

CIRCULATING COPY
Sea Grant Depository

LOAN COPY ONLY

NATIONAL SEA GRANT DEPOSITORY
PELL LIBRARY BUILDING
URI, NARRAGANSETT BAY CAMPUS
NARRAGANSETT, RI 02882

LOAN COPY ONLY

**FLOW DYNAMICS
OF THE
NEUSE RIVER ESTUARY**

C. E. Knowles

LOAN COPY ONLY

FLOW DYNAMICS OF THE NEUSE RIVER,
NORTH CAROLINA

FOR THE PERIOD 7 AUGUST TO 14 SEPTEMBER 1973

by

C. E. Knowles
Department of Geosciences
North Carolina State University
Raleigh, North Carolina

This work is partially sponsored by Office of Sea Grant, NOAA, U. S. Department of Commerce, under Grant number 04-3-158-40 and the North Carolina Department of Administration, and the Center for Marine and Coastal Studies. The U. S. Government is authorized to produce and distribute reprints for governmental purposes notwithstanding any copyright that may appear hereon.

SEA GRANT PUBLICATION UNC-SG-75-16, August 1975

Sea Grant Program, 1235 Burlington Laboratories,
North Carolina State University, Raleigh, North
Carolina 27607

ABSTRACT

A 38-day definitive study of the Neuse River circulation was undertaken from 7 August to 14 September 1973. From this study the following conclusions can be made:

(1) The net circulation in the river is slow and complicated (has circular flow patterns across river and return flow up-stream). A rough estimate of the mean net flow for the river is 1.81 cm/sec and the corresponding transit time for water starting near New Bern and entering Pamlico Sound is 32 days. Because of the complicated cross-stream, up-stream flow waste materials could remain in a local area for a time considerably longer than that predicted by the rough transit time included above.

(2) Lunar tides may be the driving mechanism for the observed circulation at all stations up-stream from Pamlico Sound. All these stations have a near tidal period in the up-stream, down-stream current fluctuations. Only one of two stations at the mouth of the river does not have a significant semi-diurnal component in its flow.

(3) The winds tend to, but do not always enhance the river circulation. They are most generally diurnal (land breeze in morning, sea-breeze in afternoon) and seem to have the largest effect on flow at Station 6B but these effects may be indirect; i.e. may be due to Pamlico Sound circulation which is generally understood to be wind-driven

This report and the results of this study should be valuable to the North Carolina Department of Air and Water Resources, to coastal and land-use planning agencies and to other investigators studying the Neuse River.

TABLE OF CONTENTS

INTRODUCTION	1
PRESENT STUDY	5
General Considerations - Instrumentation	5
Data Analysis Techniques	5
Results	9
River Flow	9
Correlation of wind to river circulation	13
Water temperature	15
Lunar tidal currents	16
Conclusions	17
REFERENCES	18
ACKNOWLEDGEMENTS	18
APPENDIX A Film-recording Sensors Used	
APPENDIX B Wind and Climatological Data	
APPENDIX C Computer Programs	
APPENDIX D River Flow Data	
APPENDIX E Water Temperature Data	
APPENDIX F Power Spectral Density Analysis	

I. Introduction

The Neuse River estuary, one of two emptying into Pamlico Sound (Figure 1), is important as a fishing ground and as a recreational site. Industrial and residential growth has and will continue to put increasing environmental pressures on the river. It has, therefore, become vitally important to understand it's biological and hydrological dynamics so that intelligent decisions concerning the growth can be made.

Most studies to date have been concerned primarily with factors that affect the biological conditions of the river: e.g. Hobbie, (1975) has been monitoring the source and fate of nutrient concentrations; the State of North Carolina has been monitoring heavy metals and other trace elements. No long-term definitive study of the circulation and flow dynamics of the river has been made; the present 38-day study was designed to satisfy that need.

It has generally been understood (Marshall, 1951; Posner, 1959) that there are no lunar tides in North Carolina Sounds except near inlets, which of course, implies a general lack of tidal currents. Wind tides are dominant (Roelofs and Bumpus, 1953) and easterly winds can cause 3 to 4 foot tides above normal at New Bern (Neuse River) and Washington (Pamlico River). Marshall (1951) indicates that the sounds are too small to have an appreciable tide generated within and any tide issuing from the ocean by way of the inlets would be rapidly damped away from the inlets. Roelofs and Bumpus (1953) calculated a hypothetical tidal range assuming the waters flowing in through the inlets were uniformly distributed over the entire sound; they came up with range of 5 cm (about 2 inches).

Magnuson (1967) indicates that it may be a lack of firm data, however, that fails to discern tidal ranges in the sounds. Indeed, in a House Document (1935) it was reported that some slight tidal variations have been detected as much as 15 miles from Oregon Inlet near the northern end of Roanoke Island. Singer and

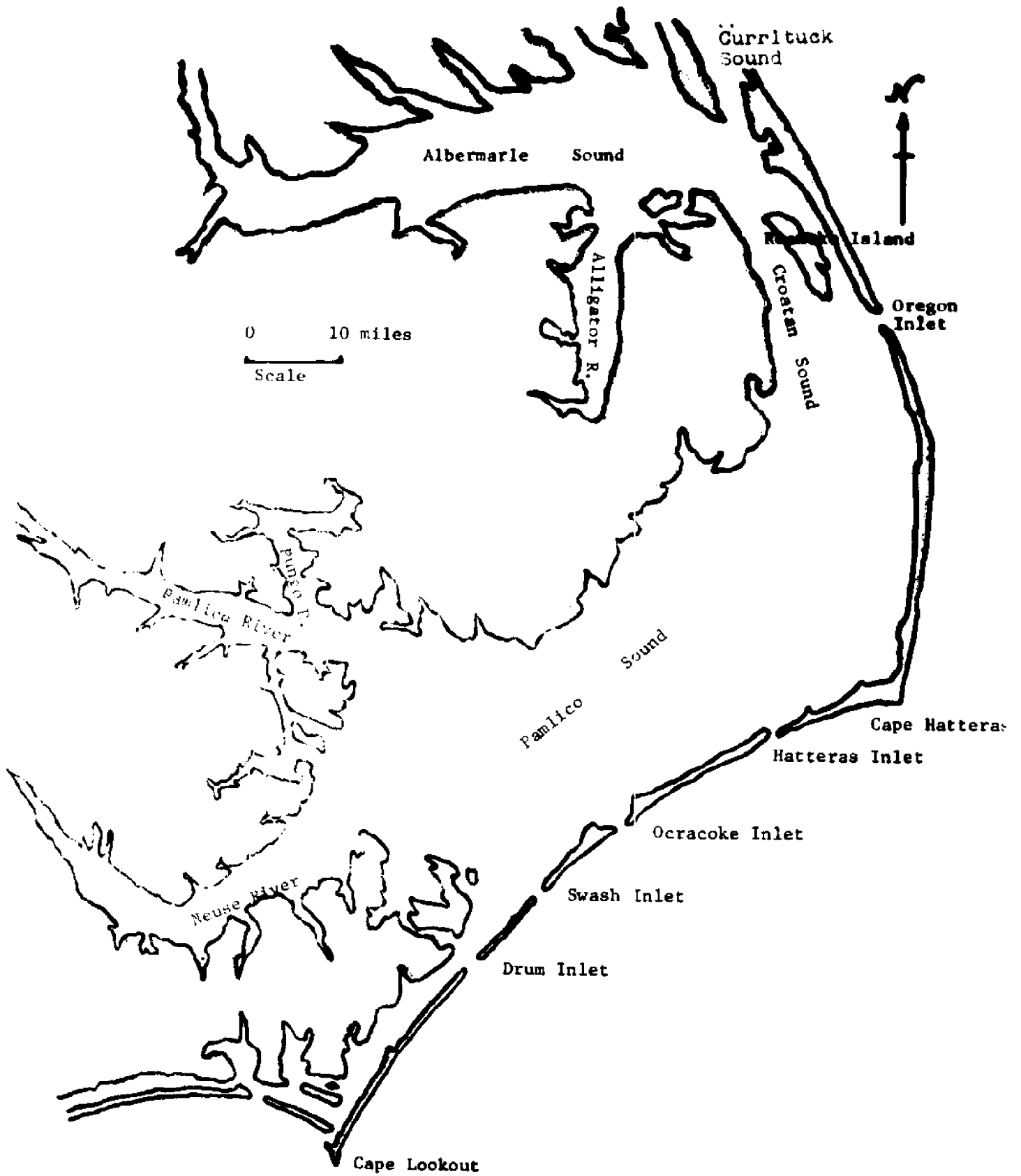


Figure 1. Upper North Carolina coast and estuarine system.

Knowles (1975), using a power spectral density analysis of United States Army Corps of Engineers tidal height records (20-30 June 1973) at Engelhard, NC (26 miles NW of Hatteras Inlet) and Stumpy Pt., NC (12 miles SW of Oregon Inlet), and data they recorded at Oregon Inlet itself for the same period, found a semi-diurnal tidal period of 12.8 hours at each of these locations.

B. J. Copeland (personal communication) has unpublished current meter data collected periodically in 1968-69 in the Bay River, NC, that indicates possible lunar tidal action. The present study will also present strong evidence for semi-diurnal tidal currents in the Neuse River.

NEUSE RIVER

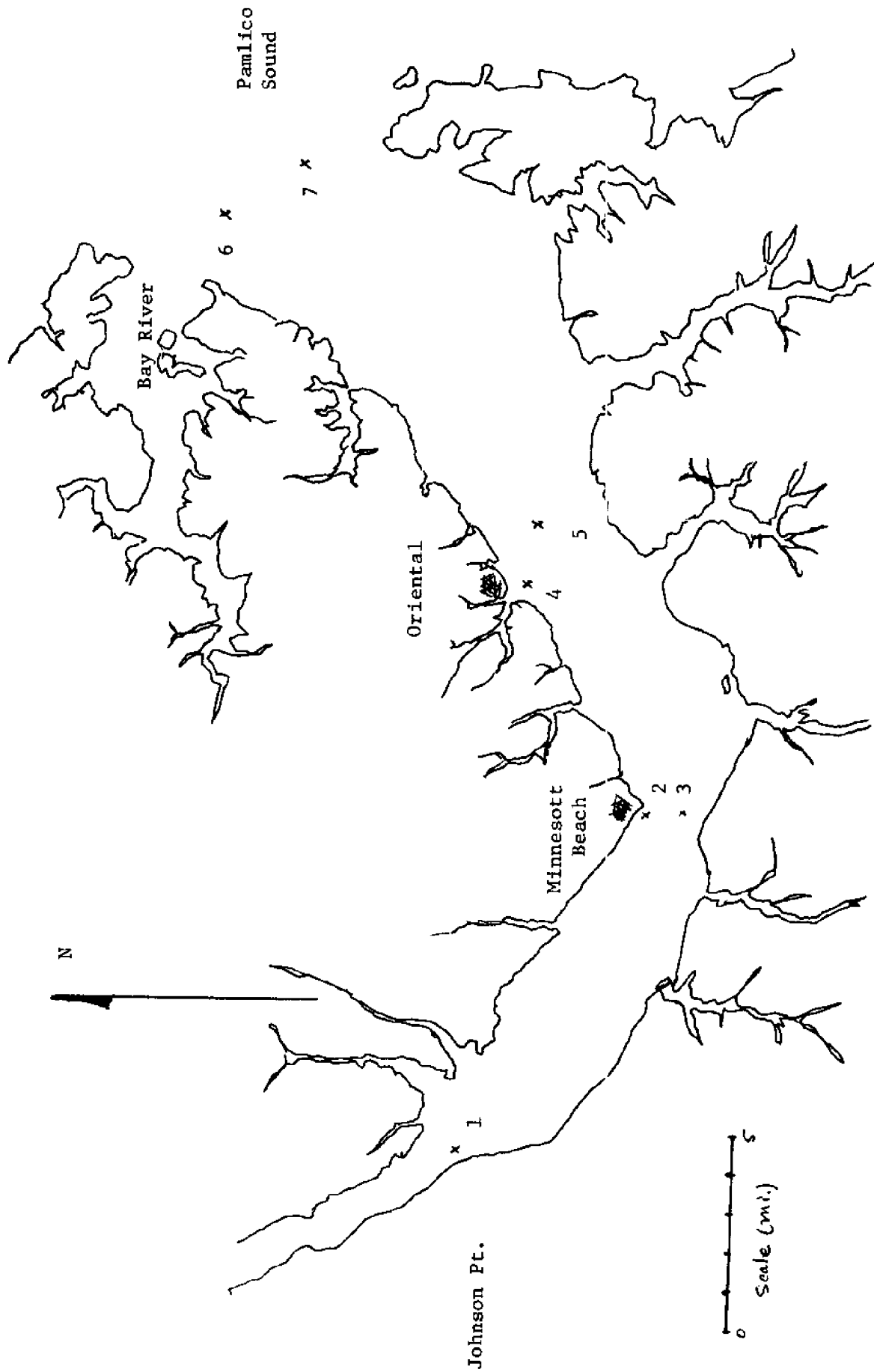


Figure 2. Neuse River sensor station locations.

II. Present Study

A. General Considerations - Instrumentation

Seven stations in the Neuse River (Figure 2) were instrumented with current and temperature sensors (see Appendix A for specifications) for the period 7 August to 14 September 1973 (a period known generally for its low-flow conditions). The data was recorded at approximately 15 minute intervals by a film-recording data logger in each of the sensors for the entire study period.

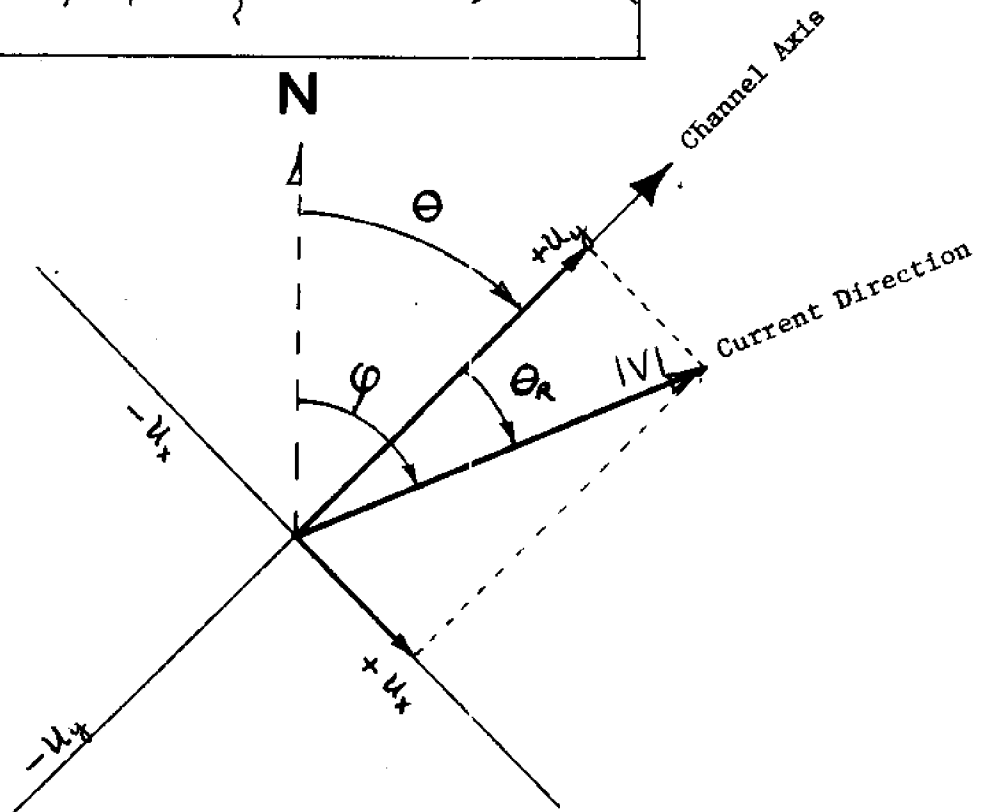
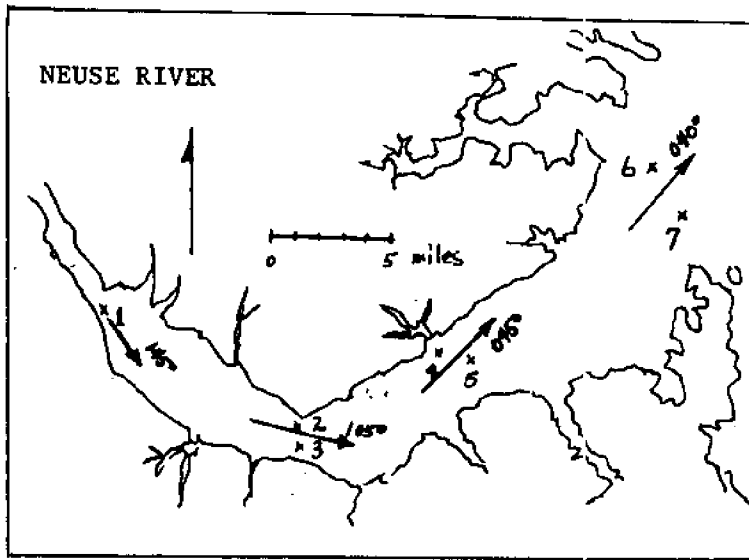
At stations 1, 3, 5, 6, and 7 river flow was measured by bottom-mounted current meters only; at stations 2 and 4 the flow was measured by both bottom and near-surface current meters. Bottom temperatures were recorded at stations 6 and 7. Tide gauges at stations 2, 3, and 7 were put in place but failed to record any data.

A portable weather station was maintained at Oriental, North Carolina, on the open lawn area adjacent to the River Neuse Motel and near the water, a location giving good southern but somewhat restricted northern, eastern, and western wind exposure. Except for periods of instrument malfunction, wind data was recorded continuously (at a height of nine feet above ground) for nearly the entire study period. It is included in this report (Appendix B) and will be correlated to the river flow.

Climatological data was obtained from the Monthly Summary for North Carolina published by the National Weather Service and is also included in Appendix B.

B. Data Analysis Techniques

The current meter data, recorded as a time sequence of the deflection angle, $Def(t)$, and the direction, $\phi(t)$, were read from the data logger film, key-punched, and used as input for the analysis program (see Appendix C for copies of this and all computer programs).



$$\theta_R = \varphi - \theta$$

$$u_y = |V| \cos \theta_R$$

$$u_x = |V| \sin \theta_R$$

Figure 3. Neuse River channel axes and vector diagram relating river current direction to the channel axes.

The deflection data, Def(t), were converted into speed (cm/sec) using the sixth-order polynomial

$$V(t) = A + B*Def(t) + C*Def(t)^2 + D*Def(t)^3 + E*Def(t)^4 + F*Def(t)^5 + G*Def(t)^6 \quad (1)$$

which the author obtained by taking a least-square fit of the deflection-speed calibration data supplied with the instruments by General Oceanics, where the coefficients of (1) are

$$\begin{aligned} A &= 2.3909 \\ B &= 1.1197 \\ C &= 2.8287 \times 10^{-3} \\ D &= -1.2010 \times 10^{-3} \\ E &= 3.8422 \times 10^{-5} \\ F &= -5.1582 \times 10^{-7} \\ G &= 2.6831 \times 10^{-9}. \end{aligned} \quad (2)$$

The polynomial in (1) had an R^2 correlation of 0.999857 and a RMS deviation from the calibration curve of ± 0.1995 cm/sec.

To facilitate analysis of the river circulation, the angle of the axis of the river channel for each station was estimated and each current vector in the time sequence was converted into its down-stream and cross-stream components as shown in Figure 3, where θ is the angle of the channel axis (in degrees) from magnetic north, ϕ , the current direction in degrees magnetic, and θ_R , the angle of the current direction from the channel axis, i.e., $\theta_R = \phi - \theta$. The down-stream and cross-stream components are given by

$$\begin{aligned} U_y &= |V| \cos \theta_R \\ U_x &= |V| \sin \theta_R \end{aligned}$$

respectively, where $|V|$ is the current magnitude (cm/sec), with signs as shown in Figure 3.

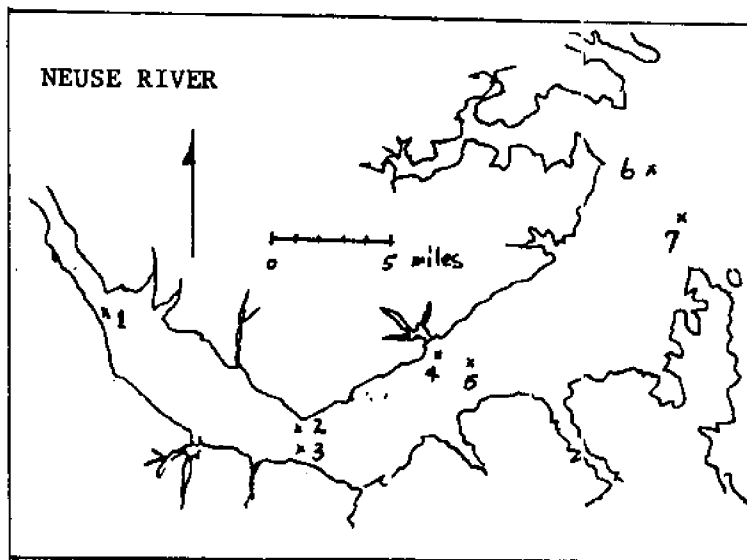


Table 1. Station locations and mean Y-component velocities (cm/sec) at each station, including the standard deviation of flow (\pm cm/sec). Negative values indicate flow up-stream.

Station #	Approximate Location and Channel Marker #	Mean Velocity Y-Comp. (cm/sec)	Standard Deviation (\pm cm/sec)
1 (Btm)	Johnson Pt., #19	4.77	8.67
2 (Top)	Minnesott Beach, #2	4.26	8.09
2 (Btm)	Minnesott Beach, #2	0.27*	7.47*
3 (Btm)	Minneostt Beach, #9	2.87	8.97
4 (Top)	Oriental Channel, #1	1.13	6.82
4 (Btm)	Oriental Channel, #1	-2.17	6.04
5 (Btm)	Oriental, #7	1.19	7.36
6 (Btm)	North Mouth	0.30	3.53
7 (Btm)	South Mouth	3.92**	6.26**

*16 days only
 **17 days only

To dampen the effects of any possible directional fluctuations in the recorded data, the components were smoothed with a 1-2-1 binomial filter, i.e., for the X-component,

$$\begin{aligned}
 U_x(1) &= [2U_x(1) + U_x(2)]/3, \\
 U_x(k) &= [U_x(k-1) + 2U_x(k) + U_x(k+1)]/4, \\
 U_x(mk) &= [2U_x(mk) + U_x(mk-1)]/3,
 \end{aligned}
 \tag{3}$$

where $t = k \Delta t$, $k = 1, 2, 3, \dots, mk$, t is time, Δt is the time increment between data points of the time sequence and mk is the last data point. A similar expression was used for U_y .

To facilitate plotting of the results, the smoothed data for each station were written into blocks of seven days beginning with Julian Day (J.D.) 219 (7 August, 1973).

The power spectral densities [in $(\text{cm}/\text{sec})^2 \text{ HR}$, where HR is hours] for the $U_y(k)$ components were calculated using the program listed in Appendix C.

The temperature data, in degrees celcius, were corrected to degrees fahrenheit and also written into blocks of seven days as discussed above for the current meter data.

C. Results

1. River Flow

The flow data will be presented in a series of figures (Appendix D) of the time sequence of the X- and Y- components of velocity (cm/sec) at each station and a table (Table 1) of the average up stream-down stream velocities and their standard deviations (also in cm/sec).

An examination of the figures show some general similarities: At every station there is an X-component of velocity, which, of course, indicates some cross-stream flow. If the X- and Y- components are considered to be

vectors (which they are), then an analysis of their phase and magnitude may be used to extract information concerning the dynamics of river circulation, i.e., if the fluctuations of U_x and U_y are always in phase ($X > 0, Y > 0$ and $X < 0, Y < 0$ (e.g., station 5B)), or 180° out of phase ($X > 0, Y < 0$ and $X < 0, Y > 0$ e.g., station 6)), then it demonstrates not only the preferred direction of flow, but also that the channel axis was not estimated properly. A rotation of the axis to a larger angle for in-phase components and to a lesser angle for 180° out of phase components could reduce U_x essentially to zero. If the components are of mixed phase ($X > 0, Y > 0$ and $X < 0, Y > 0$, etc.) then the flow direction may be due to something other than the choice of the channel axis orientation.

The positive and negative fluctuations of U_y at all stations indicates a downstream and an upstream river flow. The uniform periodicity of these fluctuations in U_y may help to explain the river circulation driving mechanisms. The river flow at some stations and for certain periods (e.g., Station 1B, J.D. 240-244 and Station 2T, J. D. 219-250) was rarely upstream, but periodically did go to zero, indicating that during those periods at least, the river flow was either sufficient to overcome the upstream driving mechanism or the mechanism itself was weaker.

In general for all stations, none of these possible high downstream flow periods have a positive correlation with the rainfall data (Appendix B). An analysis of the wind data (Appendix B) will be made later, but this also appears not to explain the semi-diurnal nature of the observations.

With these general considerations in mind, an analysis of the river flow at each station will be made.

(a) Station 1B (Figure D1). This bottom station is in the narrowest part of the river and as expected, shows the largest U_y and the smallest U_x . For the most part they are in phase ($X > 0, Y > 0$) and ($X < 0, Y < 0$) and the channel

axis is probably nearer 150° than 145° . The upstream velocities ($Y < 0$) are not generally as great as the downstream ($Y > 0$) (see Table 1), but are substantial nonetheless (max of 30 cm/sec).

- (b) Station 2T (Figure D2). This near surface station is adjacent to Minnesott Beach. With a few notable exceptions, U_y tends to be positive but periodic during all but the last seven days of data. During all but this last period, U_x is generally toward the south bank of the river ($X > 0$), is not as strongly periodic as U_y , and its phase appears in general to be only slightly correlated to it. During those periods when the flow is upstream, however, U_x is toward the north river bank ($X < 0$) and the two components are in phase and highly correlated.

As at Station 1B, the angle of the channel axis is probably a little greater; i.e., more near 110° .

- (c) Station 2B (Figure D3). In general, the trend of river flow at this bottom station is similar to 2T (located just above it). Differences lie in the magnitude of the Y-components (the phase seems to be correlated) and the phase of the X-components, i.e., the downstream velocities ($Y > 0$) are almost always greater at 2T than at 2B, the upstream velocities ($Y < 0$) are almost always less at 2T than at 2B, while the magnitude of the cross-stream velocities are about the same, but are as much out of phase as in. The phase relationship between the Y- and X-components of 2B is highly correlated, and while the upstream, downstream flow at 2B and 2T seems to be generally the same, the cross-stream flow is usually out of phase, with the flow at 2T being not so periodic and usually toward the south bank of the river.
- (d) Station 3B (Figure D4). This bottom station is opposite Minnesott Beach and Station 2, but tends to exhibit different flow patterns than Station 2T.

There appears to be a good correlation between U_x and U_y and they are in phase, which confirms the observation made above that the Channel Axis should have a larger angle. Both components have negative and positive values, though as Table 1 indicates, the mean U_y is downstream.

- (e) Station 4T (Figure D5). This near surface station is near the Oriental Channel entrance and on the same side of the river as the only other top station that recorded data (Station 2T), but has flow patterns very different from it. As with Station 3B the flow is periodic in both U_x and U_y and it seems to be highly correlated and in phase; the channel axis should probably be about 055° . The mean downstream velocity is only slightly positive (1.13cm/sec).
- (f) Station 4B (Figure D6). This station is at the same location near Oriental Channel as 4T, but on the bottom. It is the only station that shows a mean upstream velocity (-2.17 cm/sec) and since, near the surface the flow is downstream, (1.13 cm/sec), it implies that there is a vertical shear and that some external body force may be the driving mechanism for the upstream flow on the bottom. U_x and U_y are strongly periodic, but do not seem to have a consistent phase relationship; for instance, on J. D. 239 they are very much in phase, on J. D. 245-246 they are 180° out of phase. The U_x components also have a larger range of values than at the top. These two observations about phase and range imply that the bottom flow is more confused and somewhat different in direction than the top flow, which may in part be due to the proximity of the station to the Oriental Channel.
- (g) Station 5B (Figure D7). This bottom station is across from Station 4 but shows very different flow characteristics. Whereas at 4B the mean

flow is upstream, at 5B the mean flow is downstream (1.19 cm/sec) and is nearer in value to 4T than 4B. The flow is periodic, the range of velocities is larger in Uy and Ux than at Station 4, and Ux and Uy appear to be highly correlated and in phase.

- (h) Station 6B (Figure D9). This bottom station is located at the north mouth of the Neuse River at a point somewhat up from the main channel and more exposed to the influence of Pamlico Sound than any of the previous stations. The two velocity components appear to be highly correlated and 180° out of phase, implying that the channel axis should have been less, maybe 035° . As expected, the flow velocity at this location is smaller (with a mean of 0.30 cm/sec) than at the upstream stations and the fluctuations in Uy and Ux are not nearly as regularly periodic.
- (i) Station 7B (Figure D10). This bottom station is at the south mouth of the Neuse River and near the main river channel. For the most part, this 17 day record has components that appear to be highly correlated and in phase, indicating that the flow was probably oriented on an axis of 090° Mag. Both the preferred direction and magnitude of flow is greater at this station than at 6B on the opposite mouth. This result may be due to the fact that the station is more nearly in the channel than Station 6B and, therefore, more influenced by its flow.

2. Correlation of Wind Data to River Circulation

The wind speed and directional data (recorded at Oriental, North Carolina during the study period) have been expressed as time history plots of the X- and Y-components for each of the four channel axis orientations and for a N-S, E-W orientation [See Appendix B]. The former is to permit

the wind data to be used directly at each of the stations to correlate with river circulation; the latter to assess the wind patterns themselves, i.e., is there a diurnal land-breeze, sea-breeze effect, and if so when does it develop and from which direction do the winds blow. In describing the wind in the text of this report, direction will be used in the traditional meteorological sense, i.e., a north wind blows from the north; on the figures, however, the sign convention (see Appendix B) that allows a direct comparison of direction of the wind stress to the direction of water movement will be used, i.e. wind blowing upstream could cause flow upstream and both will have negative signs.

As discussed in Appendix B, there is a very strong diurnal land breeze-sea breeze nature to the wind patterns. For most of the research period, the recorded data indicates a relative no-wind condition from midnight to late morning (what wind there is is usually from North), and an increase in velocity and a shift to Southwest winds in late afternoon. If the wind patterns for each of the four channel axis orientations are examined, the same diurnal trends are evident; if they are overlayed on the river flow plots, it can be seen that the effect of the wind on the circulation seems to be only partially causative.

Unfortunately, no wind data was recorded during the period J. D. 233 to 237 (AM) when rather rapid fluctuations in the river flow was evident. It may be that the wind was the perturbation mechanism, but during one other such period (at Station 6B on J. D. 253 AM) these fluctuations occurred during calm winds.

Of all the stations, the circulation at Station 6B appears to be the most subject to wind domination; it is also (as will be discussed in the section on lunar tides) the one station that has the least amount of spectral energy at the semi-diurnal period. The circulation patterns at 6B are probably highly

affected by the circulation in Pamlico Sound, which is generally believed to be predominately wind driven. What the flow data at 6B (and the diurnal peak in the power spectral density, Appendix F) may be showing is the diurnal wind/circulation patterns of Pamlico Sound rather than the semi-diurnal patterns more evident up-stream in the river.

The effect of the wind on the Neuse River circulation should be most evident at the two top stations (2T and 4T). There appears to be some correlation of wind direction with current direction at 4T. Note in particular the Y-components on J. D.'s 240 (PM) and 249 (PM); here the strong downstream component of the wind seems to enhance the downstream flow. Look also at J. D. 251 (PM) and 252 (PM). In all four of these days except 249 (PM) there appears to be a 2 to 3 hour lag of current to the wind.

At Station 2T, the wind may also have an enhancing affect on the downstream flow on J. D. 240 (PM), 242 (PM), and 249 (PM) thru 250 (PM), and on the upstream flow on 245 (PM) and 252 (AM).

In summary, it appears that the wind tends to (particularly at the surface and usually only in the afternoons) but does not always, enhance the river circulation. Because there wind patterns are basically diurnal, however, they do not account for the semi-diurnal period of the Y-component of flow.

3. Water Temperature

The time sequence of water temperature fluctuations at Station 6B and 7B are included in Appendix E.

Both of these plots (Figure E1) show some long term trends (approx. 7 days) in water temperature with the changes at Station 7B leading 6B in time. The short term fluctuations at 6B for the period J. D. 241-248 seem generally to be diurnal, though on J. D. 245, these changes seem to be semi-diurnal. Station 7B seems to have the same characteristics,

though not for as long a time period and it shows a large unexplained drop in temperature on J. D. 249-250 that does not exist at Station 6B.

If these observations are combined with the data shown in Figure B6, it becomes apparent that neither the long nor the short term fluctuations are due to climatological conditions, but are probably due to the wind/circulation patterns of Pamlico Sound. This result is consistent with the conclusion made in the preceding section for the river circulation at Station 6B.

4. Lunar Tidal Currents.

The semi-diurnal period in U_y (see Appendix F), the diurnal wind, the vertical shear of velocities at Stations 4T and 4B, the net mean flow upstream at Station 4B and the lack of any other apparent driving mechanism, leads to the conclusion that a lunar tidal force may be necessary to explain these conditions.

The evidence for lunar tides cited earlier in the Introduction section was primarily for the Pamlico Sound and was based on tidal height data. The evidence presented here is from the first definitive study of river circulation and the first to suggest that tidal forces may be responsible for the circulation in the Neuse River. Preliminary data from a Pamlico River study in 1974 that is yet to be published also indicates a semi-diurnal component in river flow.

It is not yet clear exactly how the tidal forces drive the circulation in the river. As explained by Marshall (1951), Pamlico Sound is too small to have a tide generated within and, according to Roelofs and Bumpus (1953), the flow through the inlets when uniformly distributed over the sound would cause only a tidal range of 5 cm; these comments are even more relevant

for the Neuse River estuary. Does the tidal head and flow of the coastal inlets supply the driving force? Is a rise of 5 cm enough to support currents of 20 cm/sec?

These questions are not answerable from this study; what has been shown here for the first time is evidence of semi-diurnal fluctuations in the Neuse River circulation that may suggest lunar tides as the driving force.

D. Conclusions

It is apparent from this study that the circulation in the Neuse River is complicated and slow (at least in the sense of net flow). If an average of the mean flows at all the stations are taken, a net river flow of 1.81 cm/sec downstream is obtained. If the Neuse River is assumed to be 50 km long (from above Johnson Pt. to the mouth), then a very rough idea of the transit time of a water particle starting near Johnson Pt. can be estimated.

This value (32 days) has implications that go beyond hydrology. Excess nutrients or waste materials dumped into the river could cause considerable damage even before it empties into Pamlico Sound. The apparent circular flow patterns across the river and the return flow upstream could mean that at some locations, these wastes could remain in a local area for a time considerably longer than that predicted by the rough figures given above.

This research study was conducted during a "low-flow" period. To fully appreciate the implications of this study, further research during the winter or spring ("high-flow" conditions) should be made. Whether the semi-diurnal driving force under these conditions would be as apparent is an interesting question; whether the force is lunar is an important question.

Data collected in this study is available upon request in the form of key-punched cards (raw data), as a printed output (smoothed data) and on a

magnetic tape (smoothed data). It will be made available to anyone for the cost of reproduction.

References

- Hobbie, J. E., 1975. Nutrients in the Neuse River estuary, N. C. North Carolina Sea Grant Pub. No. UNC-SG-75-21 (in press).
- House Document No. 155, 74th Congress, 1st Session, 1935. Beach erosion at Kitty Hawk, Nags Head, and Oregon Inlet, N. C. U. S. Gov. Print. Office, Washington, D. C., 40 pp.
- Magnuson, N. C., 1967. Hydrologic implications of a deep-water channel in Pamlico Sound, North Carolina. Water Res. Inst. Report No. 5, UNC, Chapel Hill, N. C., p. 130-141.
- Marshall, N., 1951. Hydrology of North Carolina marine waters. In Taylor, H. F. editor, Survey of marine fisheries of North Carolina, UNC, Chapel Hill, N. C., 76 pp.
- Posner, G. S., 1959. Preliminary oceanographic studies of the positive bar-built estuaries of North Carolina, U.S.A. International Oceanographic Congress Reprints A.A.A.S., Washington, D. C., p. 704-705.
- Roelofs, E. W. and D. F. Bumpus, 1953. The hydrography of Pamlico Sound. Bull. of Mar. Sci. of the Gulf and Caribbean, 3(3), 181-205.
- Singer, J. J. and C. E. Knowles, 1975. Hydrology and circulation patterns in the vicinity of Oregon Inlet and Roanoke Island, North Carolina. North Carolina Sea Grant, Pub. No. UNC-SG-75-15, NCSU, Raleigh, N. C., August, 171 pp.

ACKNOWLEDGEMENTS

I want to give thanks to Mr. Jack Fulton, NCSU Computing Center Users Group for his invaluable assistance in computer graphics, to undergraduate students (too numerous to mention by name) for the difficult task of reading the data, to graduate assistants Paul Blankinship, Larry Bliven, Jim Singer, Marty Welch and Chuck McClain for help in installing and retrieving the instruments, to secretaries Nancy Beyer and Connie Harris for typing the several drafts and final copies of the manuscript and to Dixie Berg for her editorial understanding. I wish also to acknowledge the generous financial support from the UNC Sea Grant Office, the NCSU Center for Marine and Coastal Studies and the Department of Geosciences.

Appendix A. Film-recording Sensors Used

Two types of General Oceanics film-recording sensors were used in this study: (1) Model 2010 Current Meter and (2) Model 3070 Thermograph.

A. Data Logger.

Both sensors have the same type of self-contained timing and film-recording data loggers.

These film data loggers employ a super 8 camera to advance the film in single frame increments with each operation of a solenoid. This solenoid is triggered by a solid state timing circuit that has selectable timing intervals for various measurement requirements. Intervals of 5, 15, 30, or 60 minutes between photographs are used for most installations in which relatively infrequent data points over long time periods are required. A small incandescent bulb is flashed to illuminate the housing interior for each photograph; a second bulb (with appropriate sensing circuitry) is provided as a redundant light source in case of bulb failure while the instrument is on site. The circuitry is powered by 16 manganese alkaline batteries that are supposed to last up to 5 months.

The camera uses readily available super 8 film in convenient, daylight loading cartridges. Individual frames are spaced at 6 frames/inch for a total of 3600 frames in the normal 50 ft. cartridge. Approximately 3500 frames are useable for data records after beginning and end leaders are taken into account. At the 15 minute interval, the film capacity provides at least 35 days of recorded data.

B. Model 2010 Current Meter Description.

The Model 2010 operates on the principle that a buoyant wand tethered at one end will deflect into the current stream at an angle and direction that are functions of the current speed and direction. The sensing and recording of this deflection yields information that can be readily translated into current speed and direction data. A major advantage of this technique is the fact that it requires no external moving parts such as impellers or rotors which are highly vulnerable to fouling or impact damage.

The Model 2010 consists of a buoyant cylindrical housing containing a directional inclinometer and the data logger described above, which together sense and record the inclination and compass heading of the instrument. It is designed to be tethered to a ballast weight for bottom current measurements or attached to an optional mid-water frame for profile studies. The mounting method enables the instrument to be placed over any type bottom terrain. Two large vanes are affixed to the housing to assist orientation and stabilization of the current meter within the stream.

The directional inclinometer is a spherically shaped component mounted on the inner face of the lower housing end cap. The inclinometer design utilizes a transparent, fluid-filled housing containing a neutrally buoyant inner sphere. This "floating" inner sphere maintains a stable vertical attitude and an orientation towards magnetic north because of an internal bar magnet whose mounting location gives the sphere a low center of gravity. The hollow inner sphere is trimmed to neutral buoyancy by addition of silicon fluid which also serves to dampen unwanted oscillations. The outer housing is filled with water to which a wetting agent has been added to minimize drag on the inner sphere from motion of the instrument. A small circular target at the top of the transparent housing can be viewed against a grid of precision latitude and longitude lines scribed on the free inner sphere. When photographed by the camera, this target mark enables

direct reading of the instrument azimuth and inclination by its position within the grid.

Specifications:

Weight: 5.6 kgs. (12.3 lbs.) in air; 3.0 kg. (2.2 lbs.) positively buoyant in seawater.

Exposed Materials: Rigid polyvinyl chloride (PVC) housing and end caps; high density polyethylene vanes; stainless steel hardware.

Dimensions: 11.4 cm. (4½") O.D. x 51 cm. (20") long housing; 45.7 cm. (8") diameter circular sector right angle vanes tapered to housing base.

Depth Rating: 50 meters (72 psi).

Inclinometer Range: 0° to 80° from vertical (not calibrated from 80°-90°).

Inclinometer Accuracy: ±1°.

Speed Range: 0.05 to 1.7 kt. (0.08 to 2.75 fps.).

Speed Accuracy: ±3% of full scale (0.05 knots, 0.08 fps.).

Directional Range: 0° to 360°.

Directional Accuracy: approximately ±15° for inclinations less than 5° (.24 fps.), ±8° for 5° to 10° (.42 fps.), ±3° from 10° to 30° (.87 fps.) and ±1° above 30° inclination. Inclinations above 80° (2.70 fps.) are beyond range of calibration.

Main Battery Supply: Sixteen manganese-alkaline penlight cells (Mallory MN1500 size AA, or equal).

Battery Operating Life: Five months or, if sooner, 11,000 data records. (Watch battery, one year).

Mounting: Swivel eye at base of housing for mooring to ballast weight or mid-water frame.

Time Reference: Battery powered calendar watch with second, minute, and hour hands plus date window.

C. Model 3070 Thermograph.

The General Oceanics Model 3070 Film Recording Thermograph is a self-contained instrument for measurement and recording of air and water temperatures over extended periods of time. It is used to provide temperature vs. time data for a variety of meteorological, hydrological, oceanographic, and other applications. The instrument provides an accurate yet economical means for data collection in aqua-culture studies, underwater surveys, buoy installations, or detection and monitoring of thermal effluents. The fully waterproof housing enable deployment of the thermograph above water or at depths down to 50 meters. (Housings with deeper ratings can be supplied on special order).

The Model 3070 sensor is a large dial thermometer mounted on one end cap of the cylindrical instrument housing. The bi-metallic sensing element of the thermometer protrudes through the end cap out into the environment for quick response to temperature changes. This thermometer bulb is protected by a small guard piece with a number of through-holes for easy circulation of air or water. The thermometer dial is photographed at periodic intervals by a film data logger at the opposite end of the housing. A battery powered calendar watch is mounted in the center of the thermometer dial to provide an accurate time and date reference for each film frame. The use of an independent watch for the data time base yields much more accurate time data than can be achieved with instruments in which a single timing mechanism is utilized for both the data reference and film (or chart) drive functions.

Specifications:

Weight: 3 kgs. (6½ lbs.) in air; approximately 1 kg. (2.2 lbs.) positively buoyant in water.

Exposed Materials: Rigid polyvinyl chloride (PVC) housing, end caps, and thermometer bulb guard; stainless steel hardware and thermometer bulb.

Dimensions: 11.4 cm. (4½") O.D. x 38 cm. (15") overall length less thermometer bulb guard piece.

Depth Rating: 50 meters (72 psi).

Temperature Range: 0° to 55° C.

Accuracy: ±1% of full scale (.55° C).

Time Reference: Battery powered calendar watch with second, minute, and hour hands plus date window.

Watch Accuracy: ±0.0035% (30 seconds per 24 hours).

Date Interval: Selectable at 5, 15, 30, or 60 minutes. Timing intervals chosen by changing timing plugs in data logger circuit. A 15 minute range was used in this study.

Main Battery Supply: 16 manganese-alkaline penlight cells. (Mallory MN 1500, size AA, or equal).

Operating Life: 5 months or, if sooner, 11,000 camera operations. (Watch battery, one year).

Appendix B. Wind and Climatological Data

Included in this appendix are time history plots of the X- and Y- components of the wind data collected at Oriental, North Carolina, and the air temperature and rainfall at New Bern (FAA), both for the study period. The list given below includes the figure number, the channel axis orientation (in deg. mag) used to calculate the components, the use made of the particular plot and the page numbers of each plot.

<u>Figure</u>	<u>Axis</u>	<u>Use</u>	<u>Pages</u>
B1	360°	Diurnal wind analysis	B-3 thru B-8
B2	145°	Correlation with flow @ STA 1	B-9 thru B-14
B3	105°	Correlation with flow @ STA's 2 & 3	B-15 thru B-20
B4	045°	Correlation with flow @ STA's 4 & 5	B-21 thru B-26
B5	040°	Correlation with flow @ STA's 6 & 7	B-27 thru B-32

The ordinate in all the above figures and for both components show wind stress in $(\text{dynes/cm}^2) \times 10^1$ [for Figure B1, $Y > 0$ wind from south, $Y < 0$ wind from north, $X > 0$ wind from west, $X < 0$ from east; for Figures B2 - B5, $Y < 0$ wind from down-stream, $Y > 0$ wind from up-stream, $X < 0$ from right of channel axis, $X > 0$ wind from left of channel axis]; the abscissa shows time (Julian Date and hours (EDT)).

The climatological data is given in figure B6 (p. B-33)

The wind data collected for this study at Oriental was at a distance of 9 feet above the ground. The wind stress is calculated by

$$\tau(t) = \rho C_D V^2 \quad (\text{B.1})$$

where ρ is air density ($1.28 \times 10^{-3} \text{ gm/cm}^3$), V is wind velocity (cm/sec), t is time and C_D is the non-dimensional drag coefficient. A value of 2.5×10^{-3} was chosen for C_D even though the wind was not recorded at the required height of 10 meters. Because of the variable nature of the terrain surrounding the recording site, and the lack of other sufficient meteorological information to warrant a better

choice, the standard value for C_D was chosen. In all likelihood the wind stress values calculated by (B.1) are a little high, but for the purposes of this study should aid in the analysis of the dynamics of the river circulation.

The component plots at the four different channel axis orientation's (Figures B2 through B5) will be discussed in the text of the report; the NS, EW orientation (Figure B1) will be discussed below.

The diurnal nature of the winds is the most common feature of the data shown in Figure B1. In almost every case the morning winds (mid-night to about 0900) are calm or light and variable and the afternoon winds are, starting near 1800, much stronger (ave. about 10-12 knots on $.3 \text{ dynes/cm}^2$) and from the southwest. Some exceptions exist: i.e., on J.D. 220 (pm) the winds were very nearly always from the east; on J.D. 221 (mid-day) there was a predominate east wind before the shift to SW at 1400; the highest winds (SW) occurred on J.D. 222 (pm) and lasted into the next morning; on J.D.'s 247-248, except for early on 247 and late on 248 there was no wind; stronger winds (SW) reoccurred again on J.D. 249 and 250 (with early morning carry-overs); on J.D. 251 there were strong but short duration winds (SW) at 1500; and finally on J.D. 252 (am) there were substantial SE winds.

If the climatological data (Figure B6) is compared to the wind (Figure B1) no clear reasons can be found for some of these variations in the diurnal nature of the winds.

Figure B1. Wind stress (dynes/cm² x 10¹) vs time, with an axis orientation of 360° mag (Diurnal Analysis).

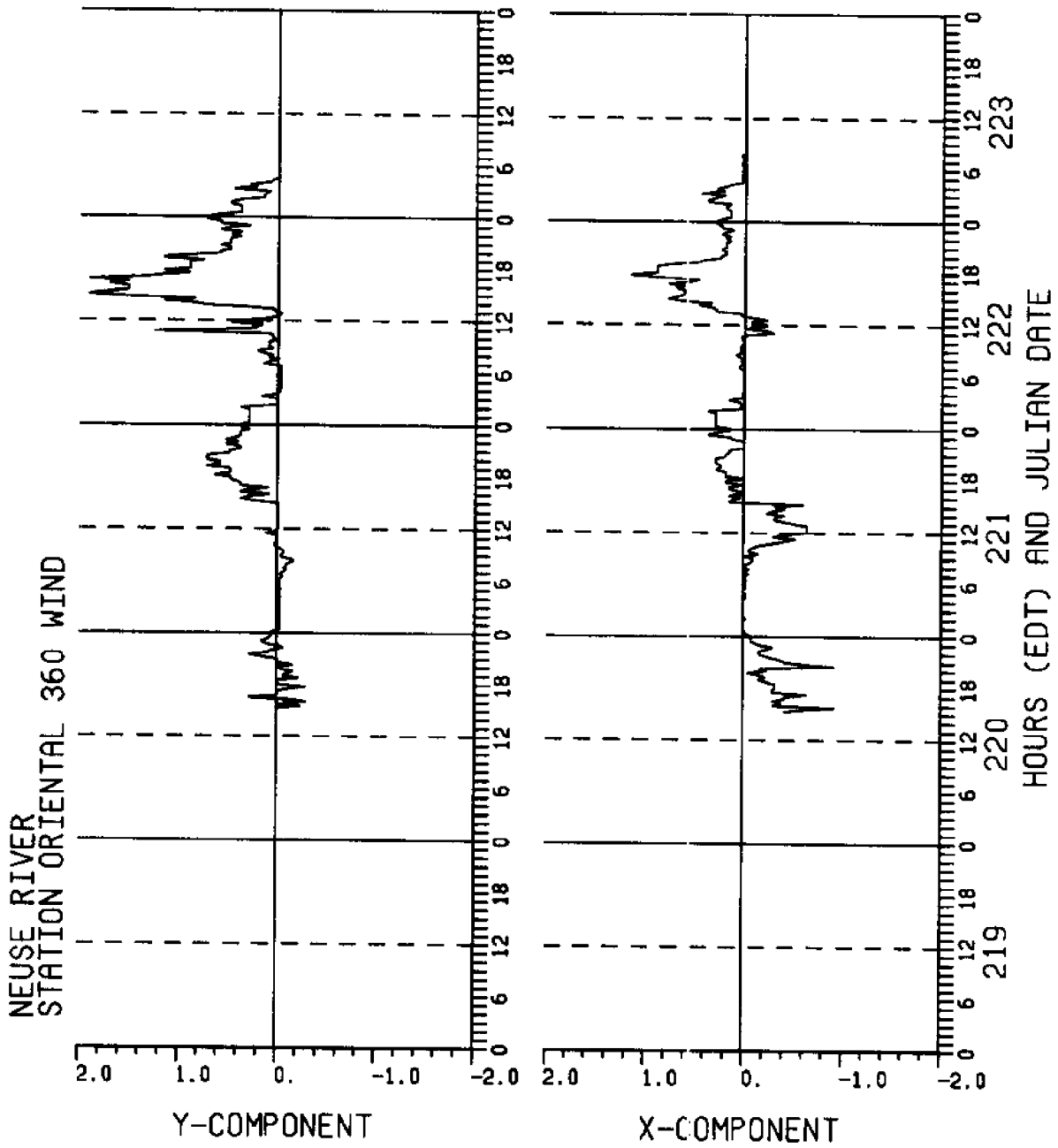


Figure B1

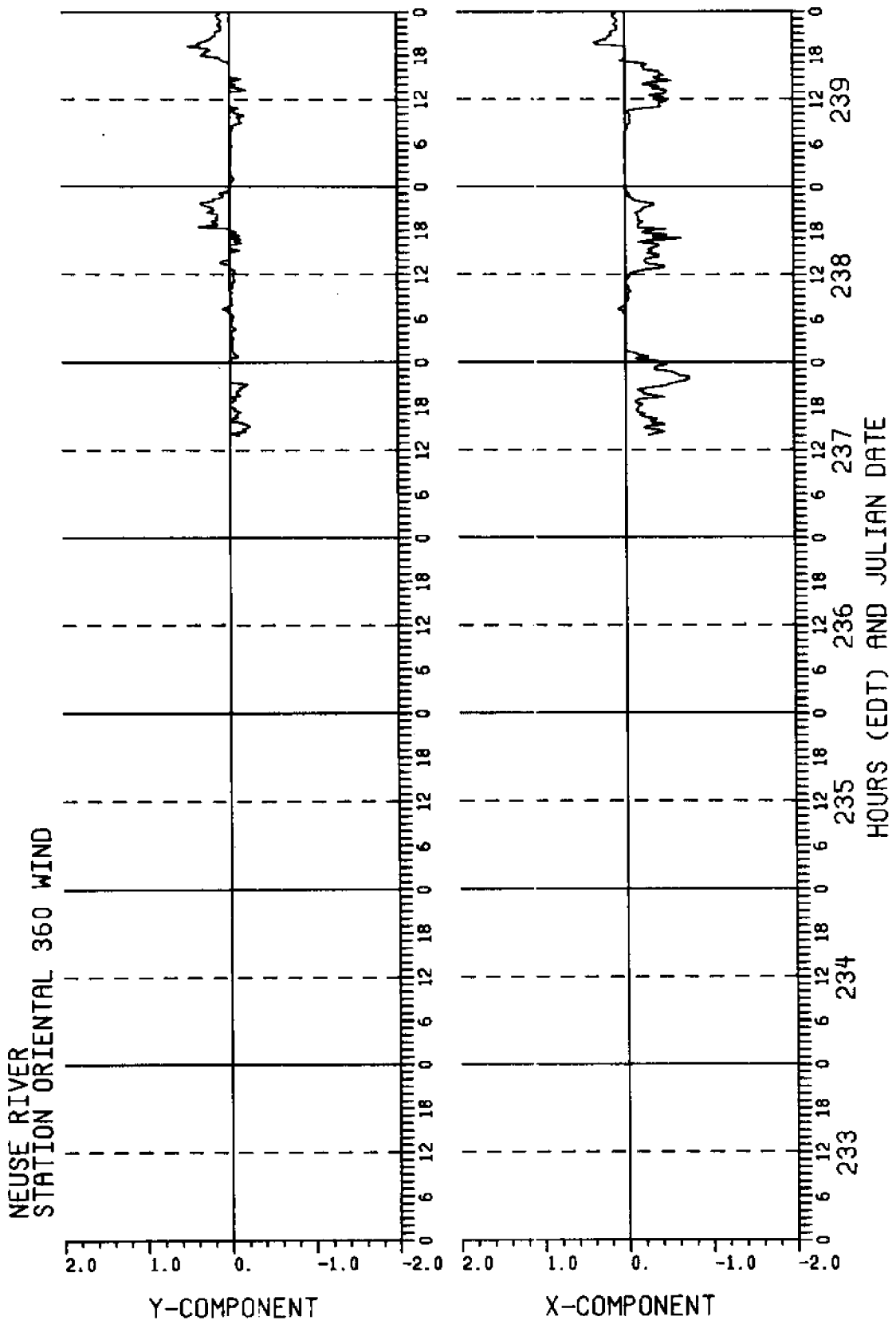


Figure B1

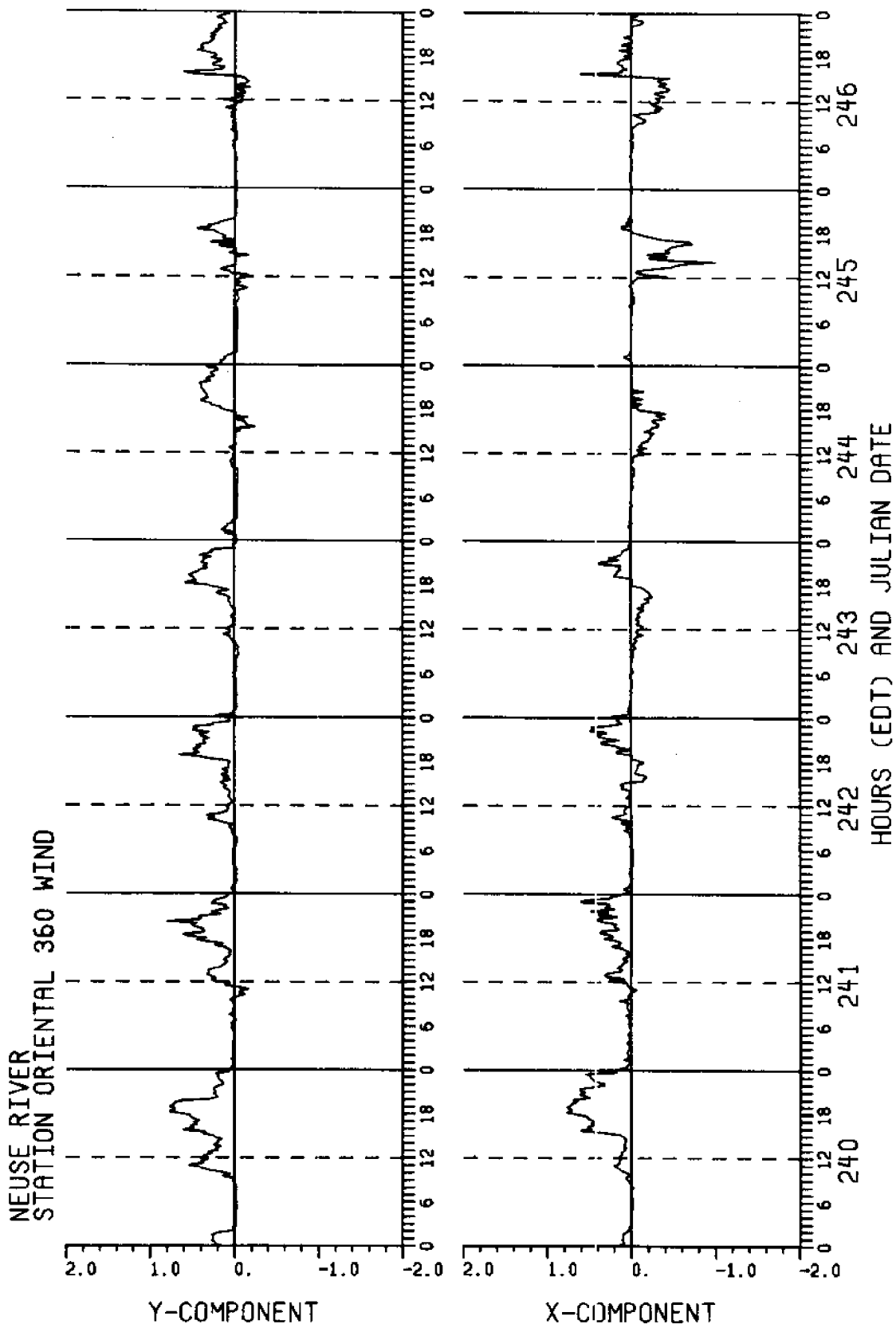


Figure B1

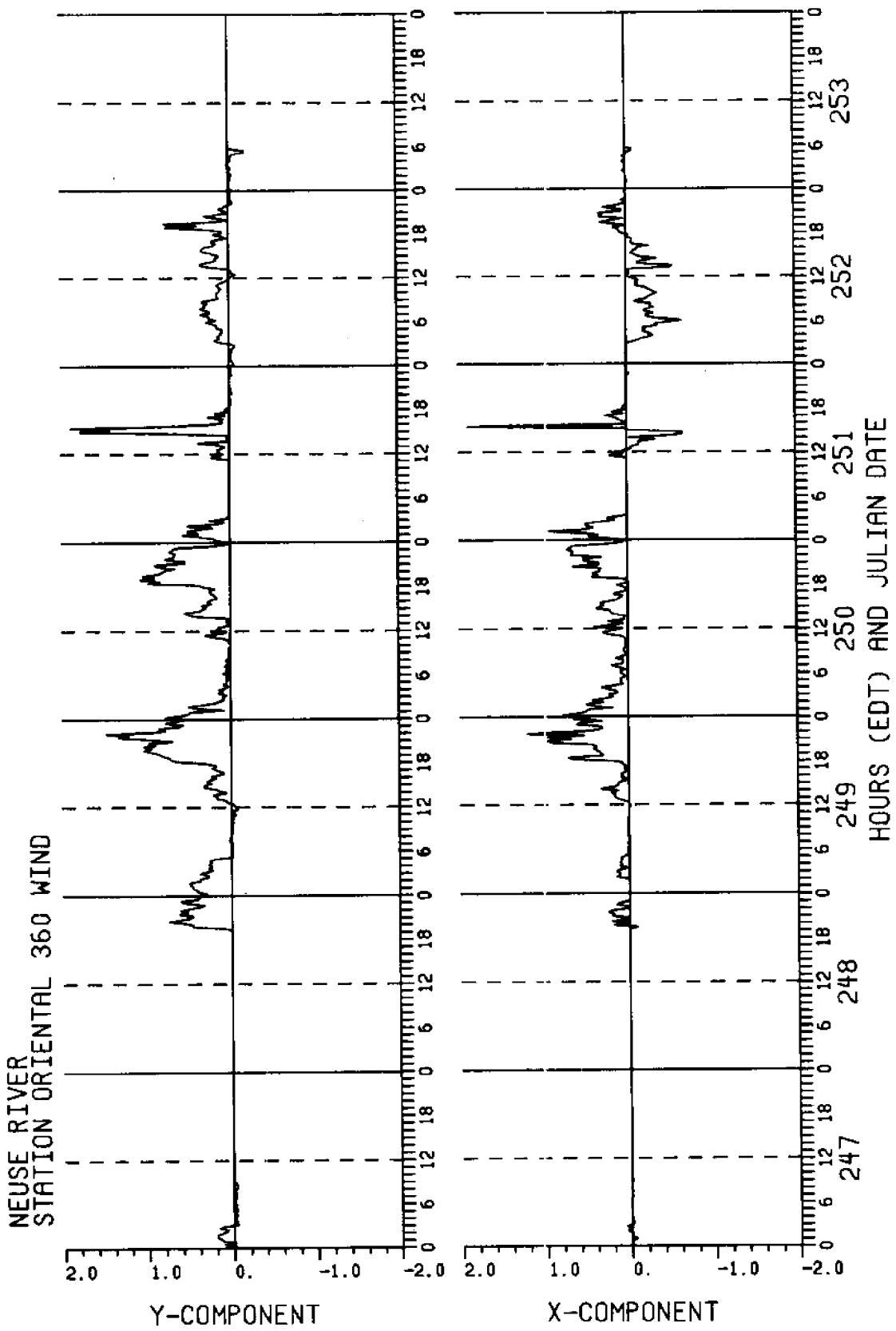
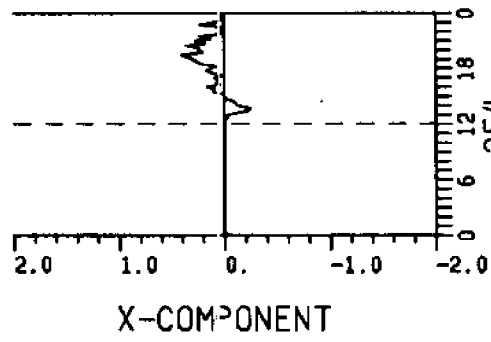
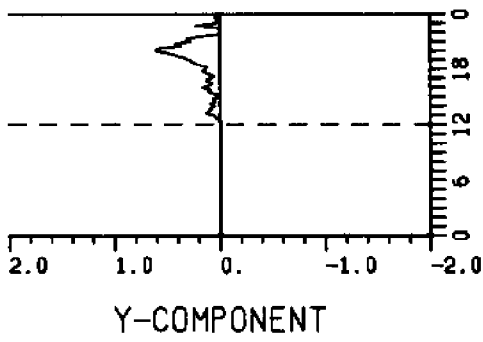


Figure B1

NEUSE RIVER
STATION ORIENTAL 360 WIND



HOURS (EDT) AND JULIAN DATE

Figure B1

Figure B2. Wind stress ($\text{dynes/cm}^2 \times 10^1$) vs time, with an axis orientation of 145° mag (Station 1).

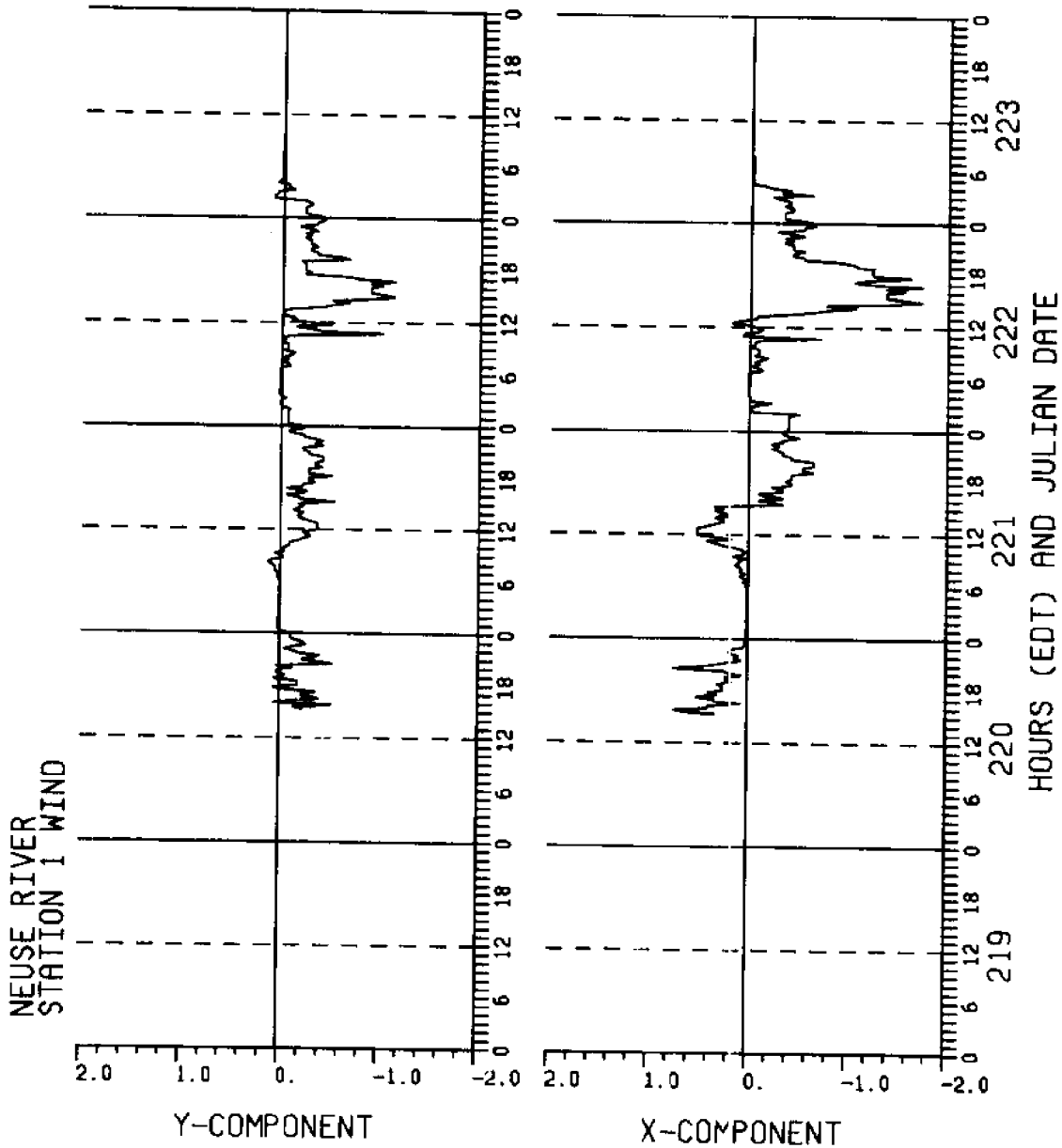


Figure B2

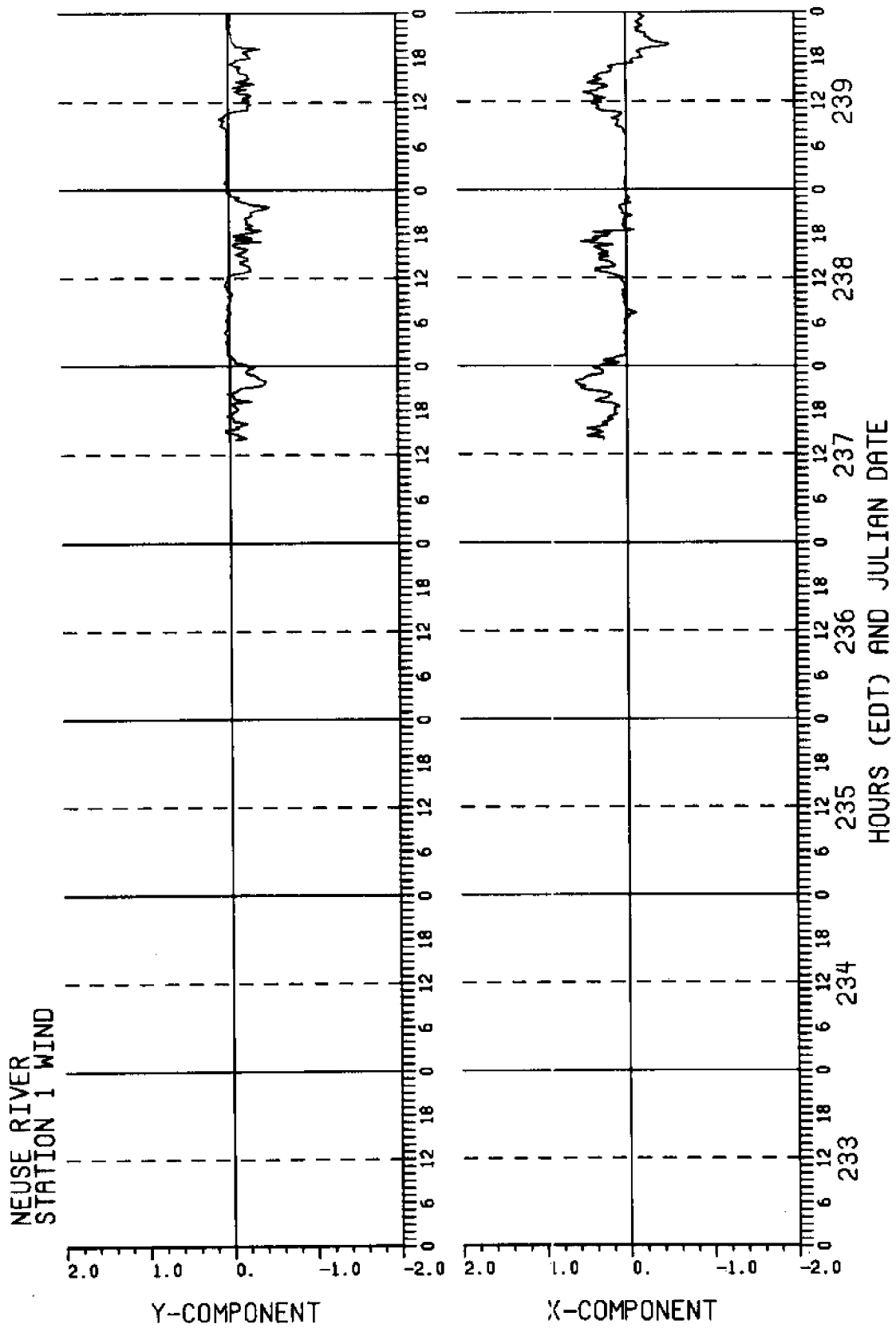


Figure B2

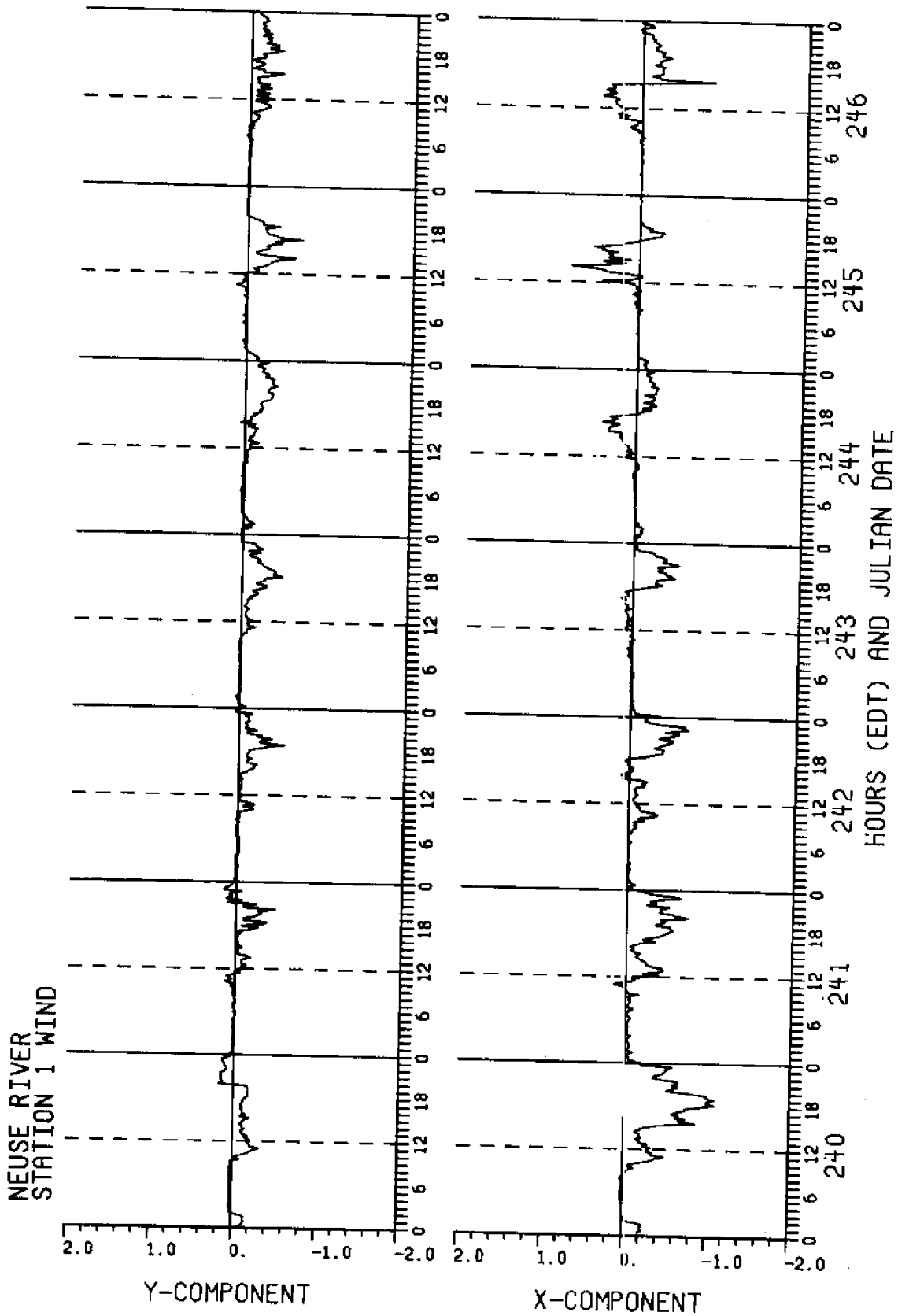


Figure B2

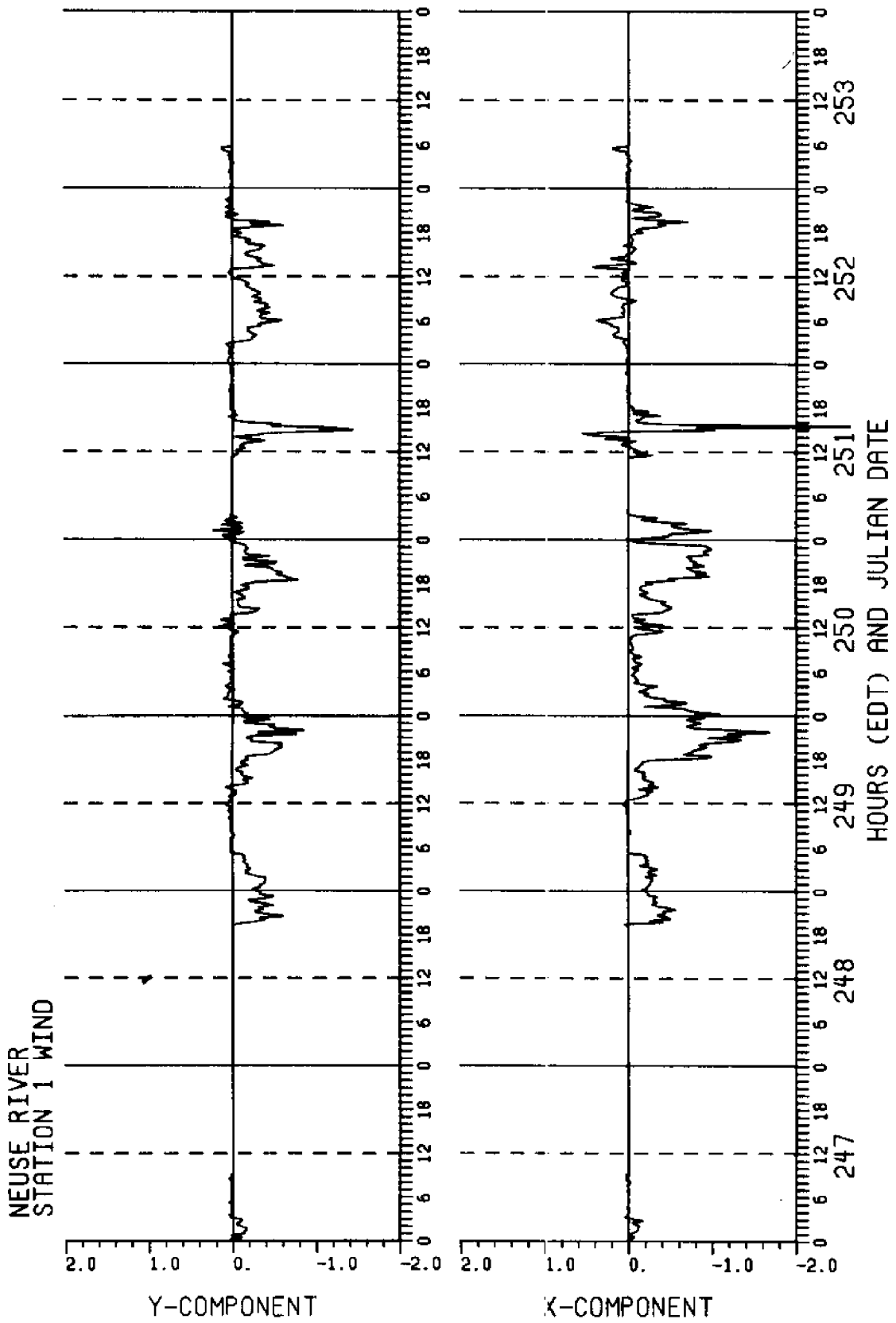
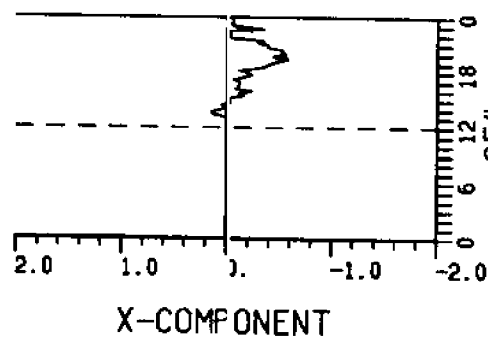
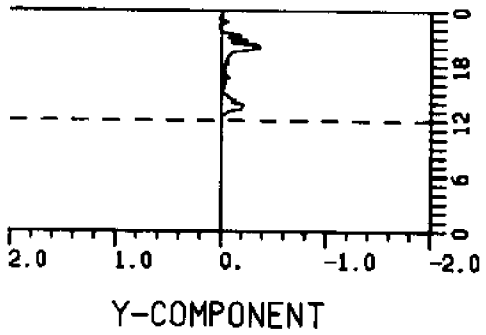


Figure B2

NEUSE RIVER
STATION 1 WIND



HOURS (EDT) AND JULIAN DATE

254

Figure B2

Figure B3. Wind stress (dynes/cm² x 10¹) vs time, with an axis orientation of 105° mag (Stations 2 & 3).

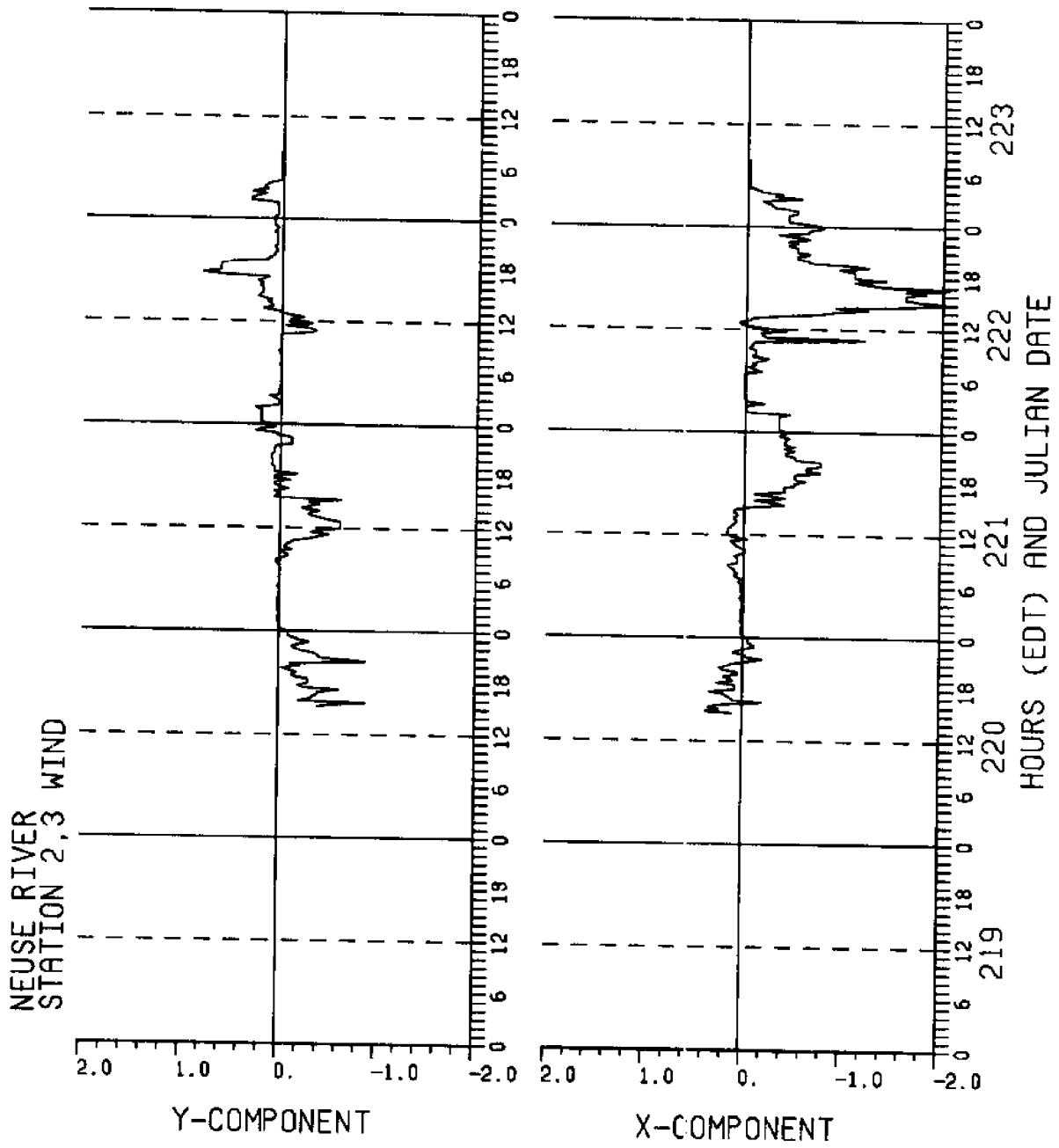


Figure B3

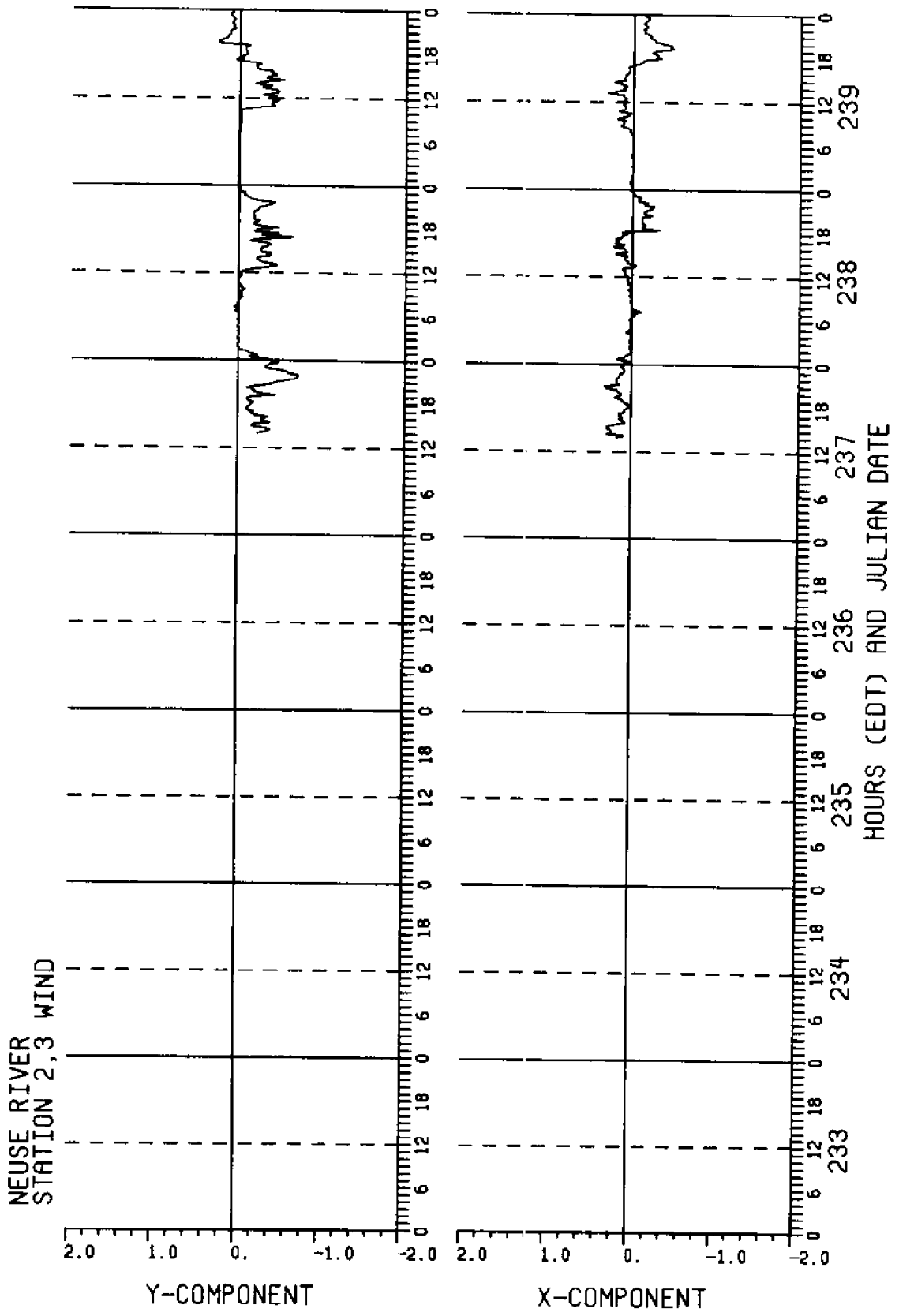


Figure B3

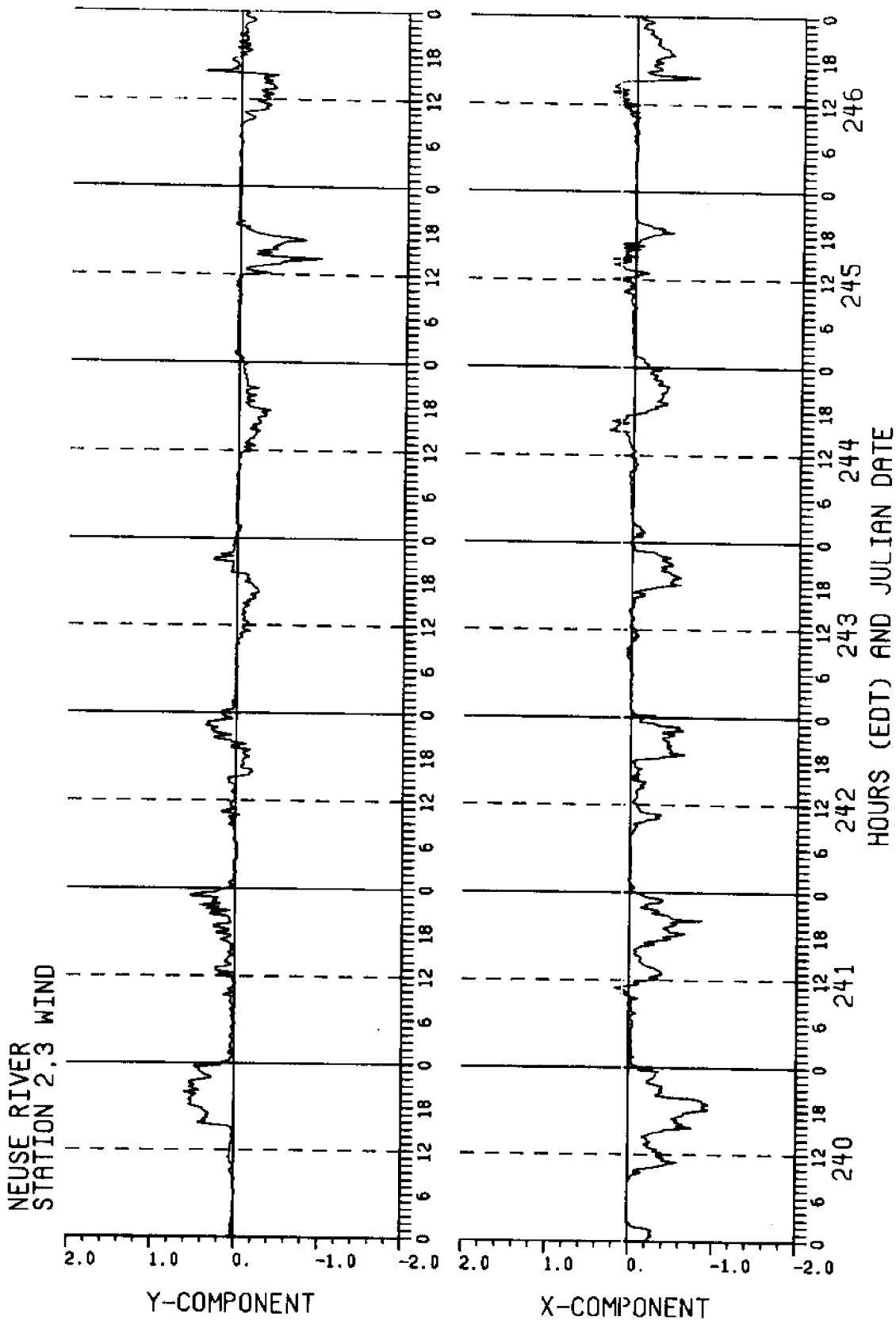


Figure B3

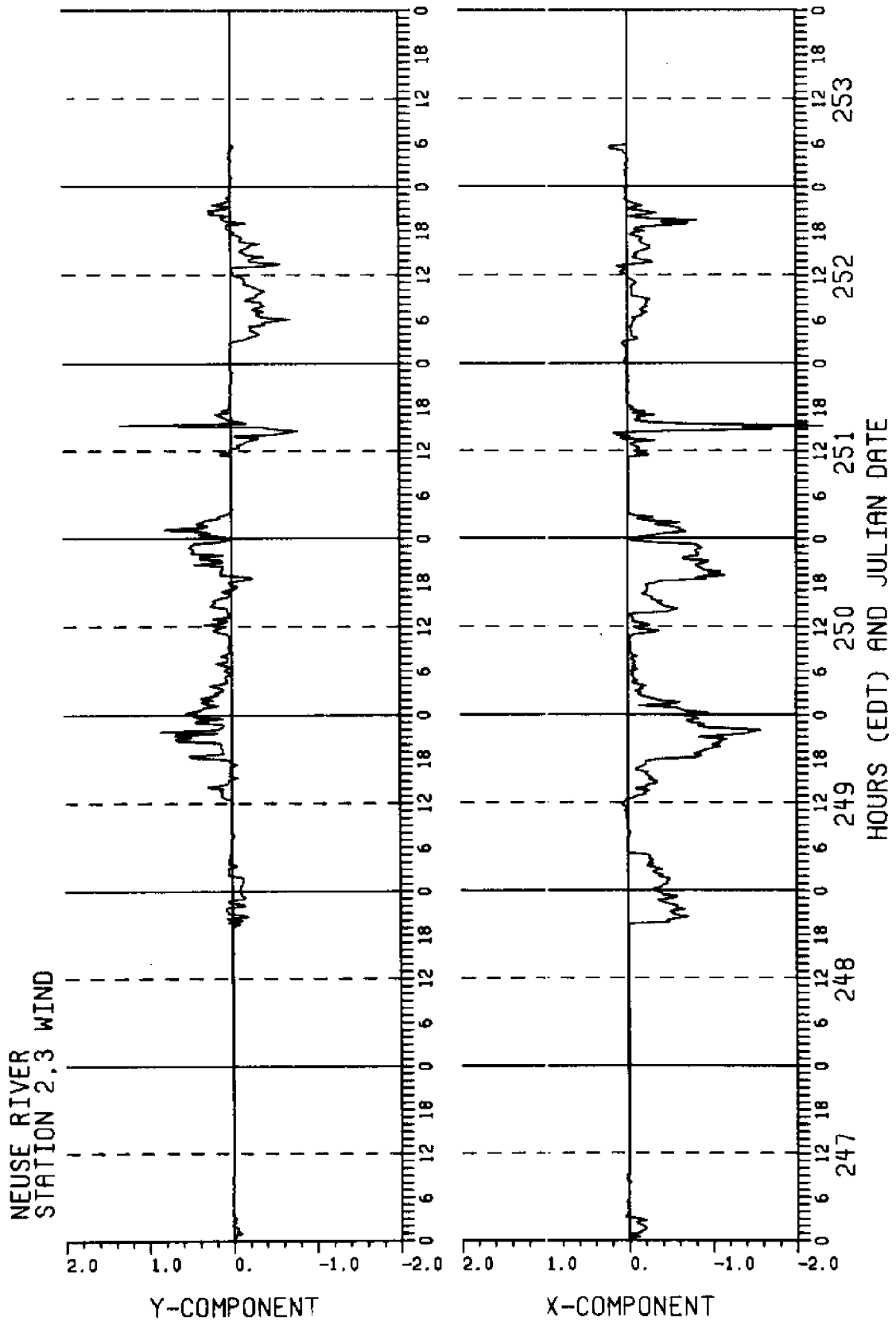


Figure B3

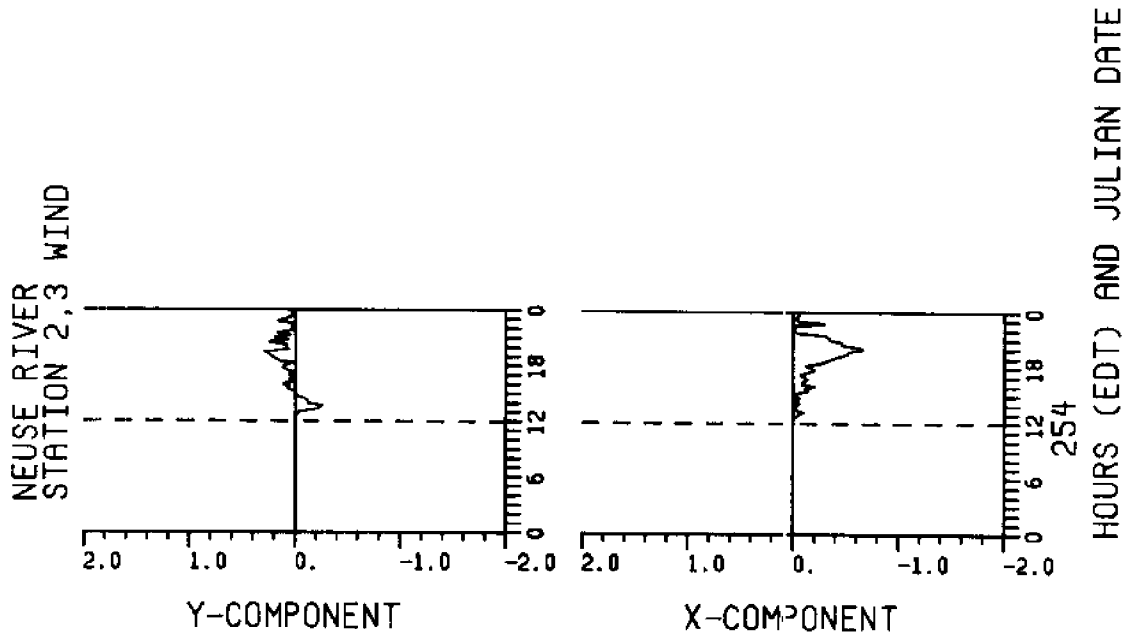


Figure B3

Figure B4. Wind stress (dynes/cm² x 10¹) vs time, with an axis orientation of 045° mag (Stations 4 & 5).

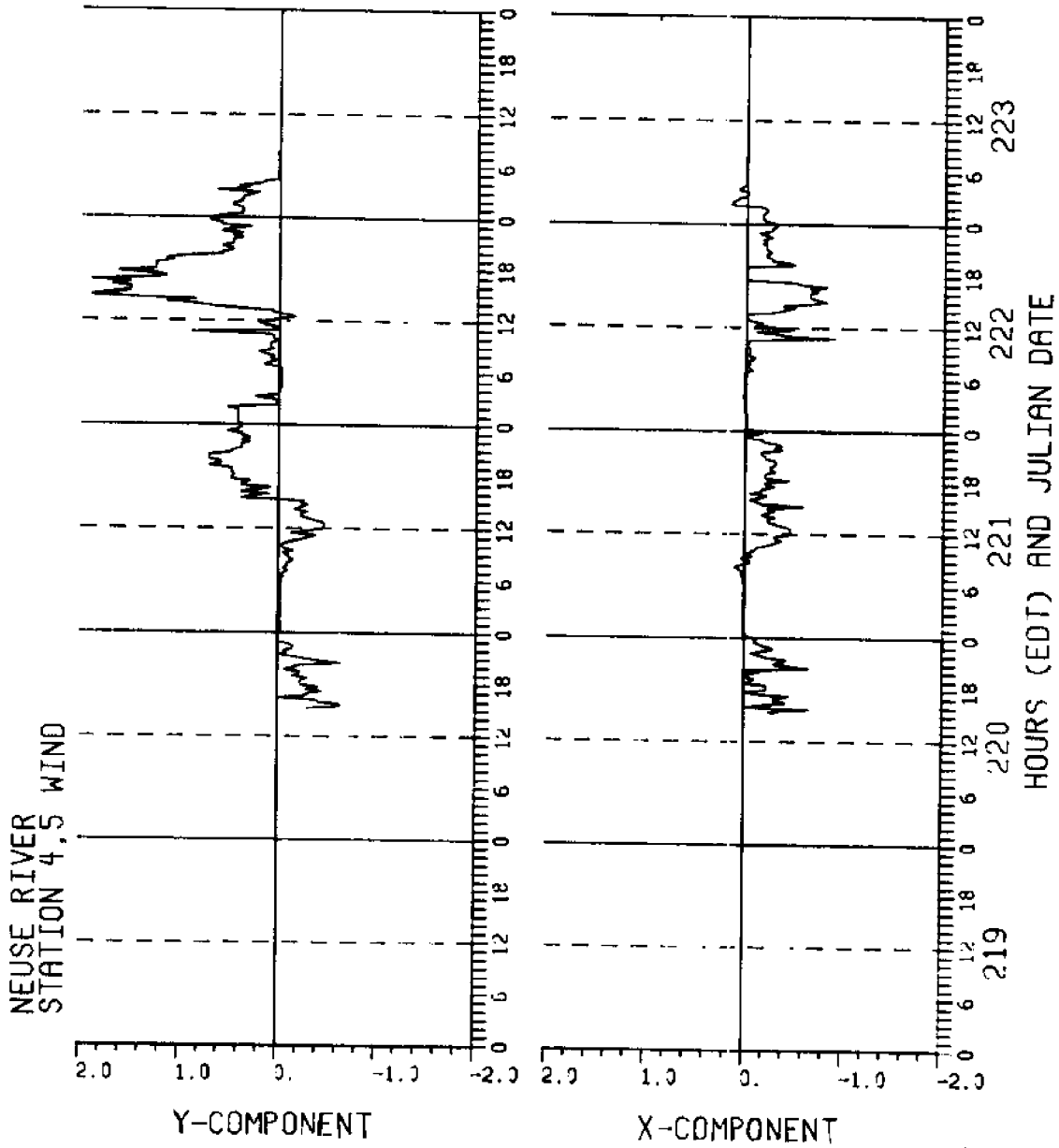


Figure B4

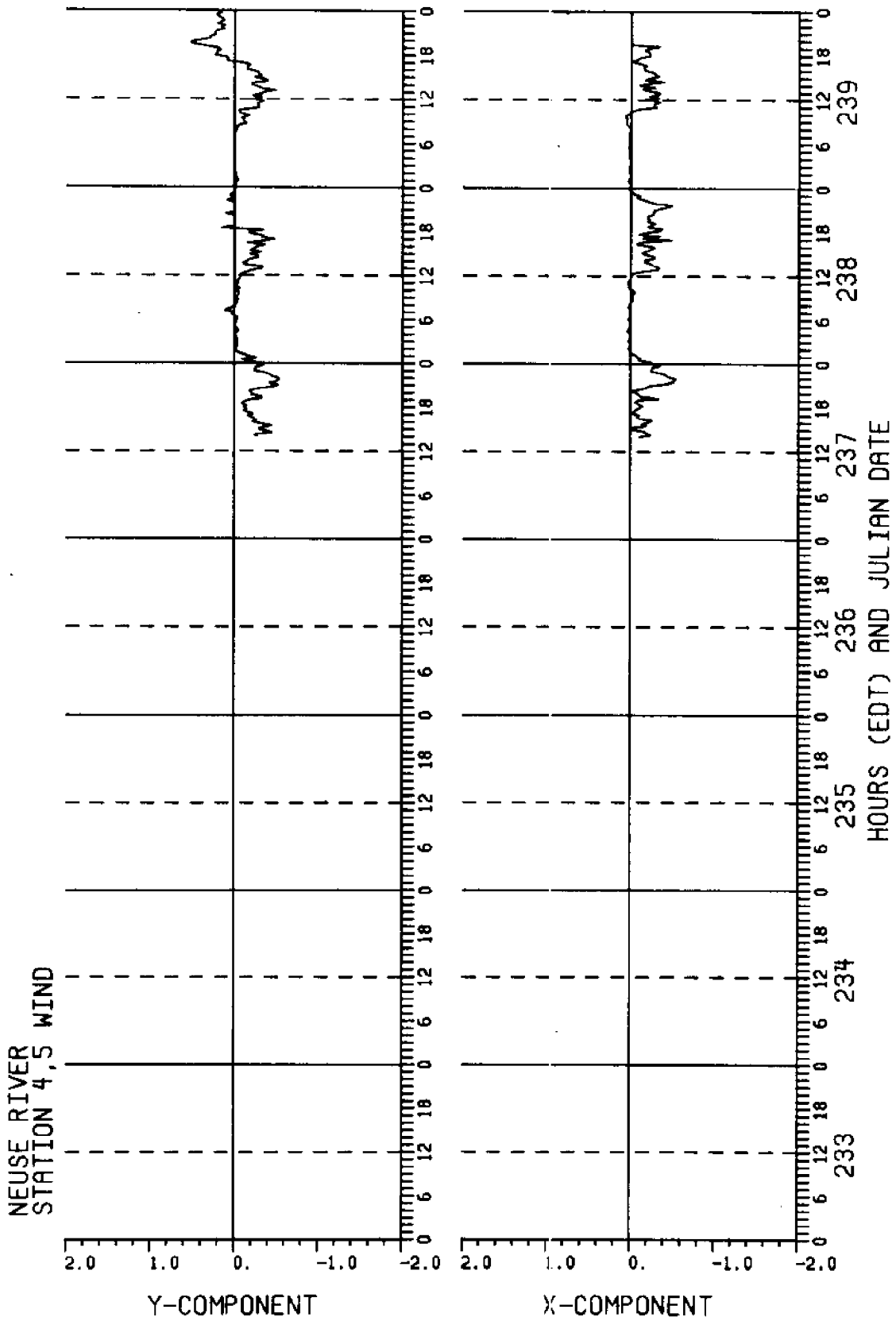


Figure B4

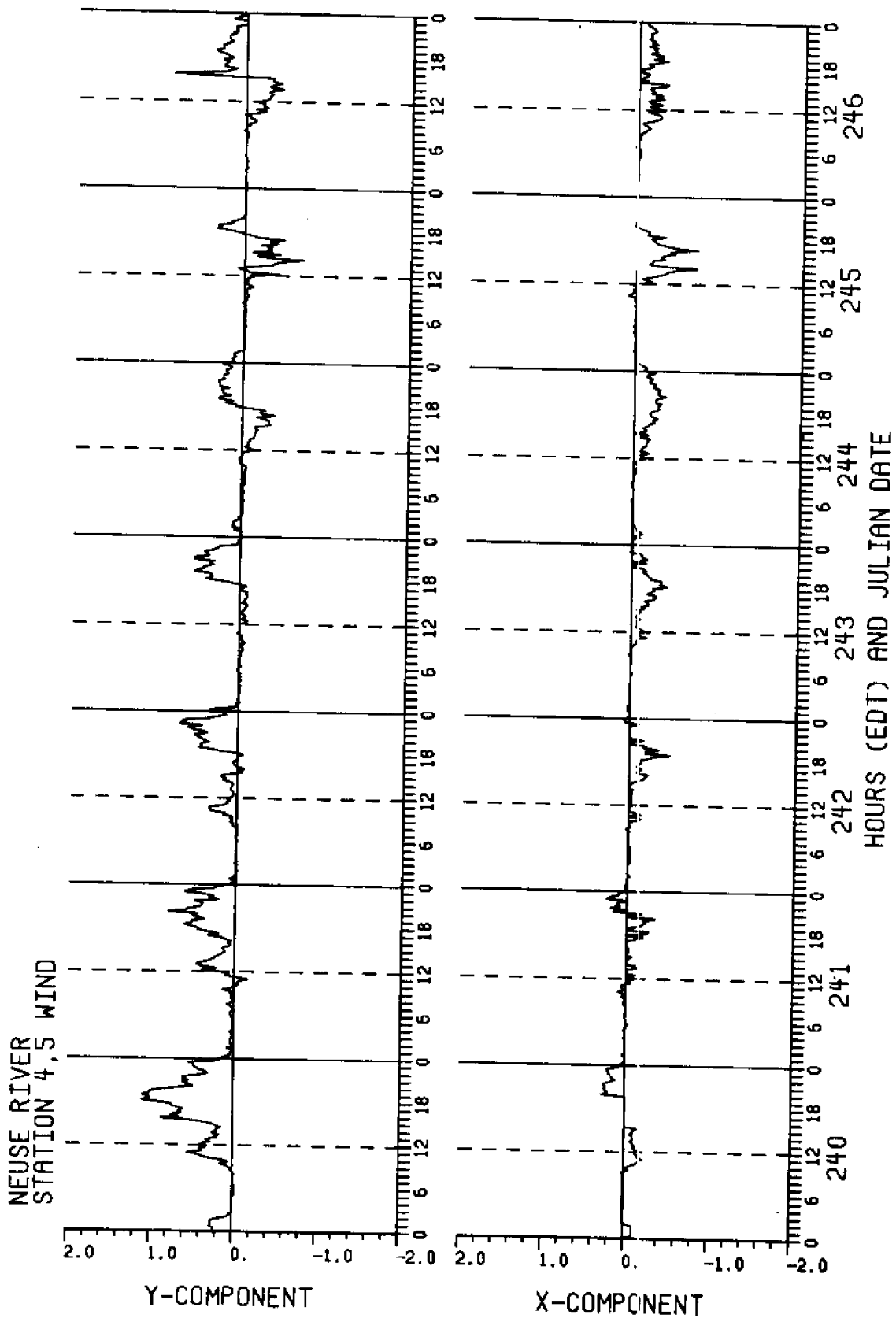


Figure B4

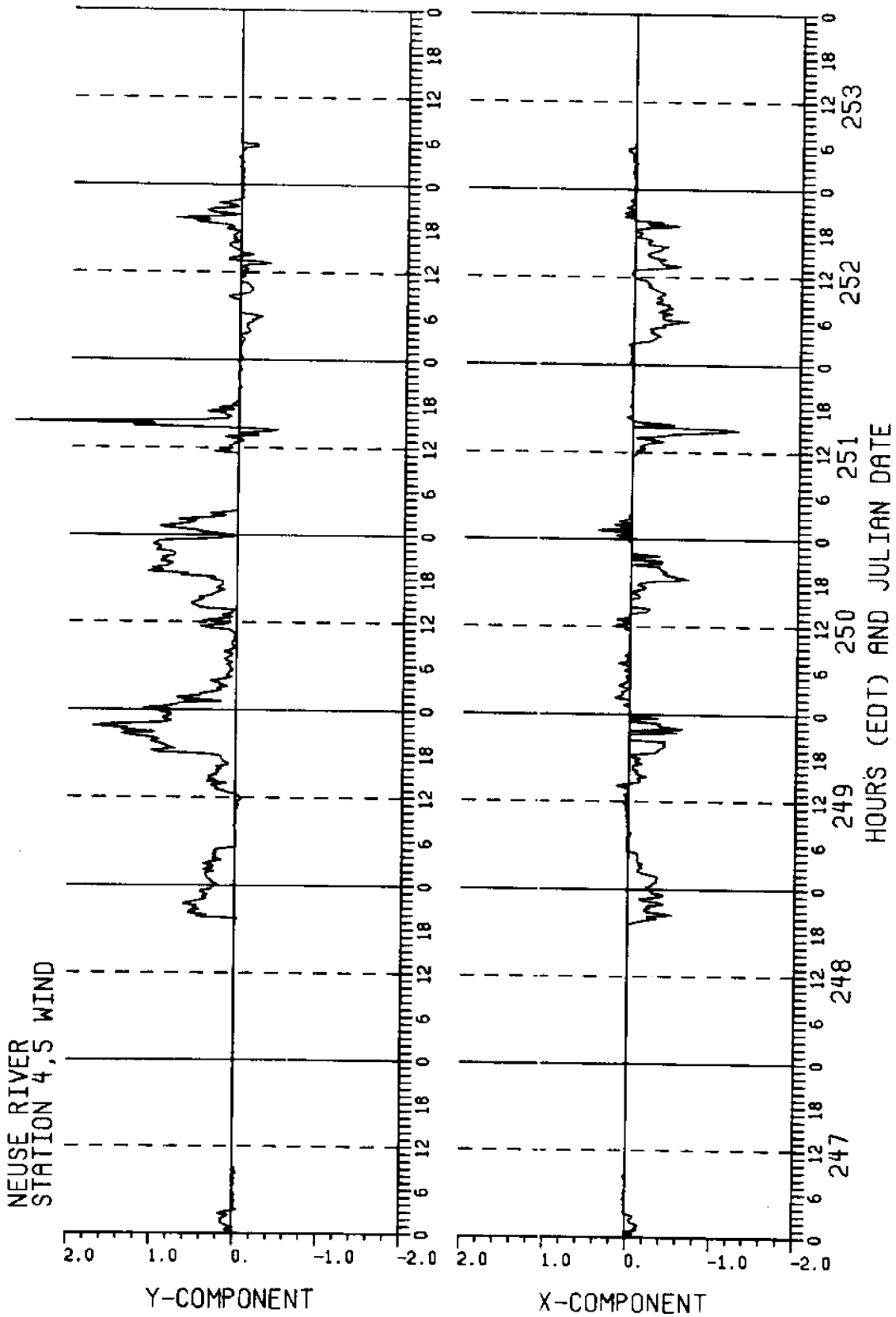


Figure B4

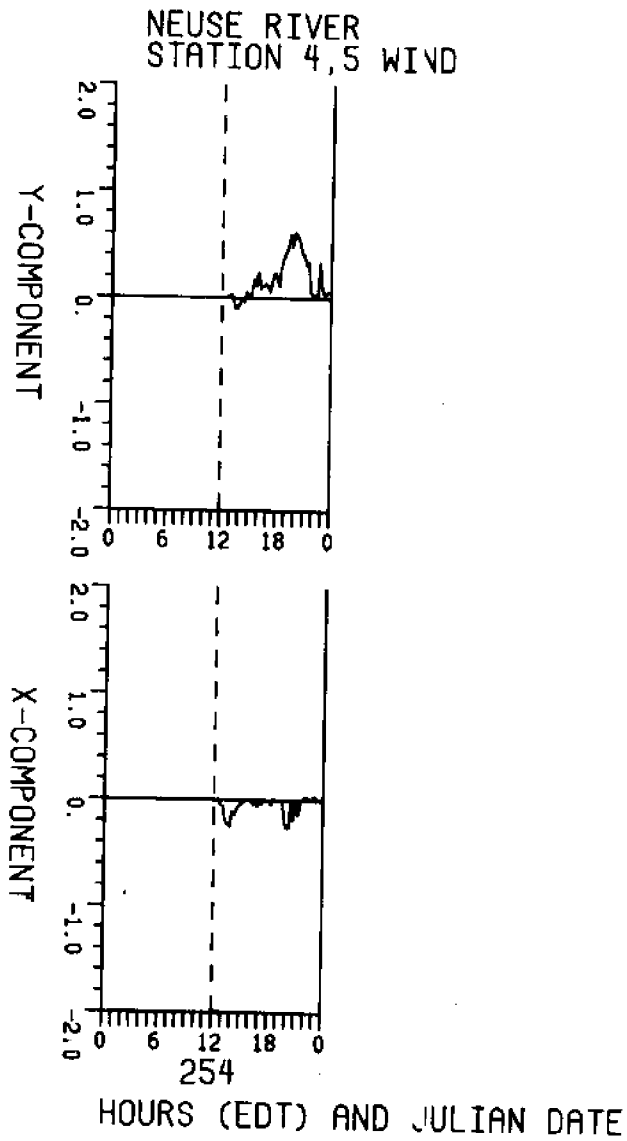


Figure B4

Figure B5. Wind stress (dynes/cm² x 10¹) vs time, with an axis orientation of 040° mag (Stations 6 & 7).

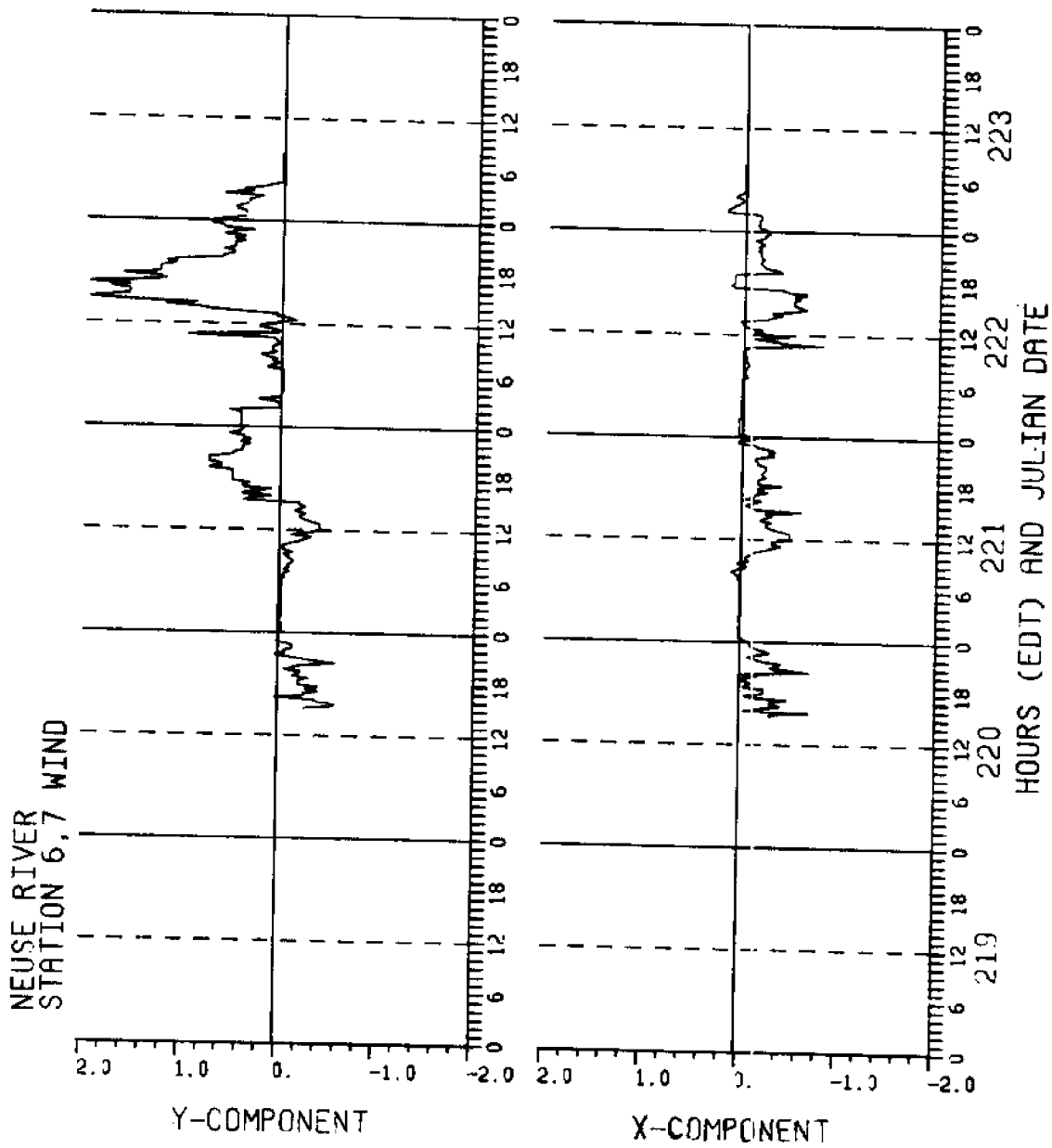


Figure B5

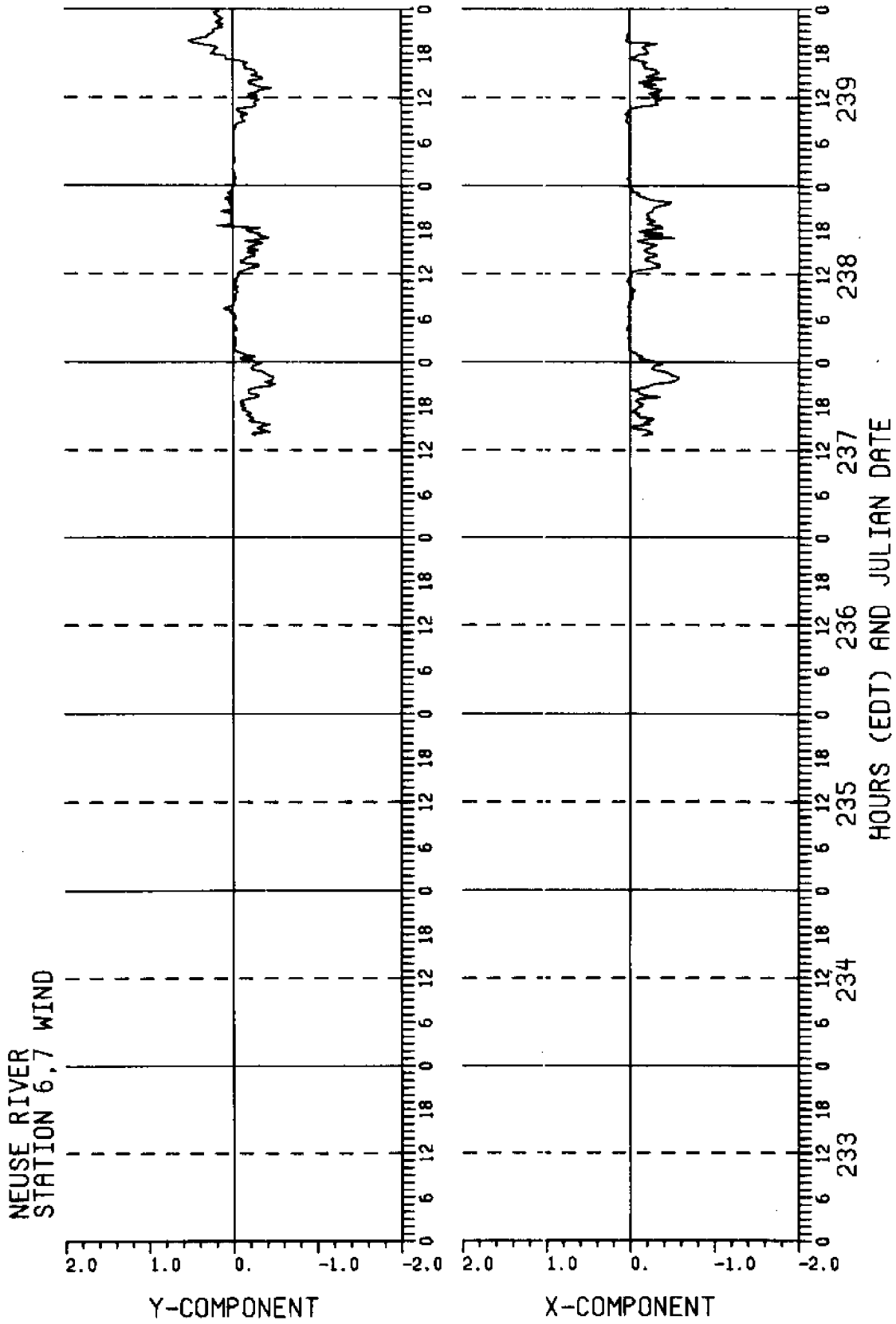


Figure B5

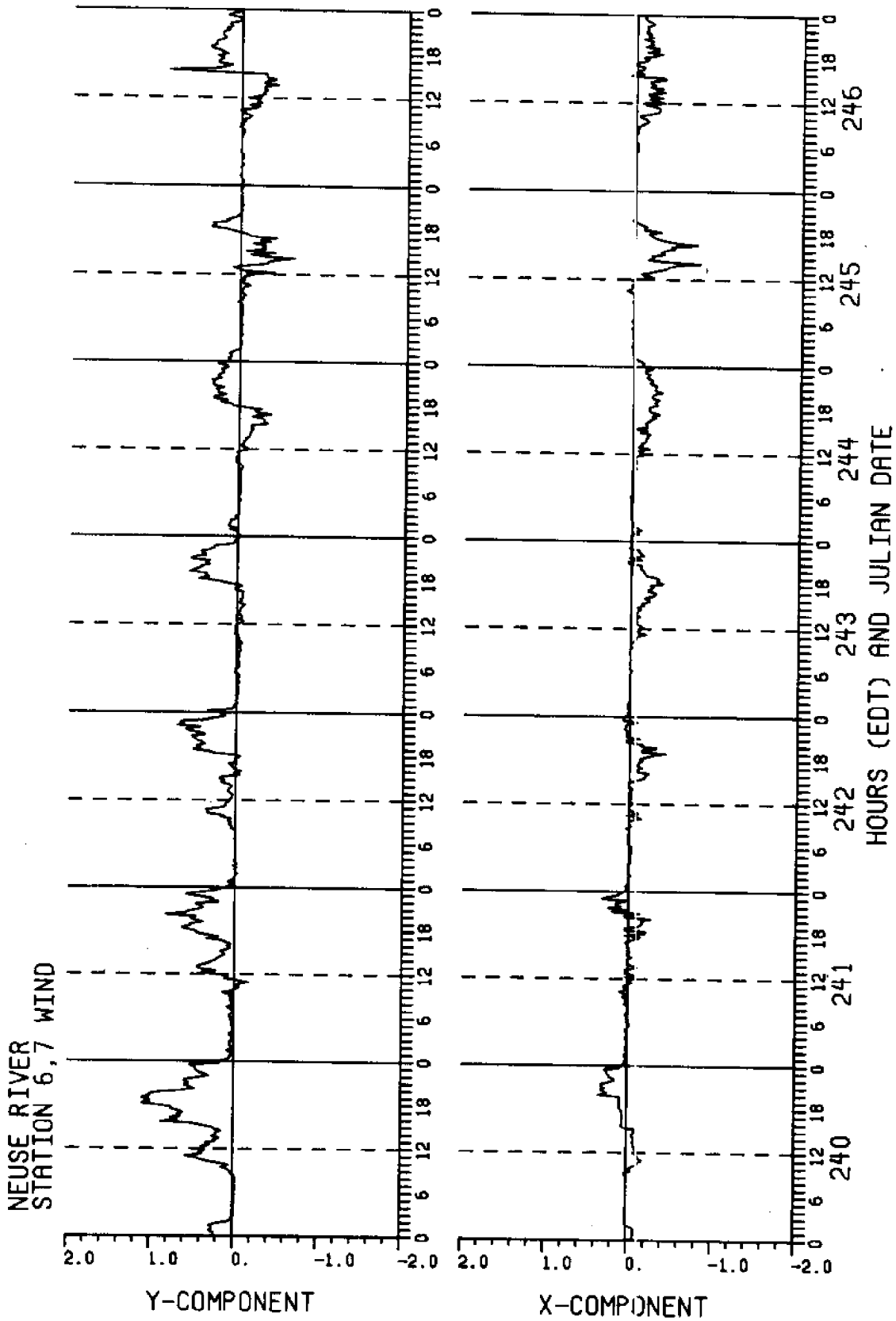


Figure B5

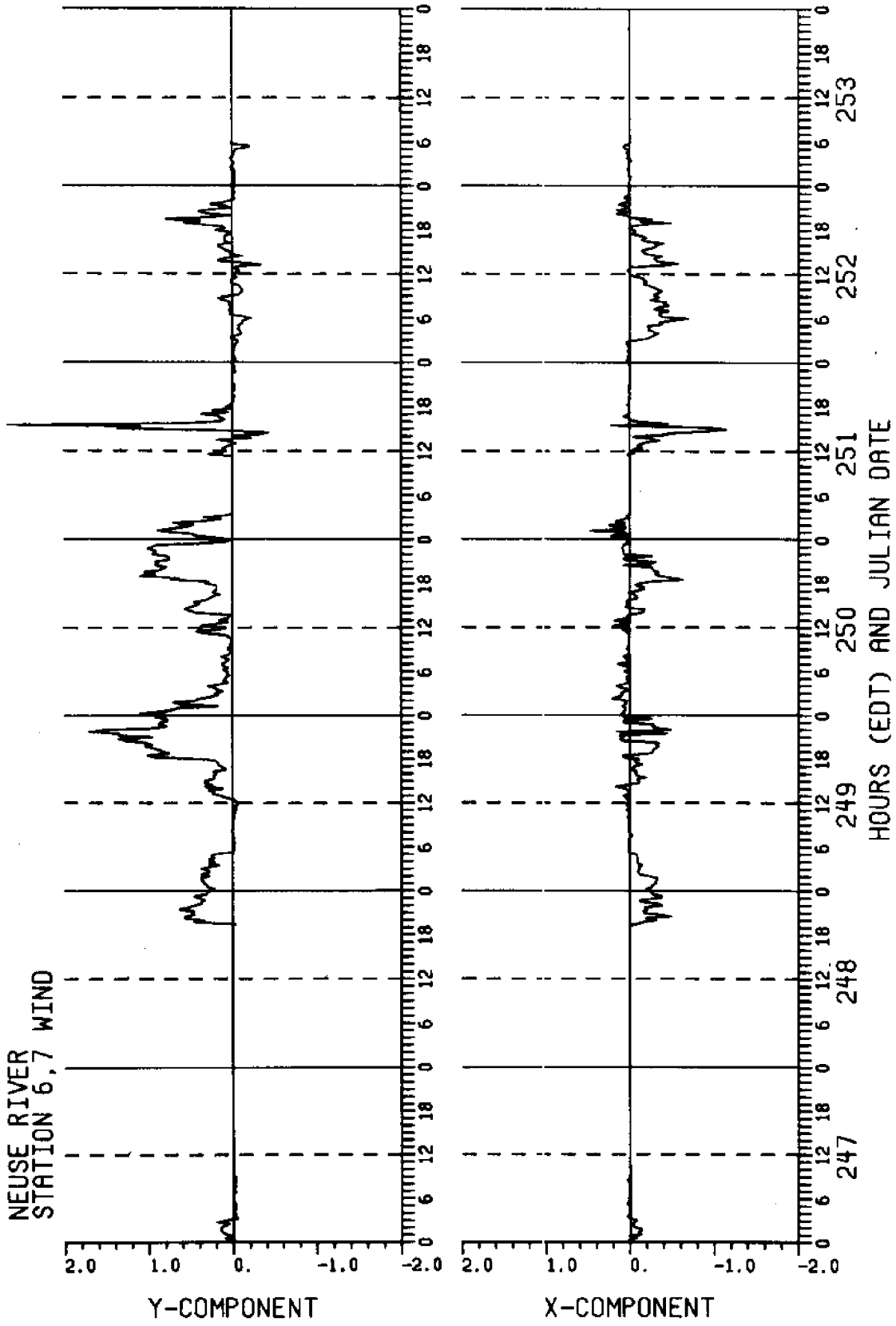
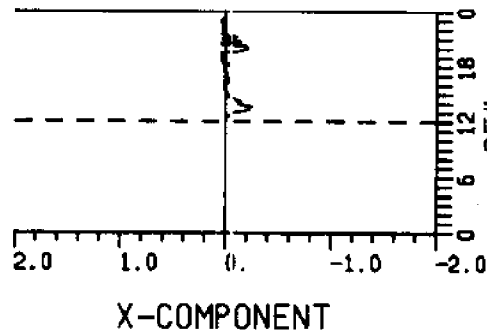
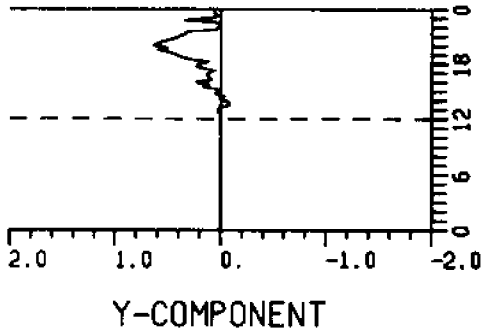


Figure B5

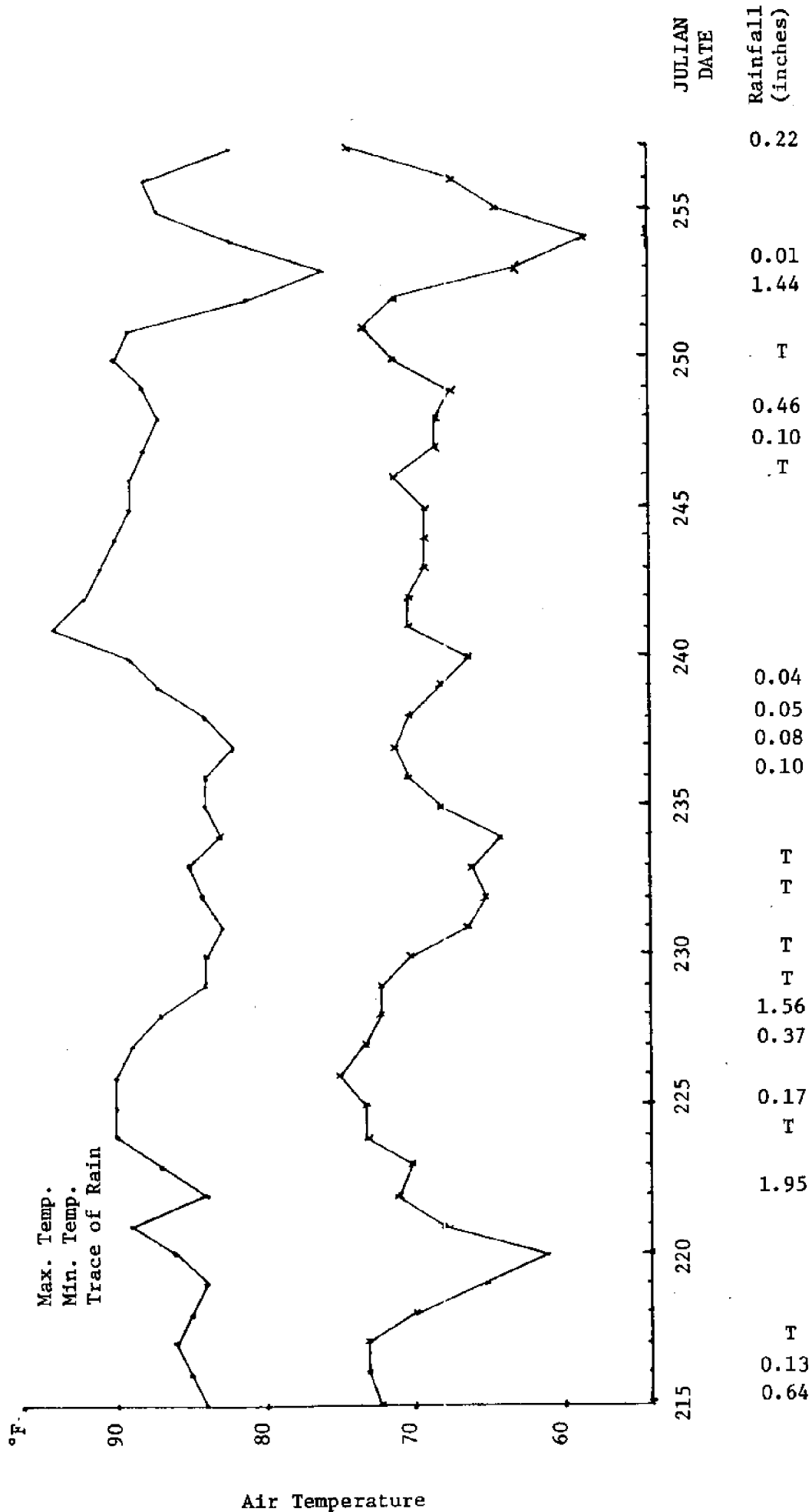
NEUSE RIVER
STATION 6, 7 WIND



254
HOURS (EDT) AND JULIAN DATE

Figure B5

Figure B6 Climatological Data, New Bern, N. C. (FAA), 1973. (From N. C. Summary, U. S. Weather Service, NOAA)



Appendix C. Computer Programs

The computer programs used to analyze the data in this study are as follows:

<u>Figure</u>	<u>Data Analyzed</u>	<u>Pages</u>
C1	River Flow	C-2 thru C-5
C2	Water Temperature	C-6 thru C-8
C3	Wind	C-9 thru C-12
C4	Power Spectral Density	C-13 thru C-15

All of these programs were run on the IBM 370/135 computer at the Triangle Universities Computation Center (TUCC), Research Triangle Park, North Carolina.

Figure C1. Computer program for the analysis of river flow data.

Figure C1. Computer program for the analysis of river flow data.


```

      IF(IHR.GE.2400) GO TO 41
      GO TO 42
41  IDTJ = IDTJ + 10000
      JD(JK) = JJ - 1
      JK = JK + 1
      IDT(JK) = IDTJ/10000
      IHR = IHR - 2400
      JJ = 1
C
42  CONTINUE
      MIN = DMIN
      IMN = IHR + MIN
      IRM(J) = IMN
      IHRM(J) = IDTJ + IMN
      DMIN = DMIN + DELT
      IF(J.EQ.NN) JD(JK)=JJ
      NANG = IANG(J) - IPHS
      IF(DEF(J).EQ.0.0) GO TO 31
      IF(IFG.EQ.1) XP = DEF(J)
      IF(IFG.EQ.1) GO TO 29
C
      CALCULATE VELOCITY FROM DEFLECTION ANGLE
C
      XP = A + B*DEF(J) + C*DEF(J)**2 + D*DEF(J)**3 + EE*DEF(J)**4
      + FF*DEF(J)**5 + G*DEF(J)**6
29  X(J) = XP
C
      GO TO 23
31  CONTINUE
      XP = 0.
      X(J) = XP
      IANG(J) = 999
23  CONTINUE
C
      CHANGE ANGLE TO RADIANS,REORIENT AXIS TO THAT OF CHANNEL AND
      BREAK VELOCITIES INTO WITH AND CROSS CURRENT COMPONENTS
C
      ANG = NANG/57.2957795
      ANG = ABS(ANG)
      AAX(J) = XP*SIN(ANG)
      AAY(J) = XP*COS(ANG)
      IF(NANG.LT.0) AAX(J) = -1.*AAX(J)
C
      JJ = JJ + 1
C
400 CONTINUE
      *****
C
      SMOOTH DATA WITH 1-2-1 FILTER
C
      DO 666 K=1,NN
C
      KM1 = K-1
      KP1 = K+1
      IF(K.EQ.1) GO TO 76
      IF(K.EQ.NN) GO TO 75
      AYY(K) = (AAY(KM1) + 2.*AAY(K) + AAY(KP1))/4.
      AXX(K) = (AAX(KM1) + 2.*AAX(K) + AAX(KP1))/4.
      GO TO 78
76  AYY(K) = (2.*AAY(K) + AAY(KP1))/3.
      AXX(K) = (2.*AAX(K) + AAX(KP1))/3.
      GO TO 79
75  AYY(K) = (2.*AAY(K) + AAY(KM1))/3.
      AXX(K) = (2.*AAX(K) + AAX(KM1))/3.
78  CONTINUE
      SUM = SUM + AXX(K)
666 CONTINUE
C
      SUM = SUM/AN
C
      WRITE(3,24) LOC,STA,DATE,SENSOR
      FORMAT(1H1,///,10X,'LOCATION: ',3A4,2X,'STATION: ',2A4,3X,'START DAT
24  IE: ',4A4,3X,'SENSOR NO.:',3A4,/)
      WRITE(3,61) JK,IPHS,NN
      FORMAT(1H,20X,'NUMBER DAYS DATA: ',I3,3X,'DOWNSTREAM CHANNEL ORIEN
61  TATION FROM MAG N: ',I4,'DEG. ',3X,'TOTAL NO. DATA PTS: ',I5)
C
      JR = 0
      LL = 0
      NM = 0
      SD = 0.
C
      *****
C
      DO 94 L=1,JK
C

```

Figure C1

```

LL = LL + 1
IF(L.GT.1) KZ=1
JO = JD(L)
C
WRITE(3,37) IDT(L),JD(L)
37 FORMAT(1H ,//,30X,'JULIAN DATE =',I3,5X,'NUMBER DATA POINTS THIS
IDATE:',I3,//,27X,'TIME',5X,'CM/S',6X,'FT/S',3X,'DIR',4X,'X-COM',
2 4X,'Y-COM',3X,'XF-COM',3X,'YF-COM',/)
C
DO 98 K=KZ,JO
C
NM = NM + 1
JR = JR + 1
AX(NM) = AXX(JR)
AY(NM) = AYY(JR)
AXF = AX(NM)/30.48
AYF = AY(NM)/30.48
XF = X(JR)/30.48
IHRM(NM) = IHRM(JR)
SD = SD + (AY(NM)-SUM)**2/AN
C
WRITE(3,38) K, IHRM(JR),X(JR),XF,IANG(JR),AX(NM),AY(NM),AXF,AYF
38 FORMAT(1H ,20X,I3,3X,I4,4X,F6.3,3X,F6.3,3X,I3,3X,F6.2,3X,F5.2,3X,
1 F6.2,3X,F6.2)
C
98 CONTINUE
C
WRITE DATA ON DISK IN 7 DAY SEQUENCES FOR PLOTTING
C
IF(LL.EQ.LP) GO TO 306
IF(L.EQ.JK) GO TO 306
GO TO 305
306 WRITE(2,49) NM,JDT
49 FORMAT(14,1X,I3)
WRITE(3,59) NM,JDT
59 FORMAT(1H1,2X,I4,1X,I3)
WRITE(2,40) (IHRM(K),AX(K),K=K7,NM)
WRITE(2,40) (IHRM(K),AY(K),K=KZ,NM)
40 FORMAT(5(17,1X,F6.2,1X))
WRITE(3,50) (IHRM(K),AX(K),K=KZ,NM)
WRITE(3,50) (IHRM(K),AY(K),K=KZ,NM)
50 FORMAT(1H ,5(1X,17,1X,F6.2))
LP = 7
JDT = JDT + LP
LL = 0
NM = 0
305 CONTINUE
94 CONTINUE
C
C -----
C
SD = SQRT(SD)
C
WRITE(3,77) SUM,SD
77 FORMAT(1H ,//,30X,'MEAN DOWNSTREAM VEL.',F6.2,1X,'CM/SEC',3X,
1 'STD.DEV.',E13.6)
C
DEBUG SUBCHK
STOP
END
//

```

Figure C1

Figure C2. Computer program for the analysis of water temperature data.


```

C      IF(IFG.EQ.1) ZF(J) = ZC(J)*1.8 + 32.
      IF(IFG.EQ.2) ZF(J) = ZC(J)*2.245
      SUM = SUM + ZF(J)
      JJ = JJ + 1
C
C 23 CONTINUE
C
      SUM = SUM/AN
      WRITE(3,24) LOC,STA,DATE,SENSOR
24  FORMAT(1H,///,10X,'LOCATION: ',3A4,2X,'STATION: ',2A4,3X,'START DAT
      IE: ',4A4,3X,'SENSOR NO.: ',3A4,/)
61  WRITE(3,61) JK,NM
      FORMAT(1H,30X,'NUMBER DAYS DATA: ',13,3X,'TOTAL NO. DATA PTS',15)
C
      JR = 0
      NM = 0
      LL = 0
      SD = 0.
C
      DO 94 L=1,JK
C
      IF(L.GT.1) KZ = 1
      LL = LL + 1
      JQ = JD(L)
      IF(IFG.EQ.1) WRITE(3,37) IDT(L),JD(L)
37  FORMAT(1H,///,30X,'JULIAN DATE = ',13,5X,'NUMBER DATA POINTS THIS
      IDATE: ',13,///,37X,'TIME',5X,'FAR',4X,'CEL',/)
      IF(IFG.EQ.2) WRITE(3,39) IDT(L),JD(L)
39  FORMAT(1H,///,30X,'JULIAN DATE = ',13,5X,'NUMBER DATA POINTS THIS
      IDATE: ',13,///,37X,'TIME',5X,'FT',4X,'PSI',/)
C
      DO 98 K=KZ,JQ
C
      NM = NM + 1
      JR = JR + 1
      DIF = ZF(JR) - SUM
      SD = SD + DIF**2/AN
      XP(NM) = ZF(JR)
      JHRM(NM) = IHRM(JR)
C
      WRITE(3,38) K,IRM(JR),ZF(JR),ZC(JR),DIF
38  FORMAT(1H,30X,13,3X,14,4X,F4.1,3X,F4.1,7X,F5.1)
C
C 98 CONTINUE
      WRITE DATA ON DISK IN 7 DAY SEQUENCES FOR PLOTTING
C
      IF(L.EQ. JK) GO TO 306
      IF(LL.EQ. LP) GO TO 306
      GO TO 305
306  WRITE(3,59) NM,JDT
59  FORMAT(1H,2X,14,1X,13)
      WRITE(2,49) NM,JDT
49  FORMAT(14,1X,13)
      WRITE(3,50) (JHRM(K),XP(K),K=KZ,NM)
50  FORMAT(1H,5(1X,17,1X,F6.2))
      WRITE(2,40) (JHRM(K),XP(K),K=KZ,NM)
40  FORMAT(5(17,1X,F6.2,1X))
      LP = 7
      JDT = JDT + LP
      LL = 0
      NM = 0
305  CONTINUE
94  CONTINUE
C
      SD = SQRT(SD)
C
      WRITE(3,77) SUM,SD
77  FORMAT(1H,///,25X,'MEAN TEMP OR TIDAL HT.',F6.2,'DEG F OR FT',3X,
      1 'STD.DEV.',F13.6)
C
      STOP
      END
//

```

Figure C2

Figure C3. Computer program for the analysis of wind data.

```

C      LUC          LOCATION OF INSTRUMENTS
C      STA          STATION NO.
C      DATE        MONTH, DAY AND YEAR OF FIRST DAYS DATA FOR THIS
C                  DATA SET
C      SENSOR      INTERNAL SENSOR NO.
C      X(J)        WIND STRESS
C      AYY(J)      Y-COMP(WITH CURRENT) OF X(J), PCS DOWNSTREAM
C      AXX(J)      X-COMP(ACROSS CURRENT) OF X(J), POS TO RIGHT
C      IANG(J)     WIND DIRECTION IN DEGREES MAGNETIC
C      VEL(J)      WIND SPEED IN CM/SEC
C      LP          FLAG FOR WRITING PLOTTING SEQUENCES INTO 7-DAY
C                  INCREMENTS
C      NN          TOTAL NO. OF DATA PTS IN DATA SET
C      DELT        TIME INCREMENT IN MINUTES
C      JK          COUNTER FOR # DAYS DATA
C      JJ          COUNTER OF # DATA PTS FOR EACH DAY
C      JR          COUNTER FROM 1 TO NN
C      IOTJ        7 DIGIT NUMBER OF JULIAN DATE WITH LAST 4 DIGITS
C                  FOR ADDITION OF TIME
C      IHR         4 DIGIT NUMBER OF HOURS
C      DMIN,MIN    2 DIGIT NUMBER OF MINUTES
C      IDT(J)      JULIAN DATE
C      IRM(J)      IHR + MIN
C      IHRM(J)     IDTJ + IRM(J)
C      IFLG        IFLG = 1, SPEED OK; IFLG = 2, SPEED HIGH, REDUCE
C      IPHS        CHANNEL ORIENTATION AXIS
C      CD          DRAG COEFFICIENT
C      RHO         AIR DENSITY
C      JDT         JULIAN START DATE FOR FIRST DATA PLOT
C      JD(L)       # DATA PTS PER DAY
C      AX(NM)      VALUES OF AXX(J) IN 7 DAY INCREMENTS
C      AY(NM)      VALUES OF AYY(J) IN 7 DAY INCREMENTS
C      NM          COUNTER FOR # POINTS IN 7 DAY INCREMENTS
C      LL          COUNTER FOR # DAYS IN 7 DAY INCREMENTS
C
C      PROGRAM TO CALCULATE JULIAN DATE AND TIME FOR EACH WIND DATA
C      POINT GIVEN THE TIME INCREMENT (DELT), AND START TIME & DATE.
C      CALCULATE THE WIND STRESS AND BREAK IT INTO ITS X- AND Y-
C      COMPONENTS
C
C      DIMENSION X(3650), IANG(3650), VEL(3650), IDT(120), JD(40), IRM(3650)
C      DIMENSION LOC(3), STA(2), DATE(4), SENSOR(3), AX(700), AY(700)
C      DIMENSION AXX(3650), AYY(3650), IHRM(3650)
C      DOUBLE PRECISION X, VEL
C
C      IPHS = 45
C      KZ = 1
C      IDT(1) = 237
C      IOTJ = IDT(1)*1.E4
C      NN = 1672
C      IHR = 1400
C      DMIN = 0.
C      JDT = 233
C      LP = 3
C      IFLG = 2
C      JJ = 1
C      JK = 1
C      DELT = 15.
C      CD = 2.5E-2
C      RHO = 1.28E-3
C      CONST = RHO*CD
C      AN = NN
C
C      READ(1,20) LOC, STA, DATE, SENSOR
20  FORMAT(3A4, 2A4, 4A4, 3A4)
C      READ(1,22) (VEL(K), IANG(K), K=1, NN)
22  FORMAT(11(1X, F2.0, 1X, I3))
C
C      IF(IFLG.EQ.1) GO TO 21
C
C      DO 71 L=1, NN
C
C      IF(VEL(L).EQ.0.) GO TO 19
C      VEL(L) = 1.5 + .2916667*VEL(L)
18  CONTINUE
71  CONTINUE
C
C      *****
C
21  SUM = 0.
C
C      DO 400 J=1, NN
C
C      CALCULATE TIME INTERVAL
C
C      IF(DMIN.GE.60.) IHR = IHR + 100
C      IF(DMIN.GE.60.) DMIN = DMIN - 60.

```

```

IF(IHR.GE.2400) GO TO 41
GO TO 42
41 IDTJ = IDTJ + 10000
   JD(JK) = JJ - 1
   JK = JK + 1
   IDT(JK) = IDTJ/10000
   IHR = IHR - 2400
   JJ = 1
C
42 CONTINUE
   MIN = DMIN
   IMN = IHR + MIN
   IRN(J) = IMN
   IHRM(J) = IDTJ + IMN
   DMIN = DMIN + DELT
   IF(J.EQ.NN) JD(JK) = JJ
   NANG = IANG(J) - IPHS
   IF(VEL(J).EQ.0.0) GO TO 31
C
C
C   CALCULATE WIND STRESS FROM WIND VELOCITY
C
   VEL(J) = 44.7*VEL(J)
   XP = CUNST*VEL(J)**2
29  X(J) = XP
C
   GO TO 23
31 CONTINUE
   XP = 0.
   X(J) = XP
   IANG(J) = 999
23  CONTINUE
C
C
C   CHANGE ANGLE TO RADIANS, REORIENT AXIS TO THAT OF CHANNEL AND
C   BREAK WIND STRESS INTO WITH AND CROSS CURRENT COMPONENTS AND
C   MULTIPLY BY -1 TO GIVE WIND COMPONENTS THE RIGHT SIGN FOR
C   PLOTTING
C
   ANG = NANG/57.2957795
   ANG = ABS(ANG)
   AYY(J) = XP*COS(ANG)
   AXX(J) = XP*SIN(ANG)
   IF(NANG.LT.0) AXX(J) = -1.*AXX(J)
   AXX(J) = -1.*AXX(J)
   AYY(J) = -1.*AYY(J)
C
   JJ = JJ + 1
C
400 CONTINUE
C
C *****
C
24  WRITE(3,24) LOC,STA,DATE,SENSOR
   FORMAT(1H1,///,10X,'LOCATION:',3A4,2X,'STATION:',2A4,3X,'START DAT
|E:',4A4,3X,'SENSOR NO.:',3A4,/)
61  WRITE(3,61) JK,IPHS,NN
   FORMAT(1H ,20X,'NUMBER DAYS DATA:',13,3X,'DOWNSTREAM CHANNEL ORIEN
|TATION FROM MAG N:',14,'DEG.',3X,'TOTAL NO. DATA PTS:',15)
C
   JR = 0
   LL = 0
   NM = 0
C
C
C *****
C
   DO 94 L=1,JK
C
   LL = LL + 1
   IF(L.GT.1) KZ=1
   JQ = JD(L)
C
37  WRITE(3,37) (DT(L),JD(L)
   FORMAT(1H ,//,30X,'JULIAN DATE =',13,5X,'NUMBER DATA POINTS THIS D
|ATE:',13,//,27X,'TIME',5X,'CM/S',6X,'DIR ',3X,'TAU',4X,'X-COM',
2  4X,'Y-COM',3X,/)
C
   DO 98 K=KZ,JQ
C
   NM = NM + 1
   JR = JR + 1
   AX(NM) = AXX(JR)
   AY(NM) = AYY(JR)
   IHRM(NM) = IHRM(JR)
C
38  WRITE(3,38) K,IRM(JR),VEL(JR),IANG(JR),X(JR),AX(NM),AY(NM)
   FORMAT(1H ,20X,13,3X,14,4X,F6.2,3X,13,3X,F6.2,3X,F6.2,3X,F6.2)
C
98  CONTINUE
C
C   WRITE DATA ON DISK IN 7 DAY SEQUENCES FOR PLOTTING

```

Figure C3


```

C      IF(L.EQ.JK) GO TO 306
      IF(LL.EQ.LP) GO TO 306
      GO TO 305
306    WRITE(2,49) NM,JDT
49     FORMAT(14,1X,13)
      WRITE(3,59) NM,JDT
59     FORMAT(11H1,2X,14,1X,13)
      WRITE(2,40) (IHRM(K),AY(K),K=KZ,NM)
      WRITE(2,40) (IHRM(K),AX(K),K=KZ,NM)
40     FORMAT(5(I7,1X,F6.2,1X))
      WRITE(3,50)(IHRM(K),AY(K),K=KZ,NM)
      WRITE(3,50)(IHRM(K),AX(K),K=KZ,NM)
50     FORMAT(1H ,5(1X,I7,1X,F6.2))
      LP = 7
      JDT = JDT + LP
      LL = 0
      NM = 0
305    CONTINUE
94     CONTINUE

C
C .....
C
      STOP
      END

/*
//
//

```

Figure C3

Figure C4. Computer program to compute the power spectral density function.

```

C      X(K)          X-COMPONENT RIVER FLOW IN BLOCKS OF 7 DAYS
C      Y(K)          Y-COMPONENT RIVER FLOW IN BLOCKS OF 7 DAYS
C      Z(J)          X-COMPONENT * TOTAL TIME SEQUENCE
C      ITM(K)        TIMES
C      XS(N)         SINE TRANSFORM OF Z(J)
C      XC(N)         COSINE TRANSFORM OF Z(J)
C      AMP(N)        POWER SPECTRAL DENSITY FUNCTION
C      R(N)          AMP(N) SMOOTHED WITH HANNING FILTER
C      C(J)          COSINE TABLE FOR USE IN TRANSFORM PROGRAM
C      S(J)          SINE TABLE FOR USE IN TRANSFORM PROGRAM
C      AKK(N)        FREQUENCIES
C      AJJ(N)        PERIODS(1/AKK(N))
C      NR            START POINT FOR PUNCHING TRANSFORM ON CARDS
C      JQ            # FREQ. VALUES CALCULATED
C      NQ            END POINT FOR WRITING TRANSFORM ON CARDS
C      DELT          TIME INTERVAL OF TIME SERIES
C      NL            COUNTER TO OBTAIN Z(J)
C
C      THIS PROGRAM WILL CALCULATE THE POWER SPECTRAL DENSITY FUNCTION
C      AND SMOOTH IT WITH A HANNING FILTER.
C
C      DIMENSION X(850),Z(3700),ITM(850),XS(1900),XC(1900),R(1900),
1      C(3700),S(3700),AMP(1900),TITLE(16),AKK(1900),AJJ(1900),Y(800)
C
C      NR = 12
C      JQ = 200
C      AJ = JQ
C      NQ = 90 + NR
C      NZ = 6
C      DELT = 14.495057
C      DELT = DELT/60.
C      NL = 0
C      READ(1,49) TITLE
49      FORMAT(16A4)
C      WRITE(3,50) TITLE
50      FORMAT(1H1,10X,16A4,/)
C      WRITE(2,61) TITLE
61      FORMAT(3X,16A4)
C
C      DO 40 J=1,NZ
C
C      READ(9,44) NN,JDT
44      FORMAT(14,1X,13)
C      READ(9,45) (ITM(K),Y(K),K=1,NN)
C      READ(9,45) (ITM(K),X(K),K=1,NN)
45      FORMAT(5(17,1X,F6.2,1X))
C
C      DO 60 L=1,NN
C
C      NL = NL + 1
C      Z(NL) = X(L)
60      CONTINUE
40      CONTINUE
C
C      CALCULATE FREQUENCY INTERVAL AND ASSIGN FREQUENCY VALUES
C      FOR ALL OF FREQUENCY SEQUENCE
C
C      AL = NL
C      DELF = 1./(DELT*AL)
C      NML = NL - 1
C
C      DO 11 N=2,JQ
C      AQ = N-1
C      AKK(N) = AQ*DELF
11      AJJ(N) = 1./AKK(N)
C      AJJ(1) = 0.
C      AKK(1) = 0.
C
C      CALL FOURK(Z,C,S,XS,XC,NML,JQ)
C
C      DO 12 N=1,JQ
C      AMP(N) = XS(N)**2 + XC(N)**2
12      CONTINUE
C
C      DO 79 N=1,JQ
C
C      NP1 = N + 1
C      NM1 = N - 1
C
C      IF(N.EQ.1) R(N) = .5*AMP(N) + .5*AMP(NP1)
C      IF(N.EQ.JQ) R(N) = .5*AMP(NM1) + .5*AMP(N)
C      IF(N.EQ.1) GO TO 76
C      IF(N.EQ.JQ) GO TO 76
C      R(N) = .25*AMP(NM1) + .5*AMP(N) + .25*AMP(NP1)
76      CONTINUE
79      CONTINUE

```

```

C
WRITE(3,51)
51 FORMAT(1H ,//,10X,'POWER SPECTRUM',//)
WRITE(3,77) JQ,DELF,NL
77 FORMAT(1H ,10X,'JQ=',I4,4X,'FREQ. INTERVAL=',F7.4,1X,'CYCLES/HR',
1 3X,'NL = ',I4,/)
C
WRITE(3,21) (AKK(N),AJJ(N),R(N),AMP(N),N=1,JQ)
21 FORMAT(1H ,3(1X,F7.4,1X,F8.4,1X,F10.4,1X,F10.4))
WRITE(2,89) (AJJ(N),R(N),N=NR,NQ)
89 FORMAT(4(F7.3,1X,F10.4,1X))
C
STOP
END
SUBROUTINE FOURK(XIN,C,S,XSIN,XCOS,NL,JQ)
DOUBLE PRECISION DTH,SUM,RUM,ARG,SUM1,PI
DIMENSION XIN(1),C(1),S(1),XSIN(1),XCOS(1)
C
C
C THIS SUBROUTINE WILL TAKE SINE AND COSINE TRANSFORM OF INPUT XIN
C
PI = 3.141592653589793
PNL = NL
NLN = NL + 1
DTH = 2.*PI/PNL
CONST = 2./PNL
C
C SINES AND COSINES
C
DO 1 J=1,NL
AJ = J-1
ARG = AJ*DTH
C(J) = DCOS(ARG)
S(J) = DSIN(ARG)
1 CONTINUE
C
C FOR ZERO FREQ
C
SUM1 = 0.
DO 33 K=1,NLN
33 SUM1 = SUM1 + DBLE(XIN(K))
XCOS(1) = SUM1*CONST/2.
XSIN(1) = 0.
C
DO 35 N=2,JQ
C
C
C SUM PRODUCTS XIN*COS(ARG) AND XIN*SIN(ARG)
C
SUM = 0.0
RUM = 0.0
NN = 1
C
DO 79 J = 1,NLN
IF(NN-NL) 70,70,72
72 NN = NN - NL
C
70 SUM = SUM + DBLE(XIN(J))*C(NN)
RUM = RUM + DBLE(XIN(J))*S(NN)
NN = NN + (N-1)
C
79 CONTINUE
C
XCOS(N) = SUM*CONST
XSIN(N) = RUM*CONST
C
35 CONTINUE
C
C
RETURN
END
/*
//

```

Appendix D. River Flow Data

Included in this appendix are the time history plots of the up-stream, down-stream (Y), and cross-stream (X) components of river flow. The list below includes the Figure no., the channel axis orientation (in deg. mag.) used to calculate the components, the Station no. and the page numbers of each plot.

<u>Figure</u>	<u>Channel Axis</u>	<u>Station Number</u>	<u>Pages</u>
D1	145°	1 Bottom	D-2 thru D-8
D2	105°	2 Top	D-9 thru D-15
D3	105°	2 Bottom	D-16 thru D-19
D4	105°	3 Bottom	D-20 thru D-26
D5	045°	4 Top	D-27 thru D-33
D6	045°	4 Bottom	D-34 thru D-40
D7	045°	5 Bottom	D-41 thru D-47
D8	040°	6 Bottom	D-48 thru D-53
D9	040°	7 Bottom	D-54 thru D-58

The ordinate in all figures and for both components show current flow in cm/sec [Y > 0 down-stream Y < 0 up-stream; X > 0 to right of channel axis; X < 0 to left of channel axis]; the abscissa shows time (Julian Date and hour (EDT)).

Figure D1. River flow at Station 1 Bottom, with channel axis of 145° mag.

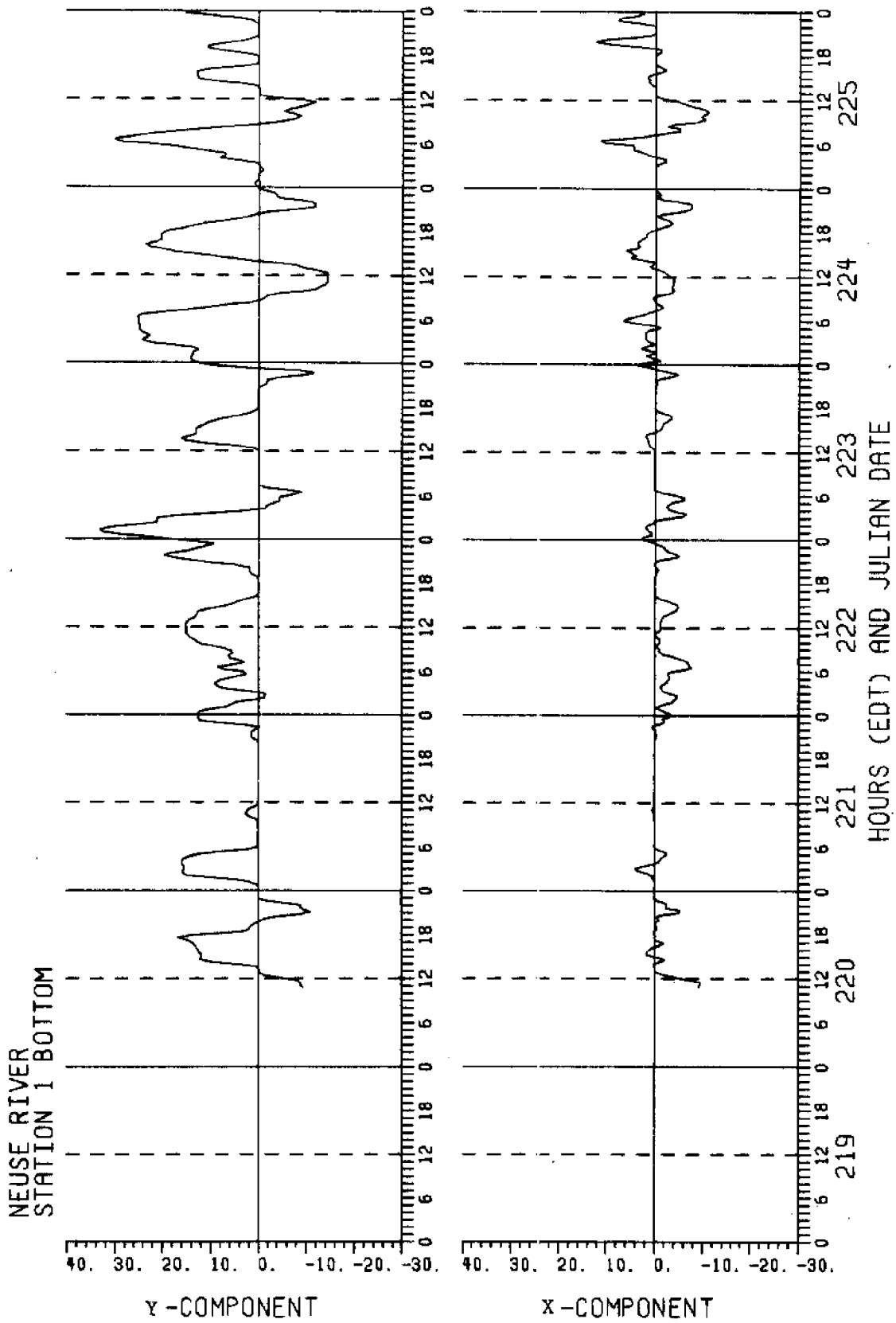


Figure D1

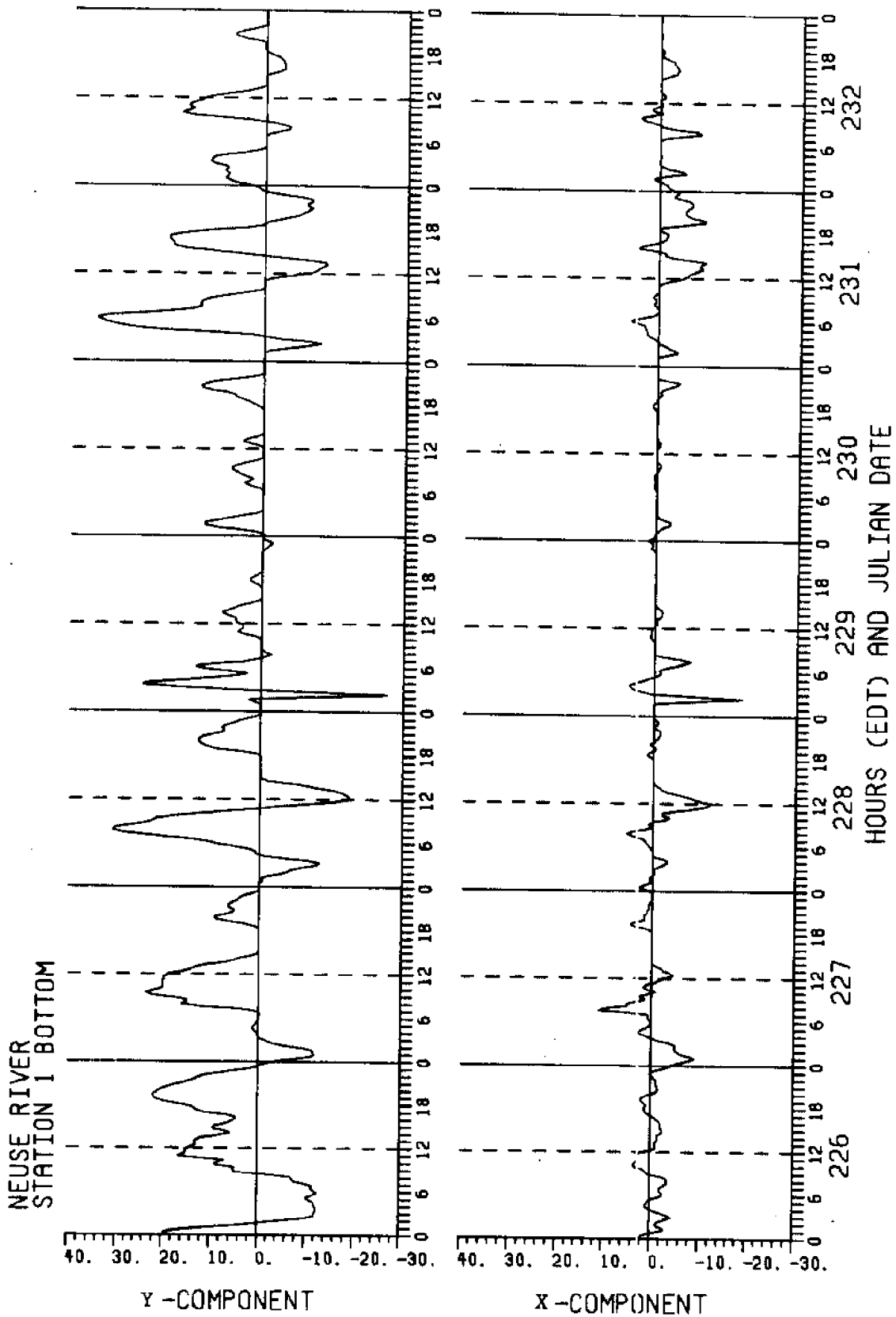


Figure D1

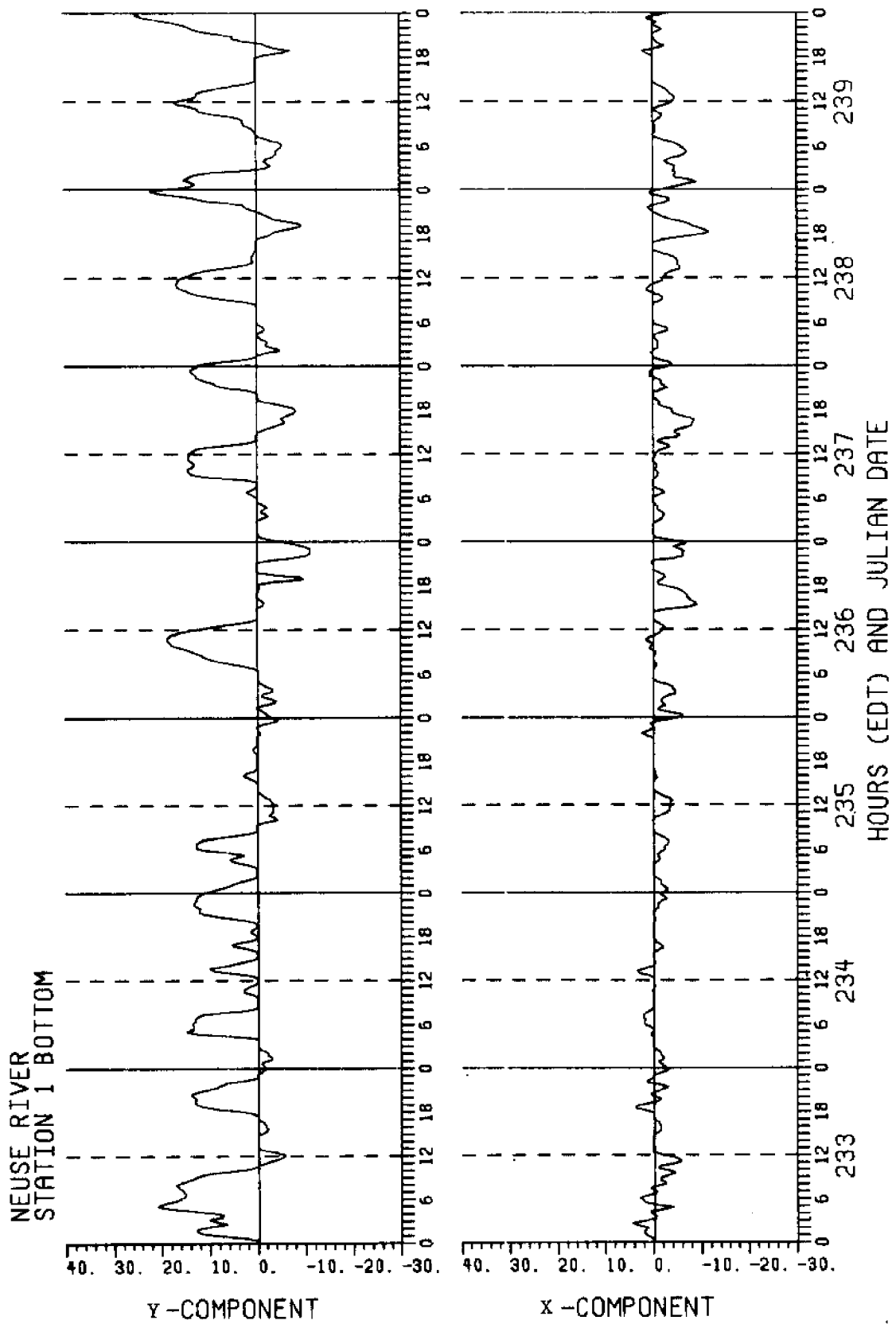


Figure D1

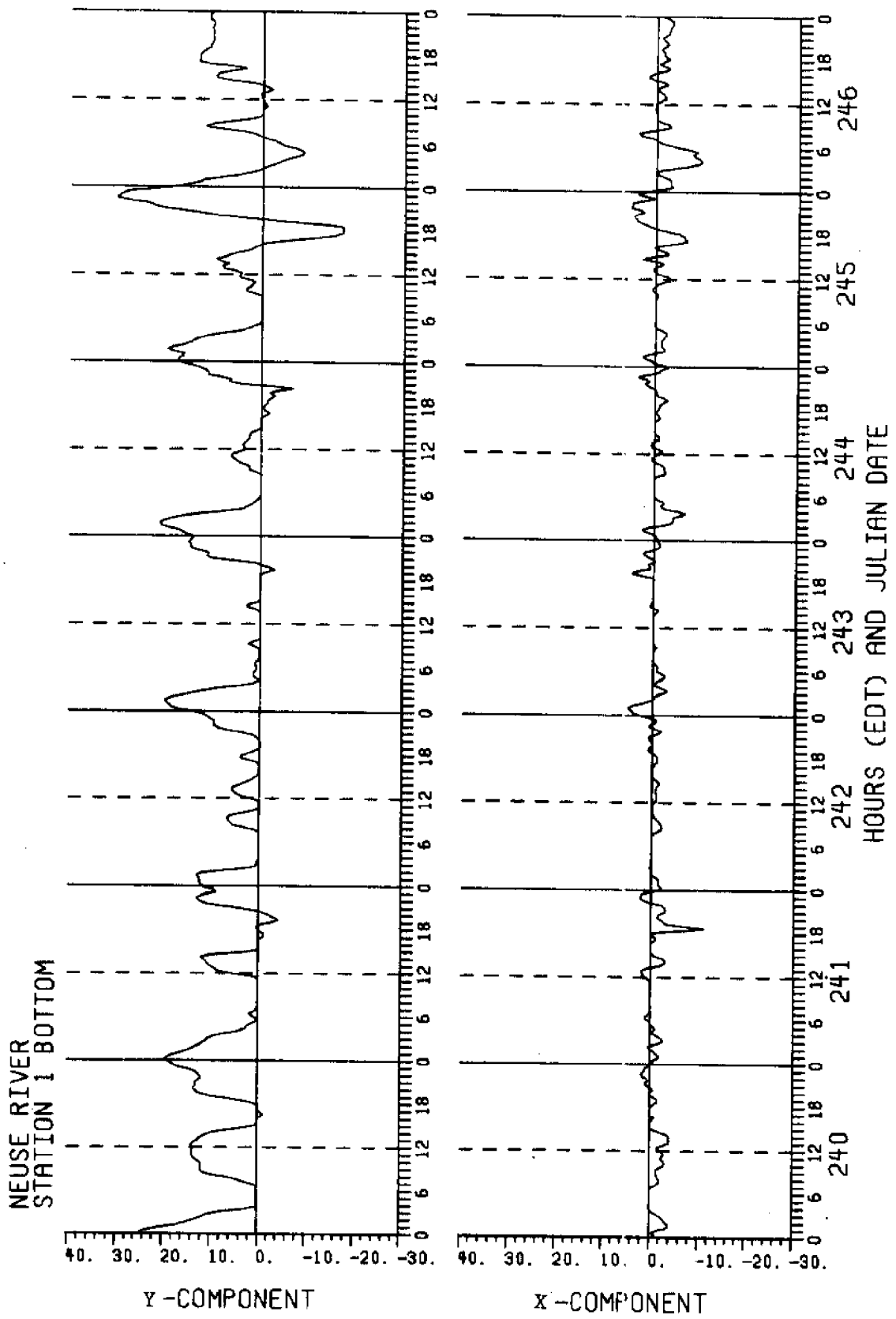


Figure D1

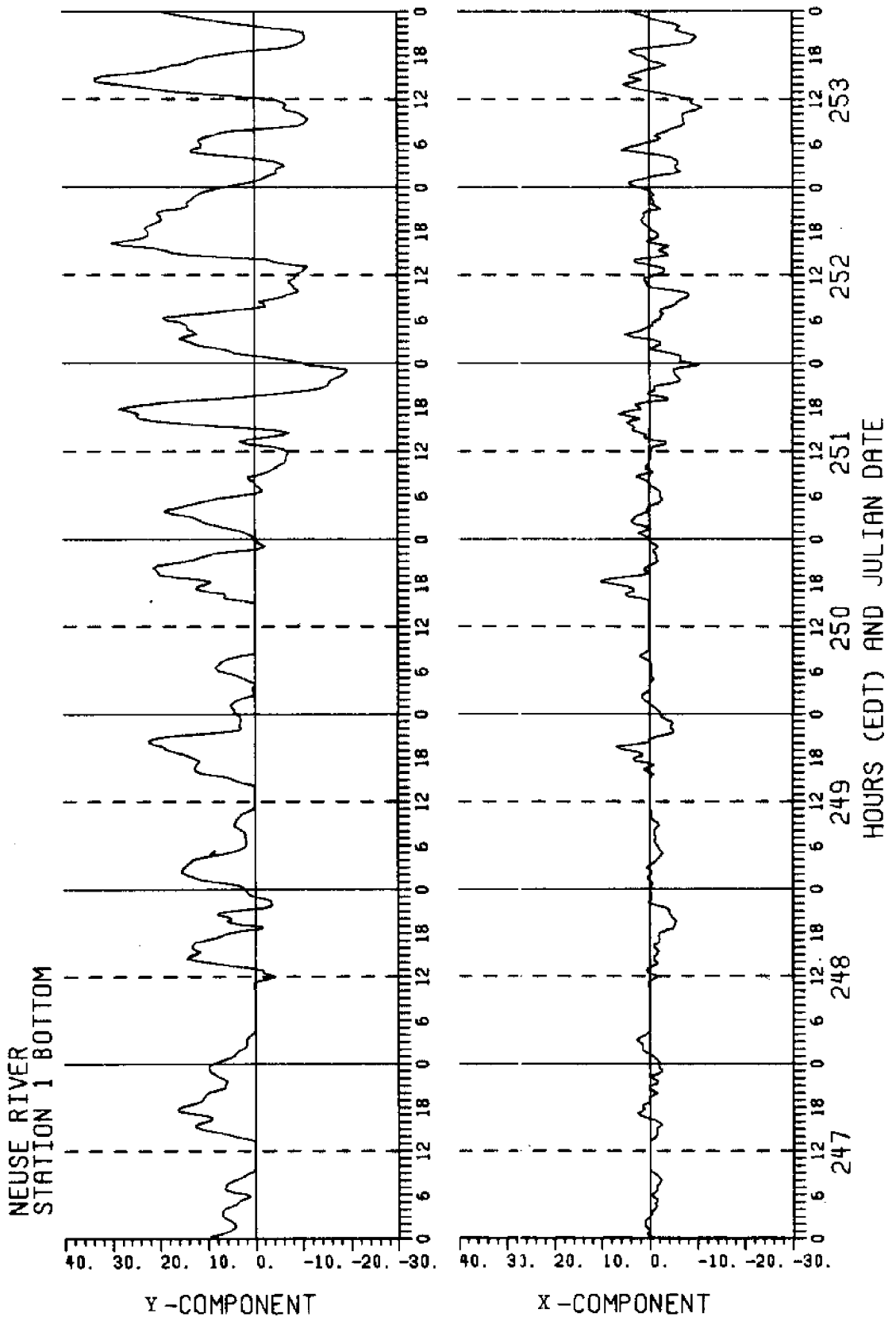


Figure D1

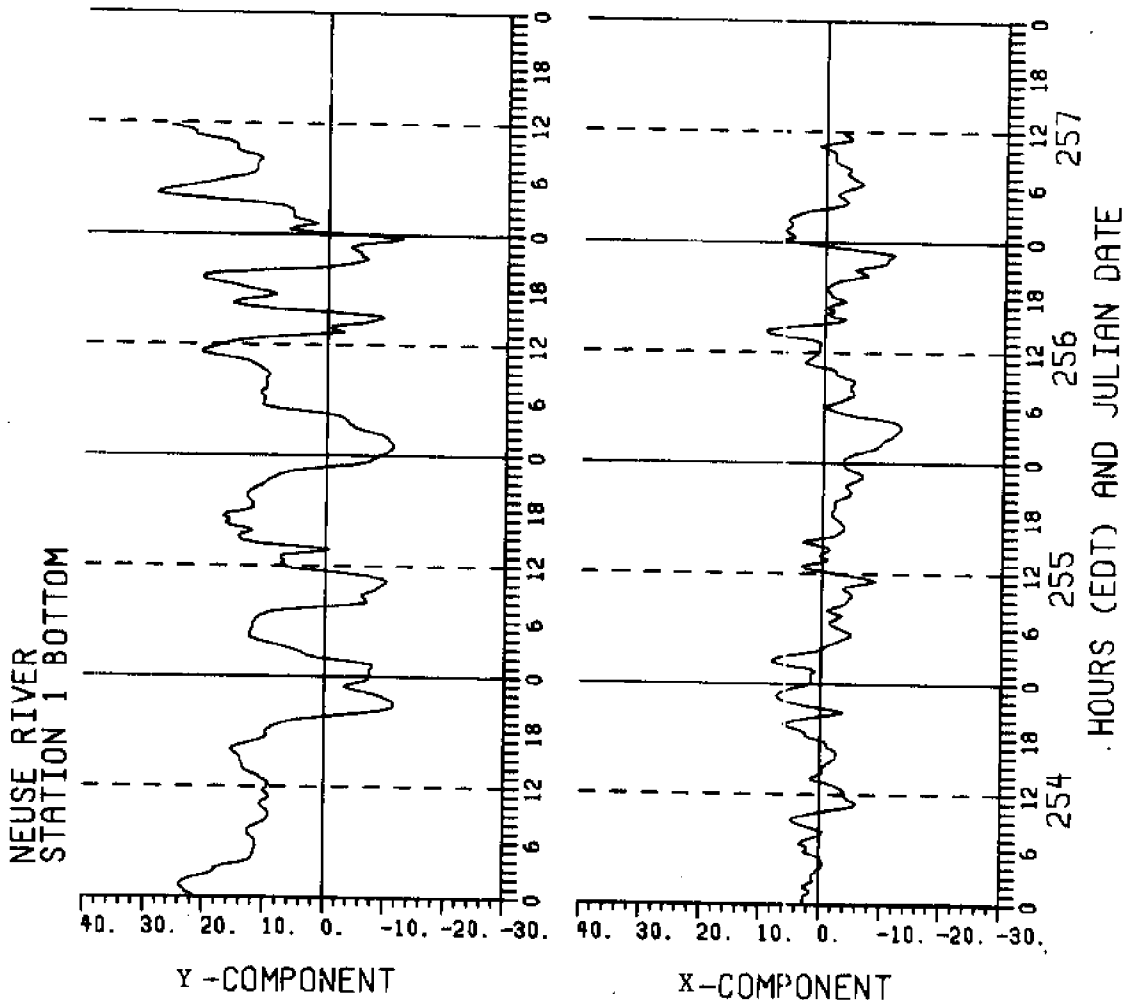


Figure D1

Figure D2. River flow at Station 2 Top, with channel axis of 105° mag.

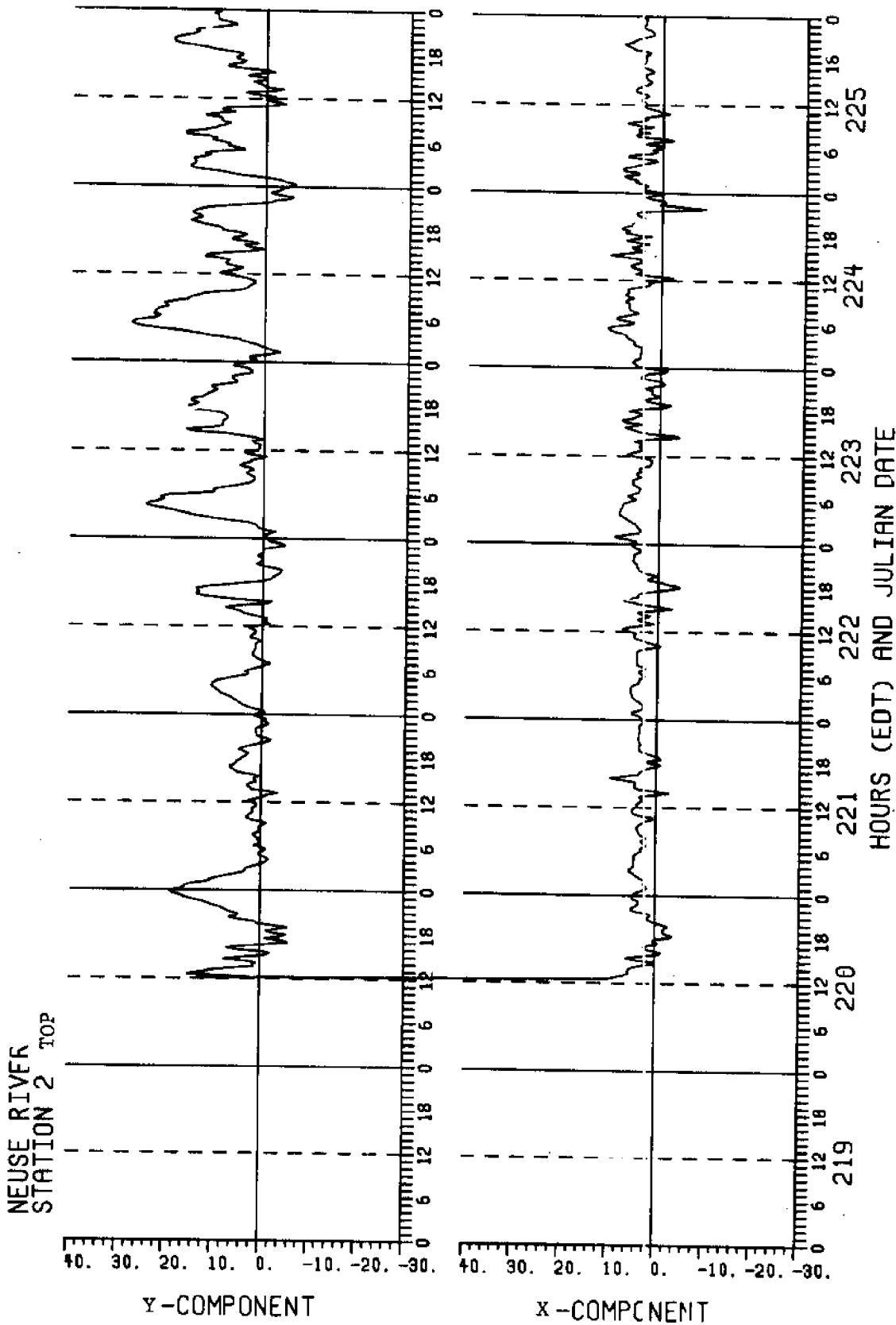


Figure D2

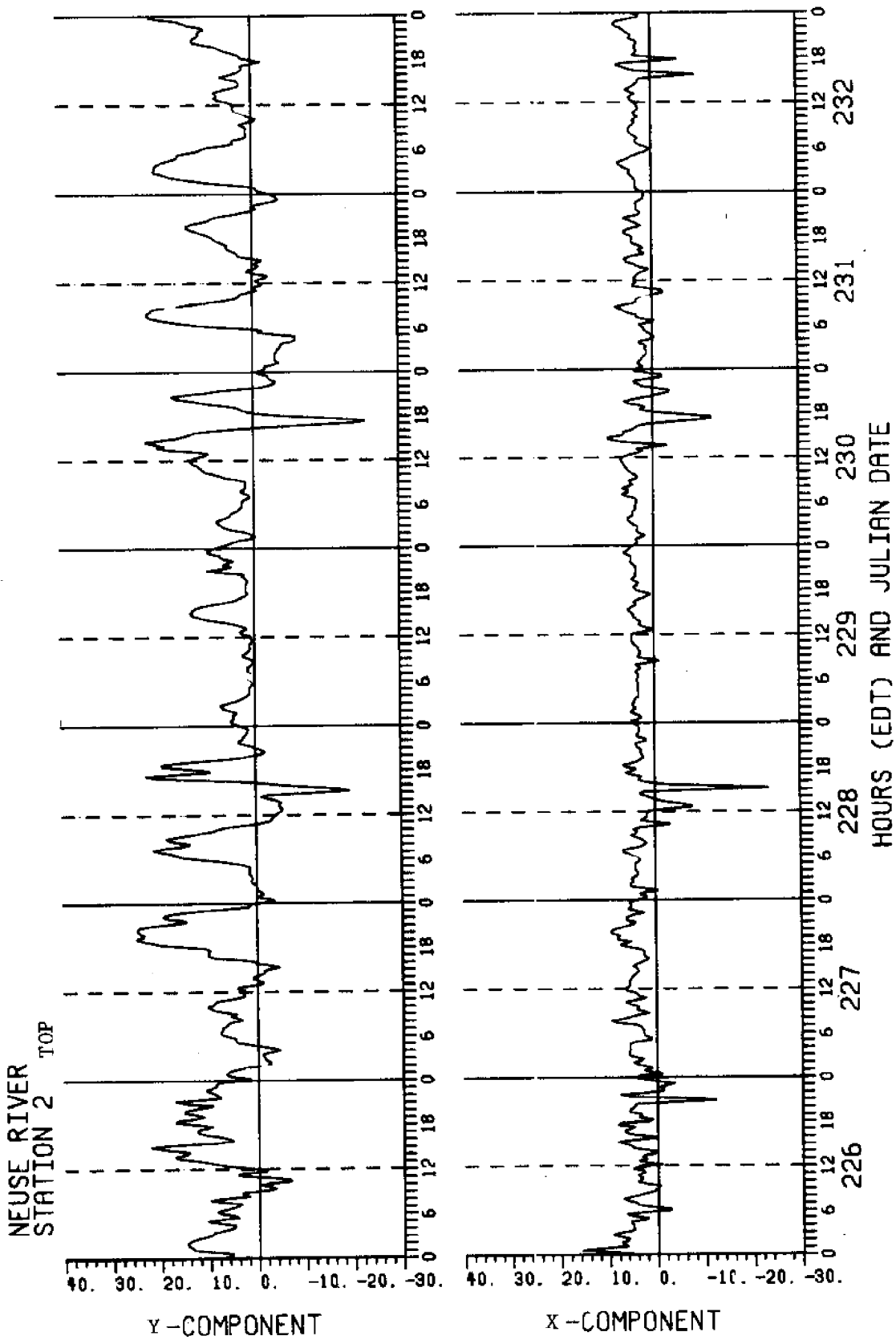


Figure D2

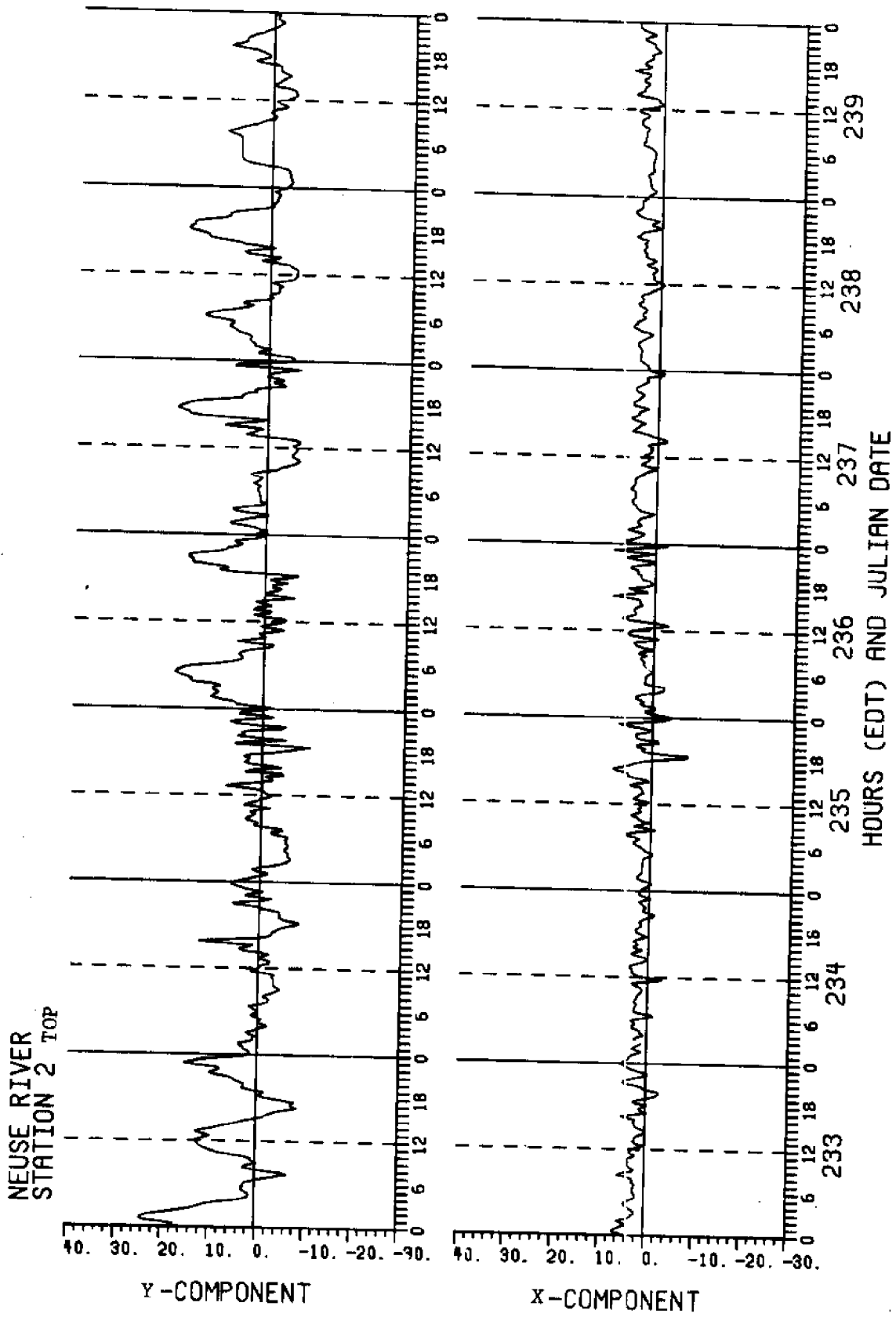


Figure D2

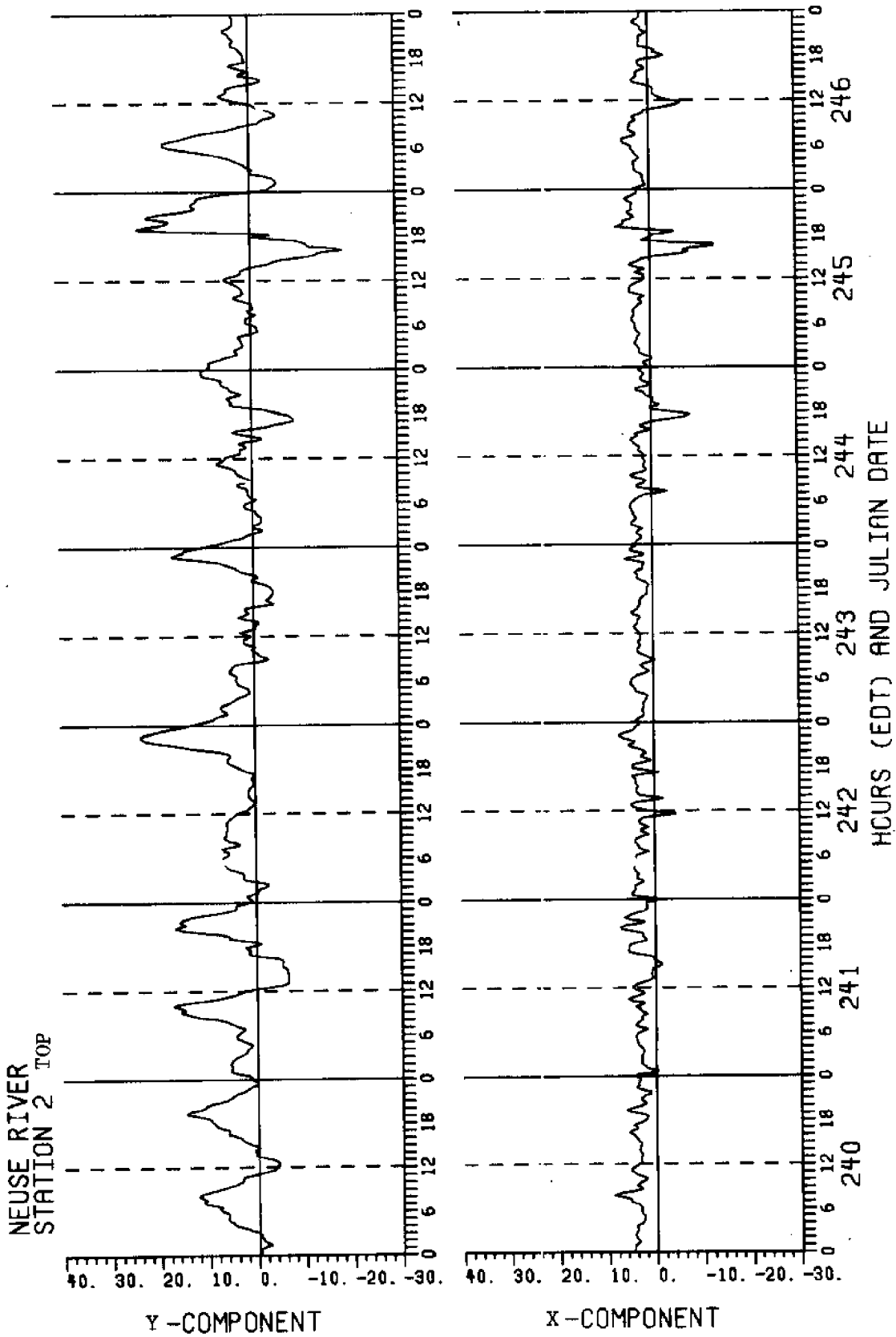


Figure D2

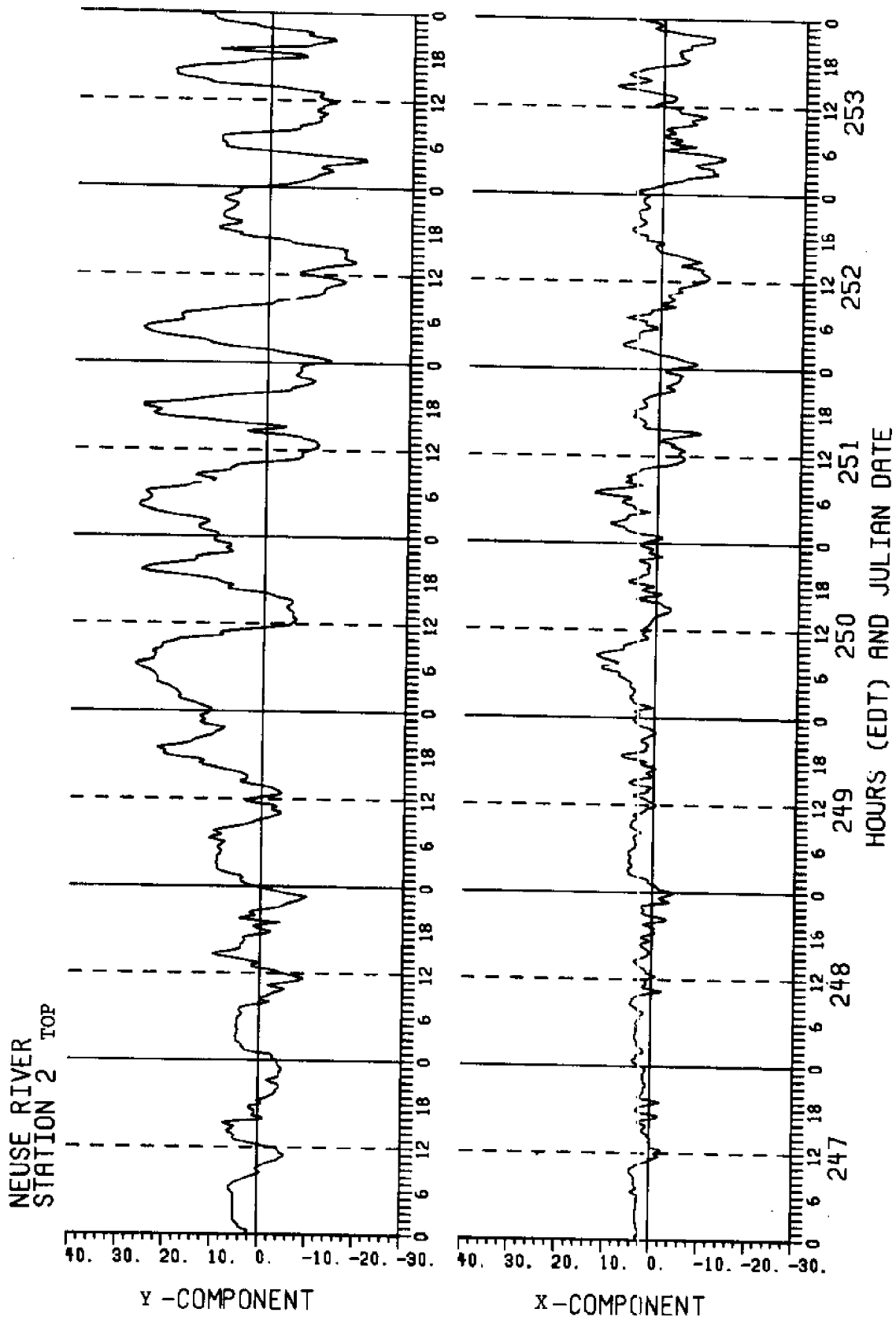


Figure D2

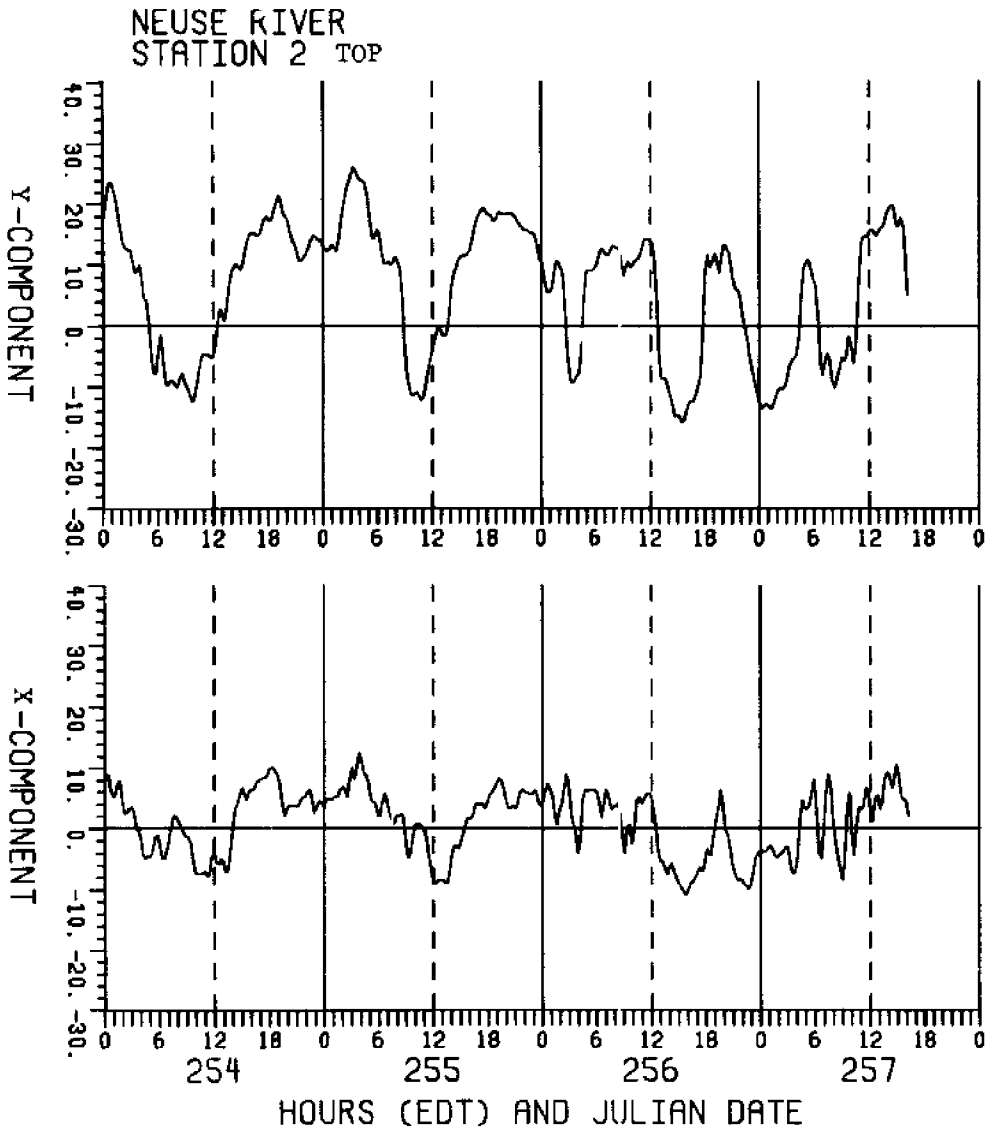


Figure D2

Figure D3. River flow at Station 2 Bottom, with channel axis of 105° mag.

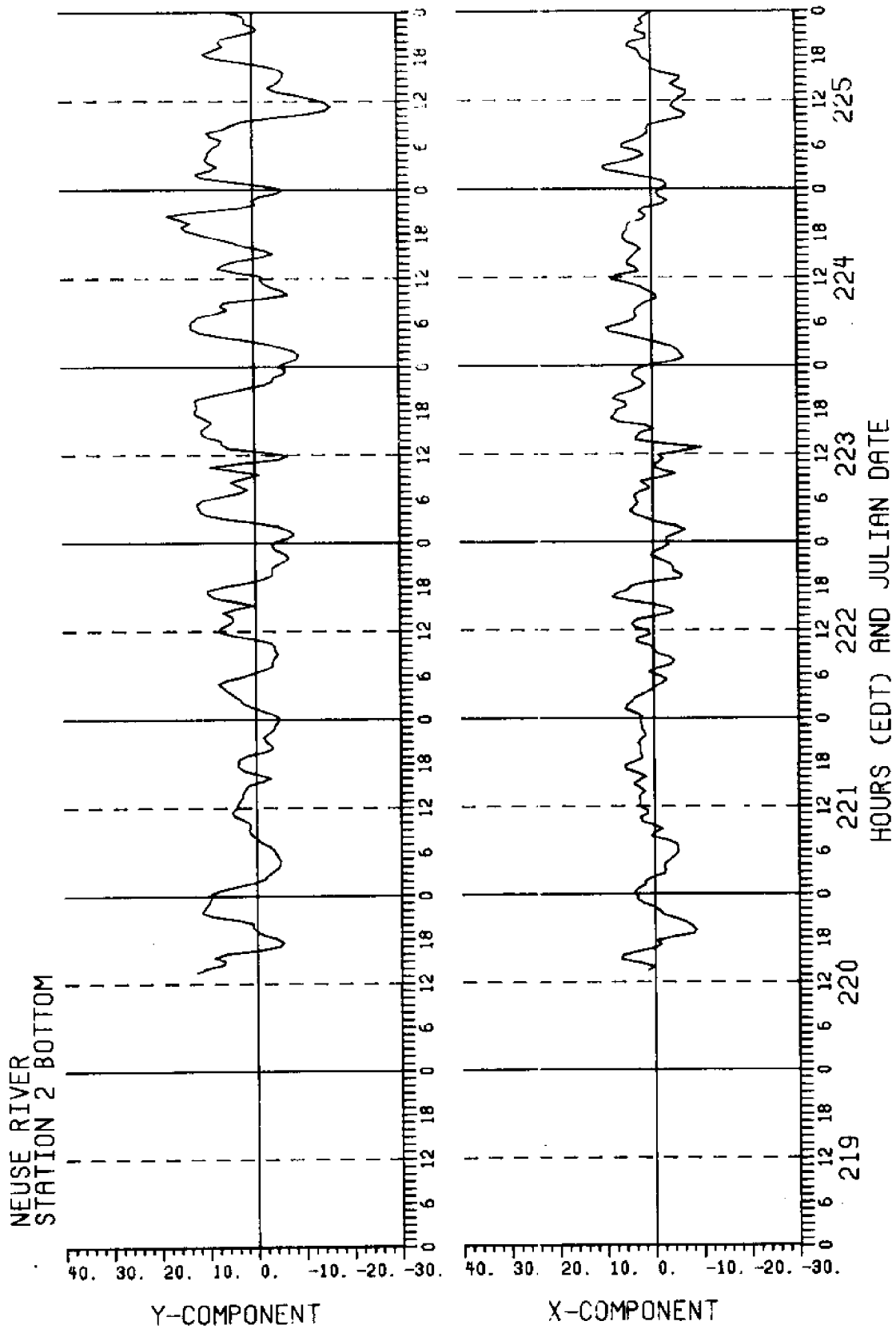


Figure D3

NEUSE RIVER
STATION 2 BOTTOM

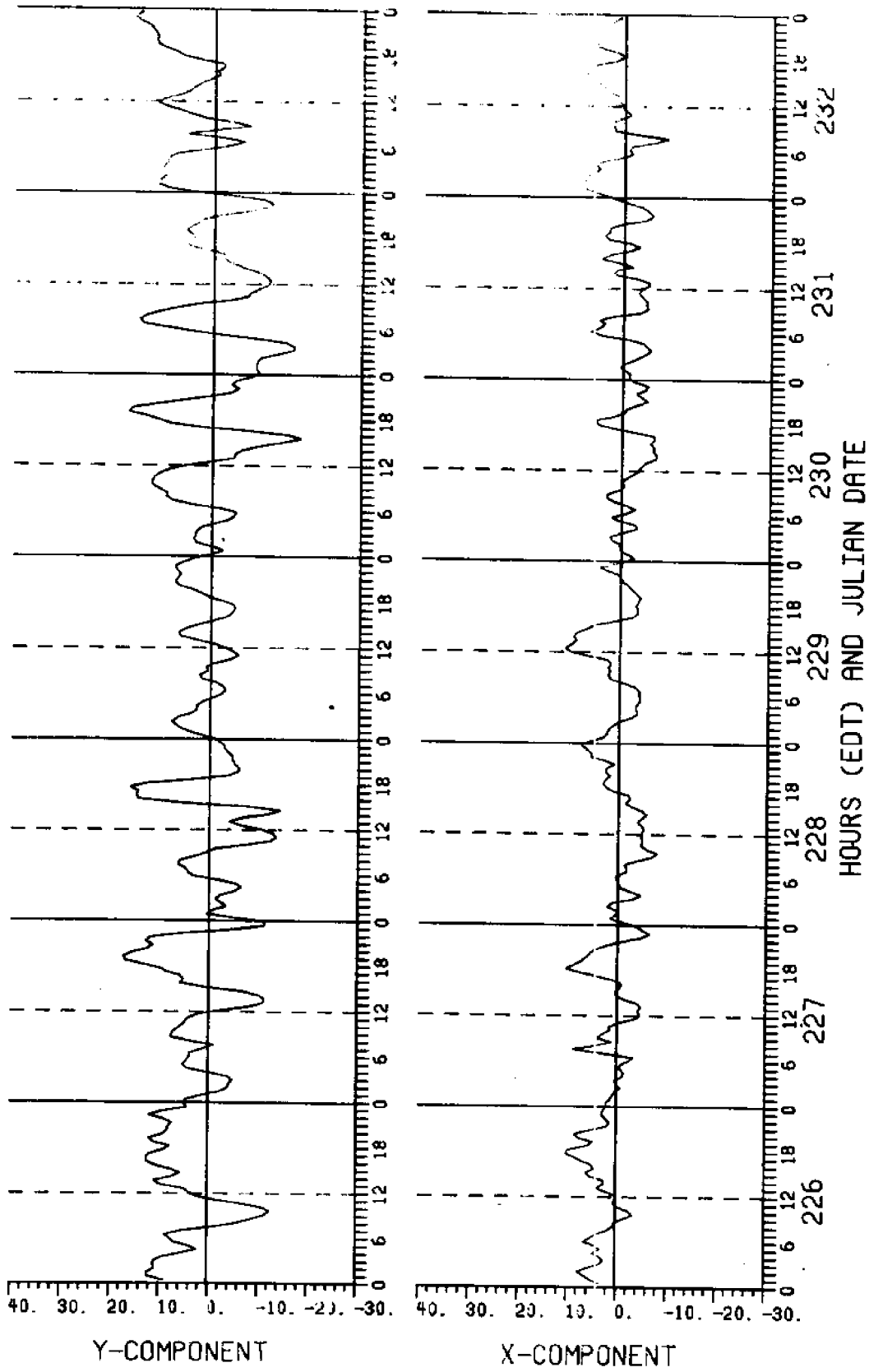


Figure D3

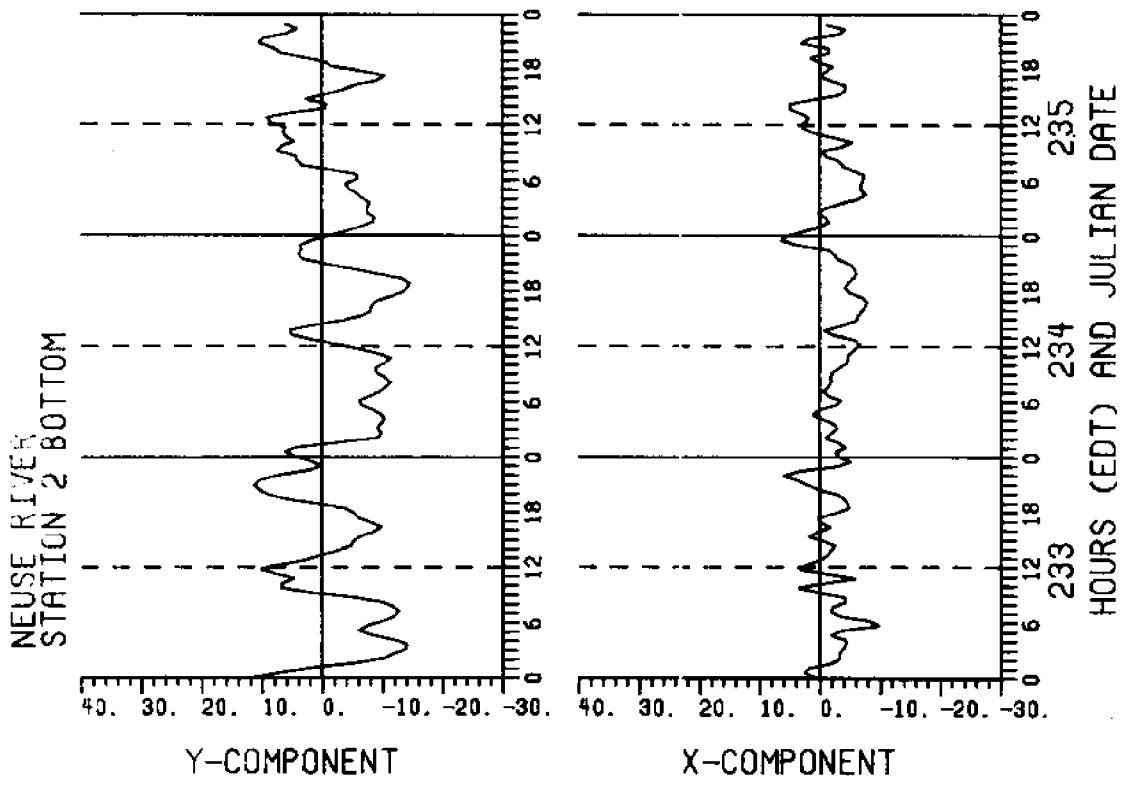


Figure D3

Figure D4. River flow at Station 3 Bottom with channel axis of 105° mag.

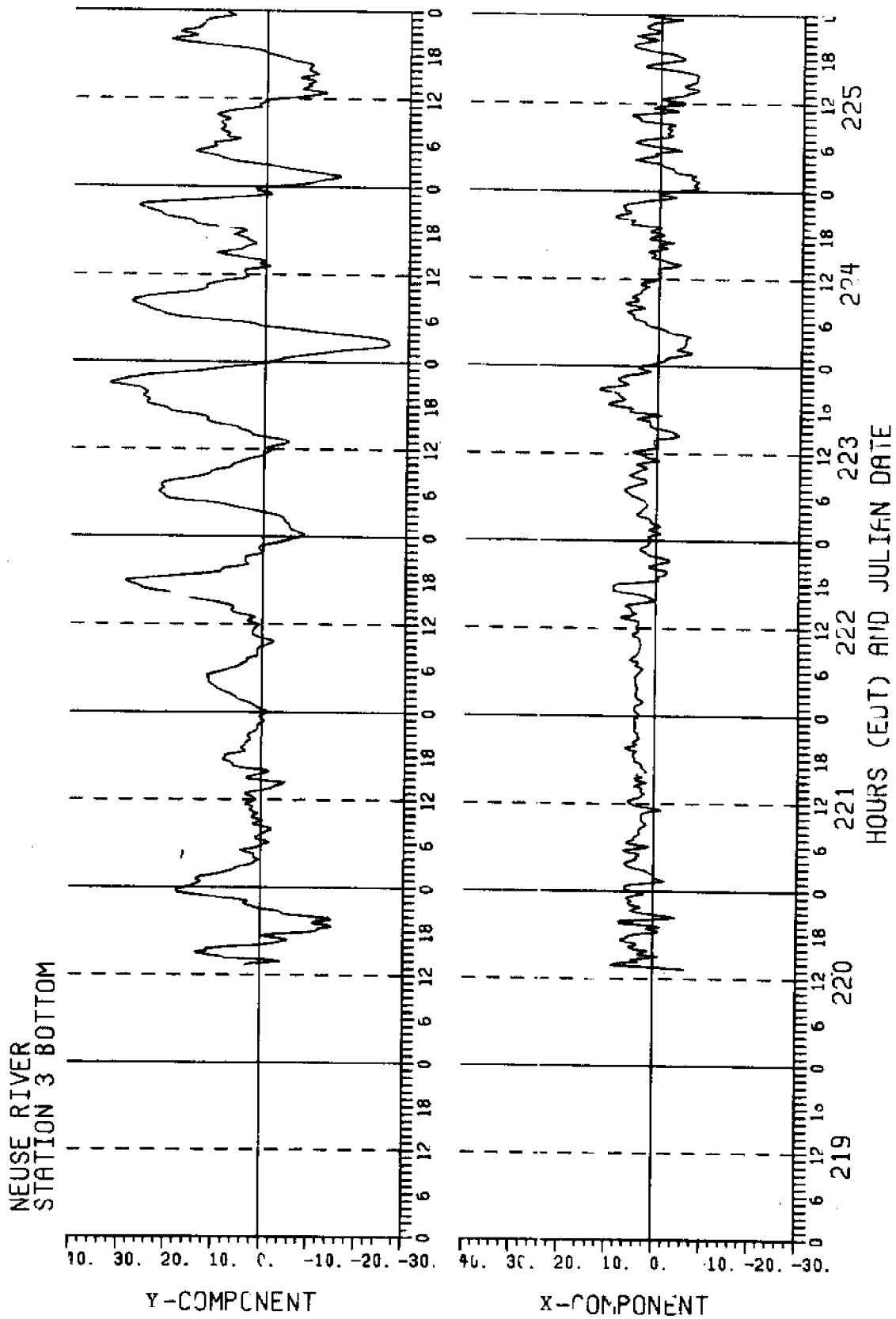


Figure D4

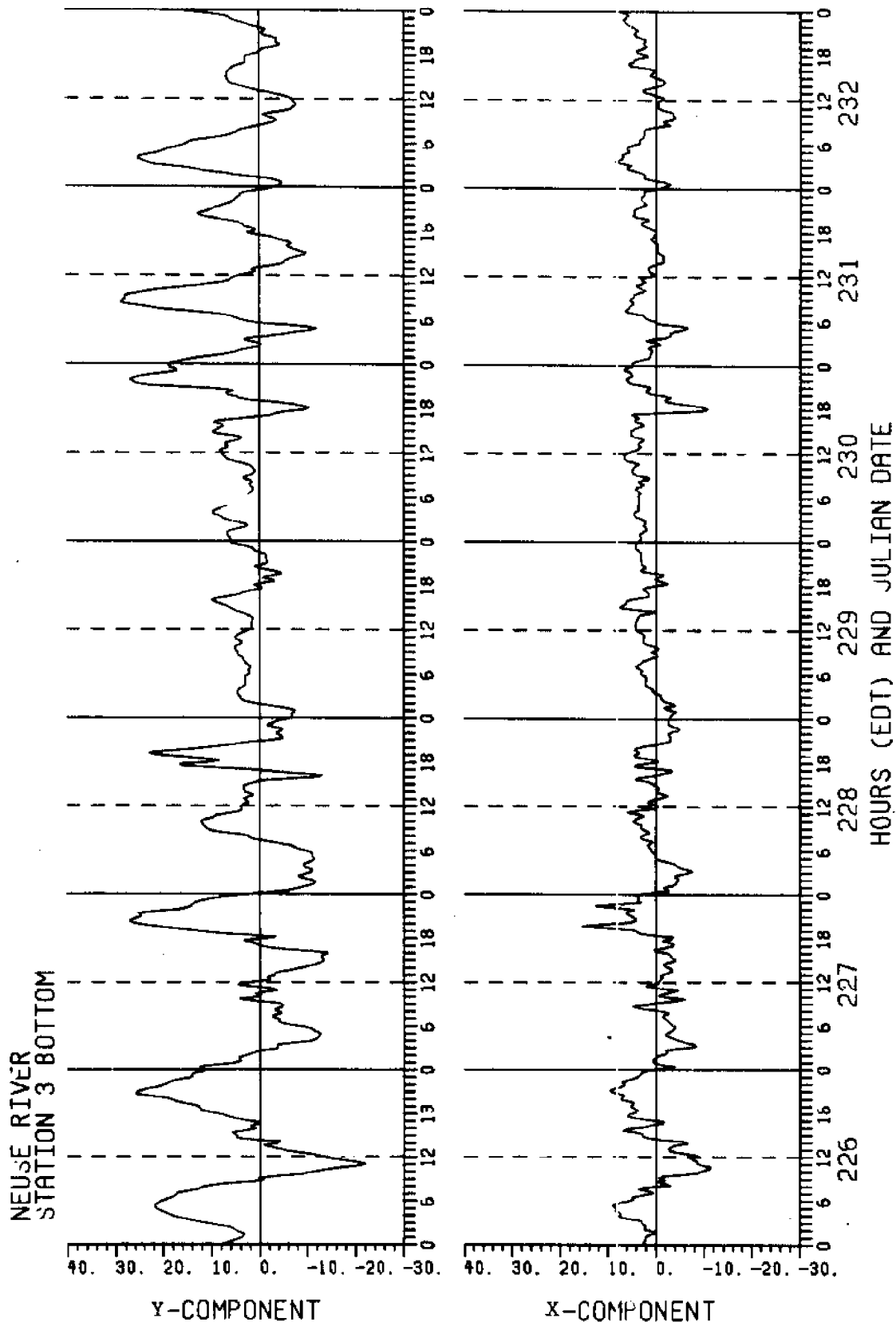


Figure D4

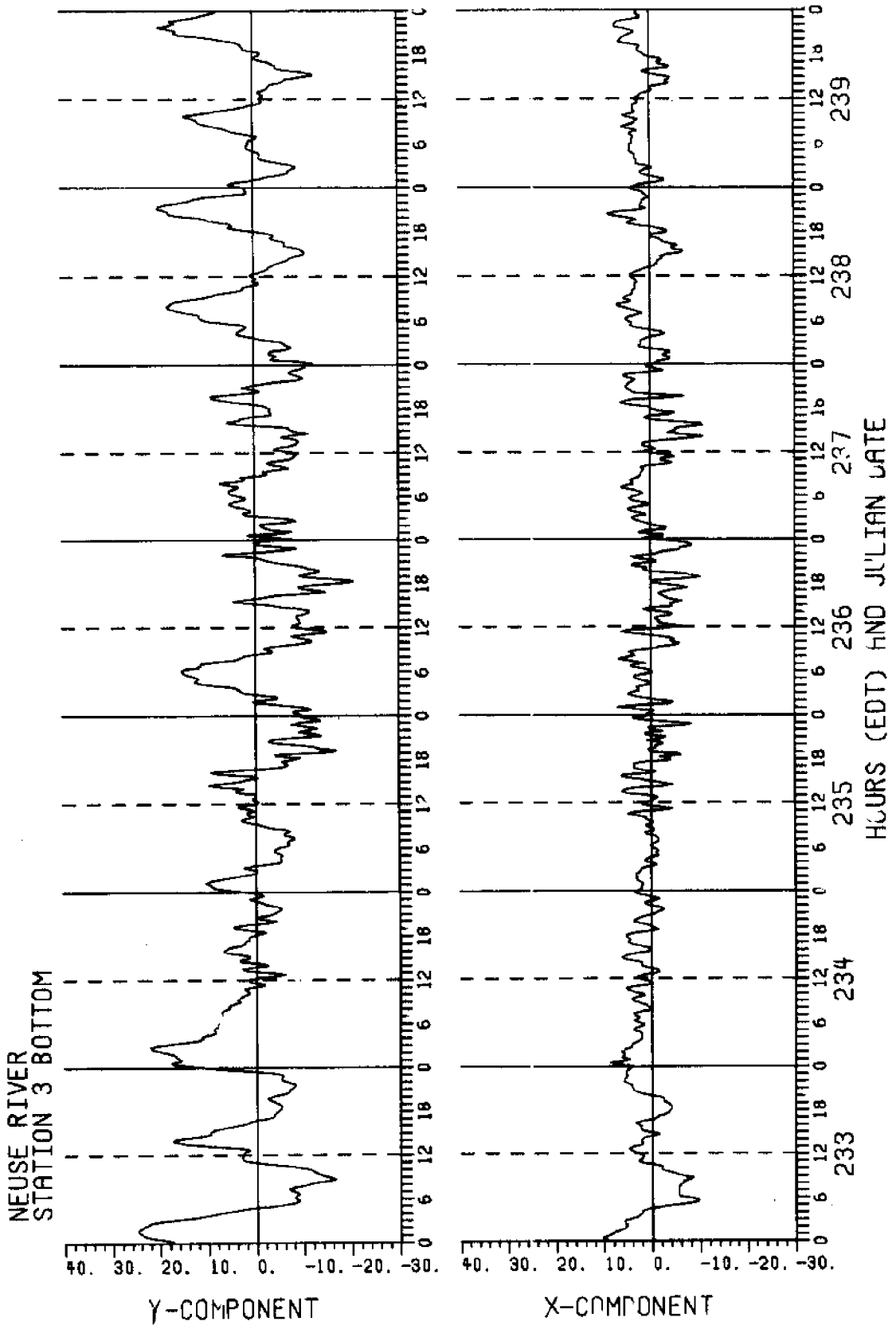


Figure D4

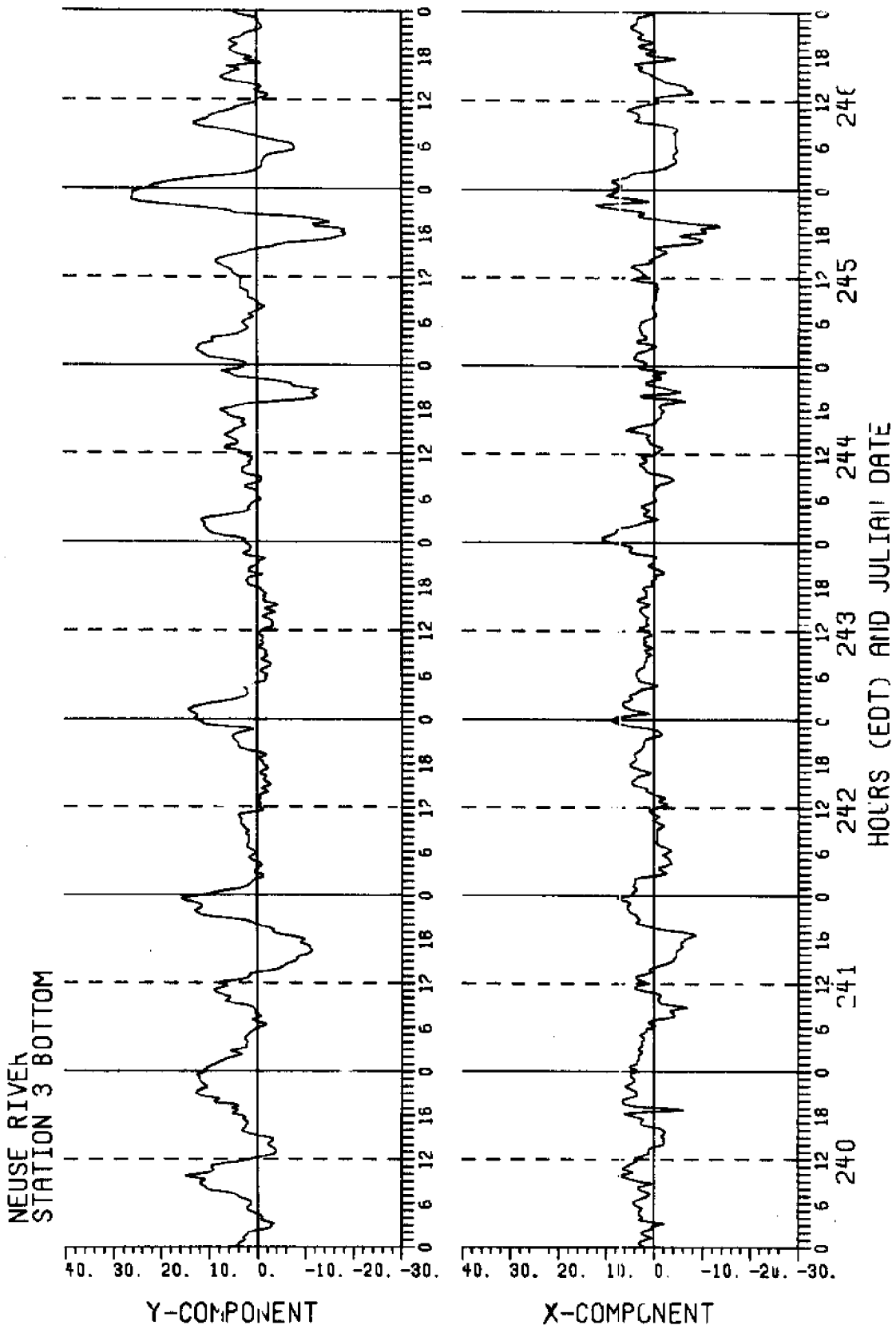


Figure D4

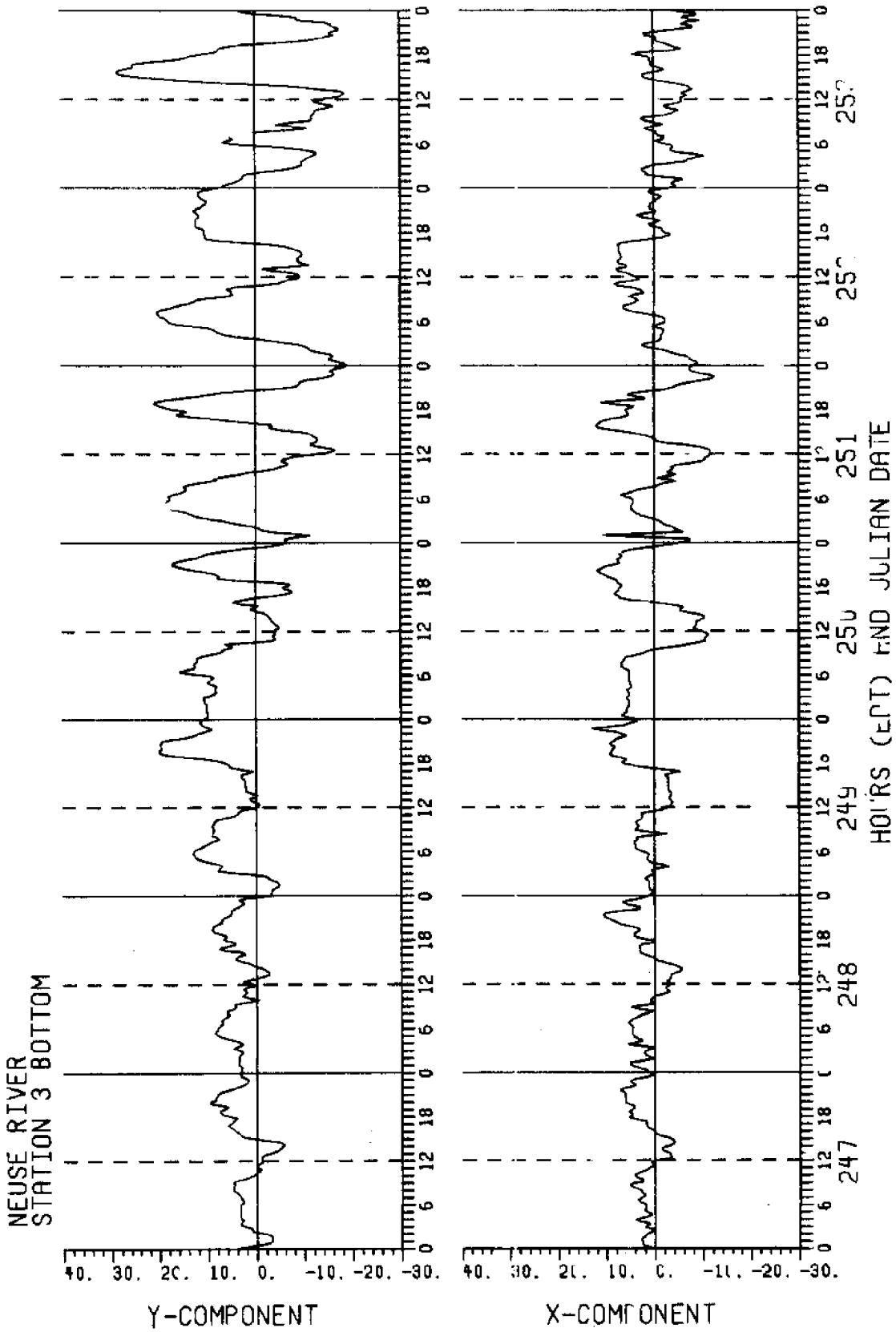


Figure D4

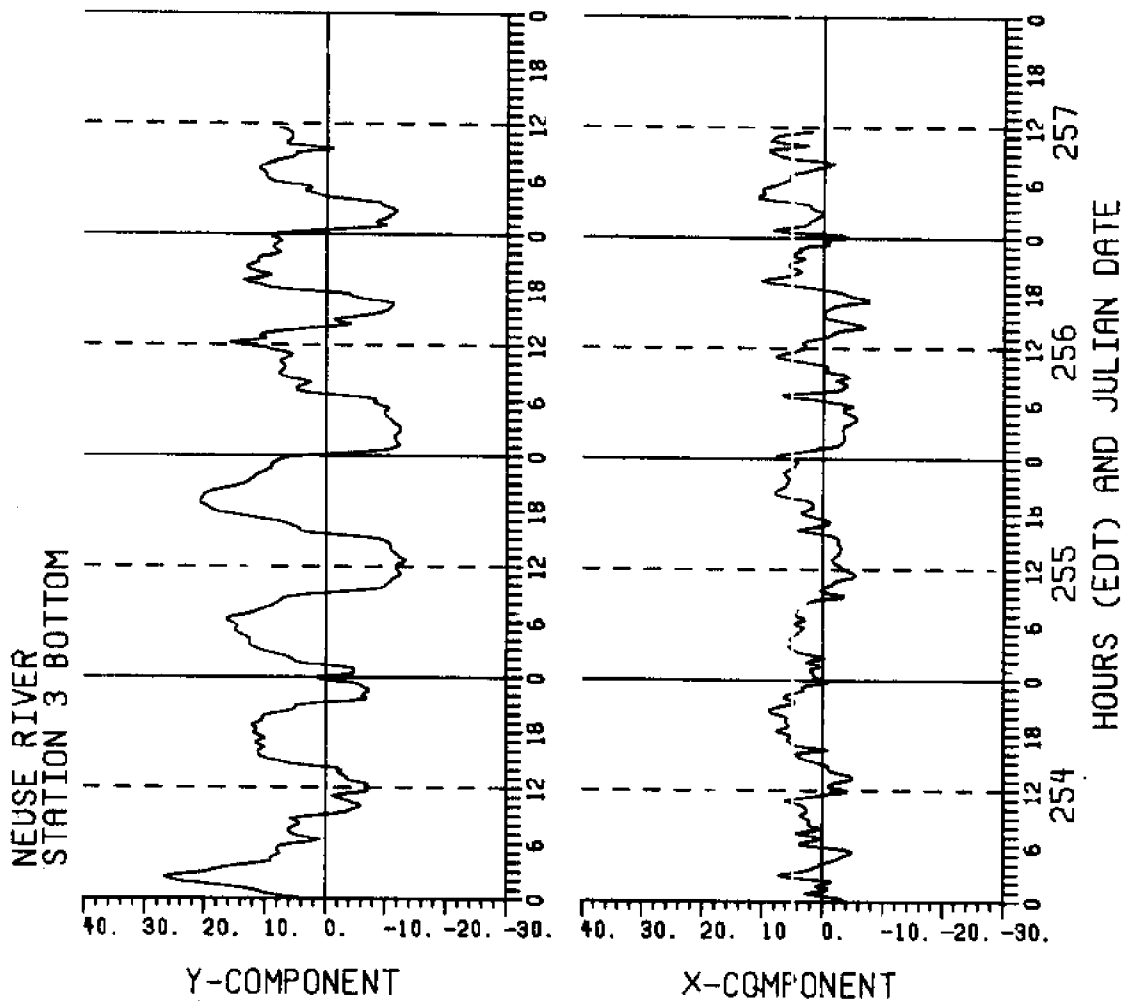


Figure D4

Figure D5. River flow at Station 4 Top, with channel axis of 045° mag.

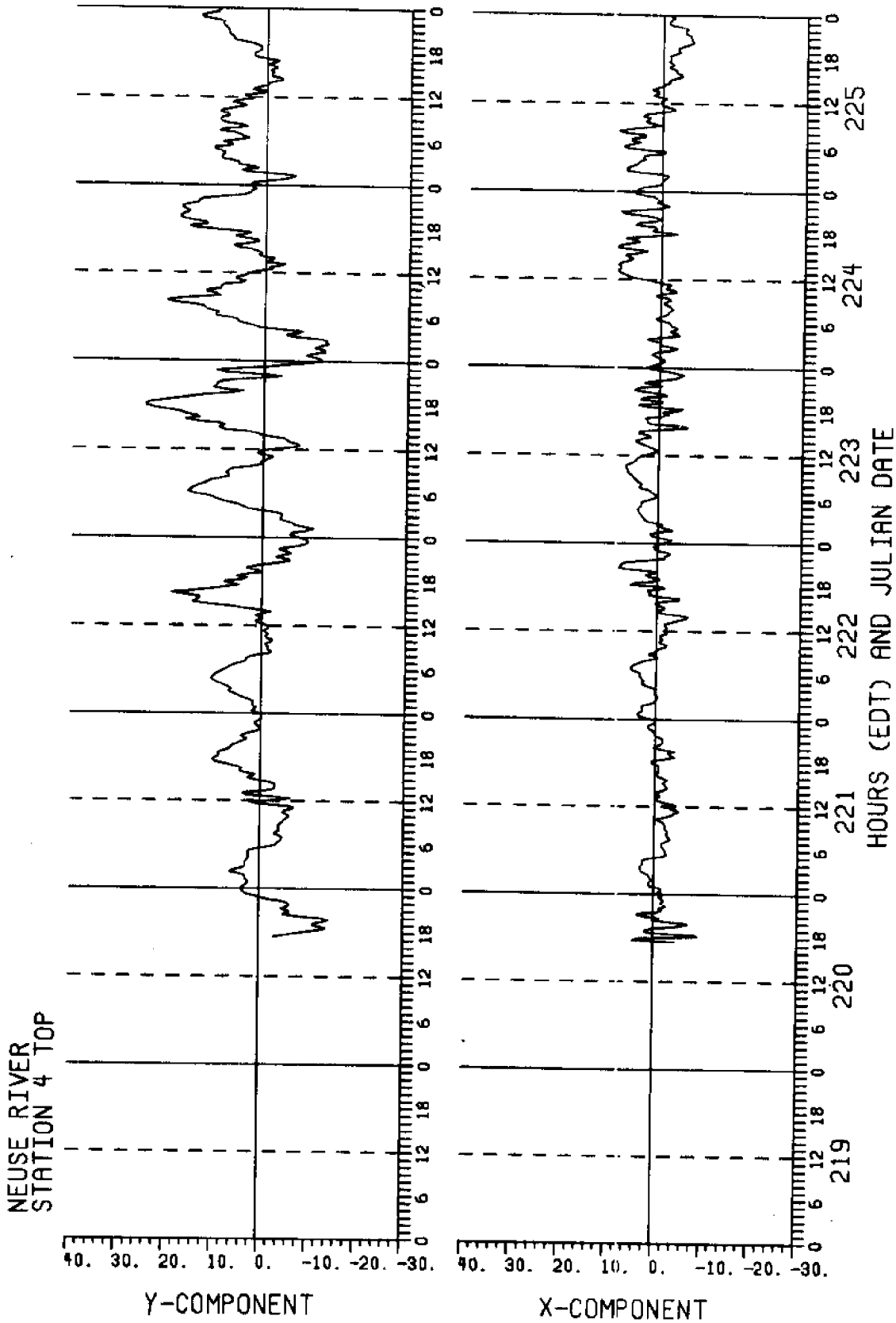


Figure D5

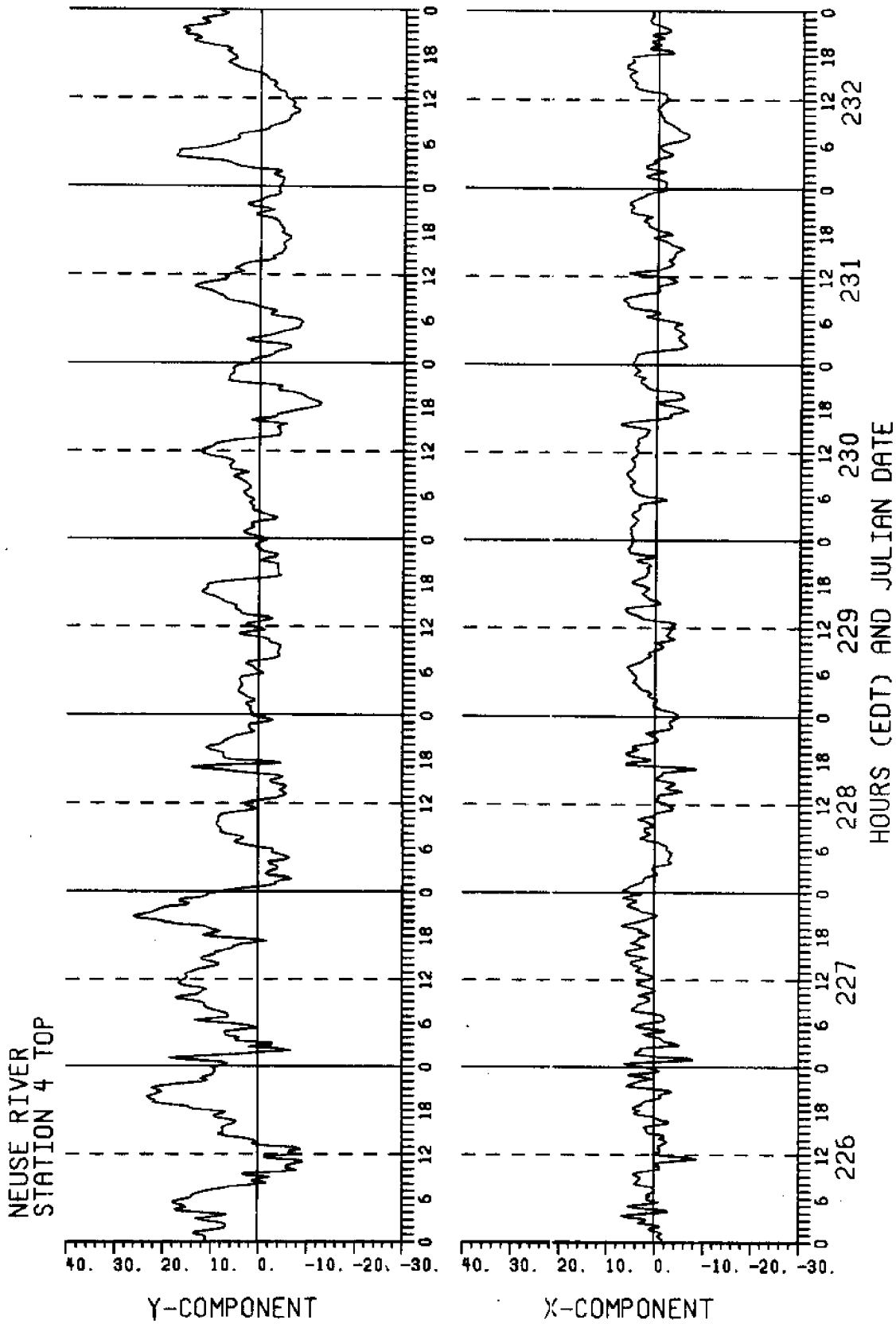


Figure D5

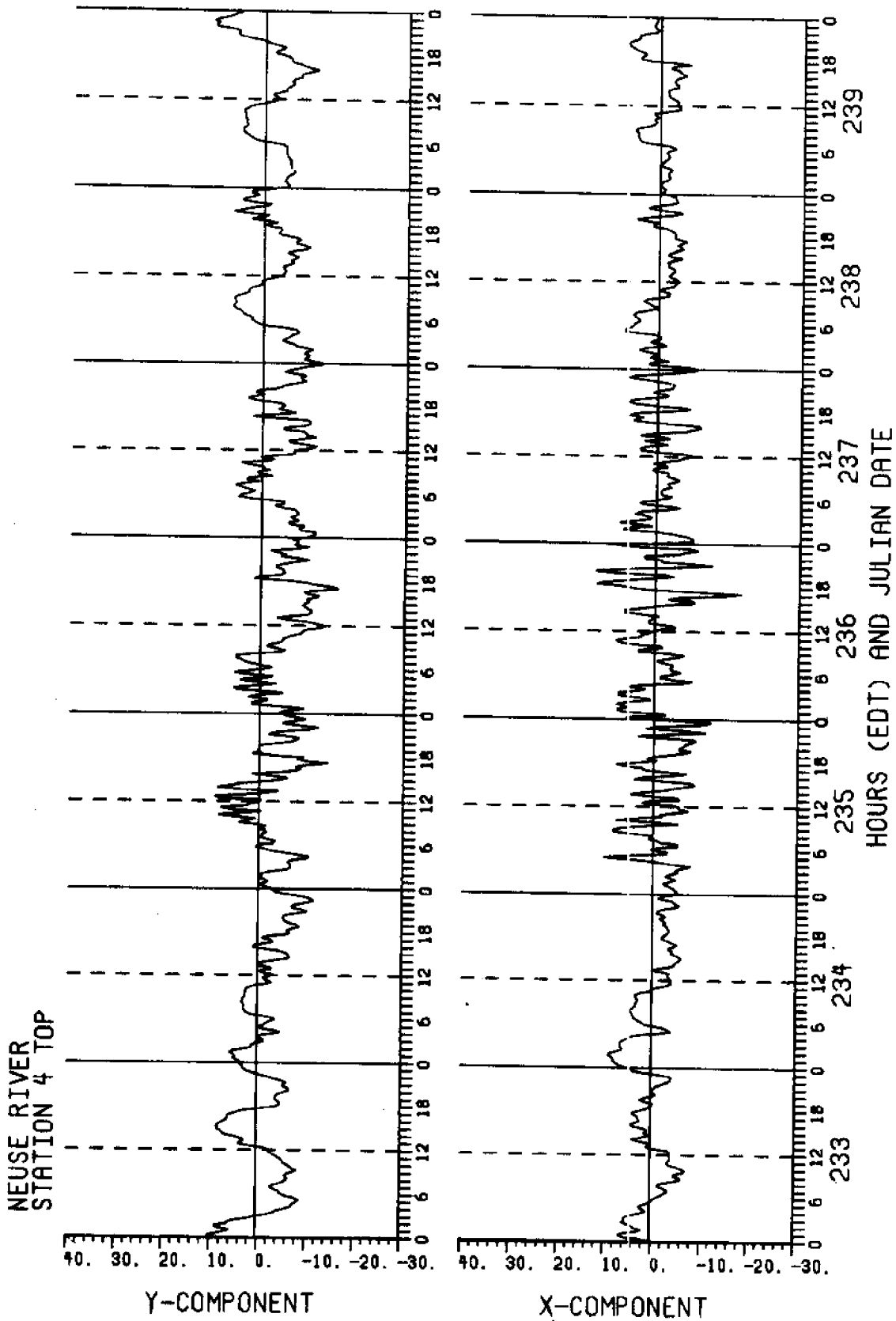


Figure D5

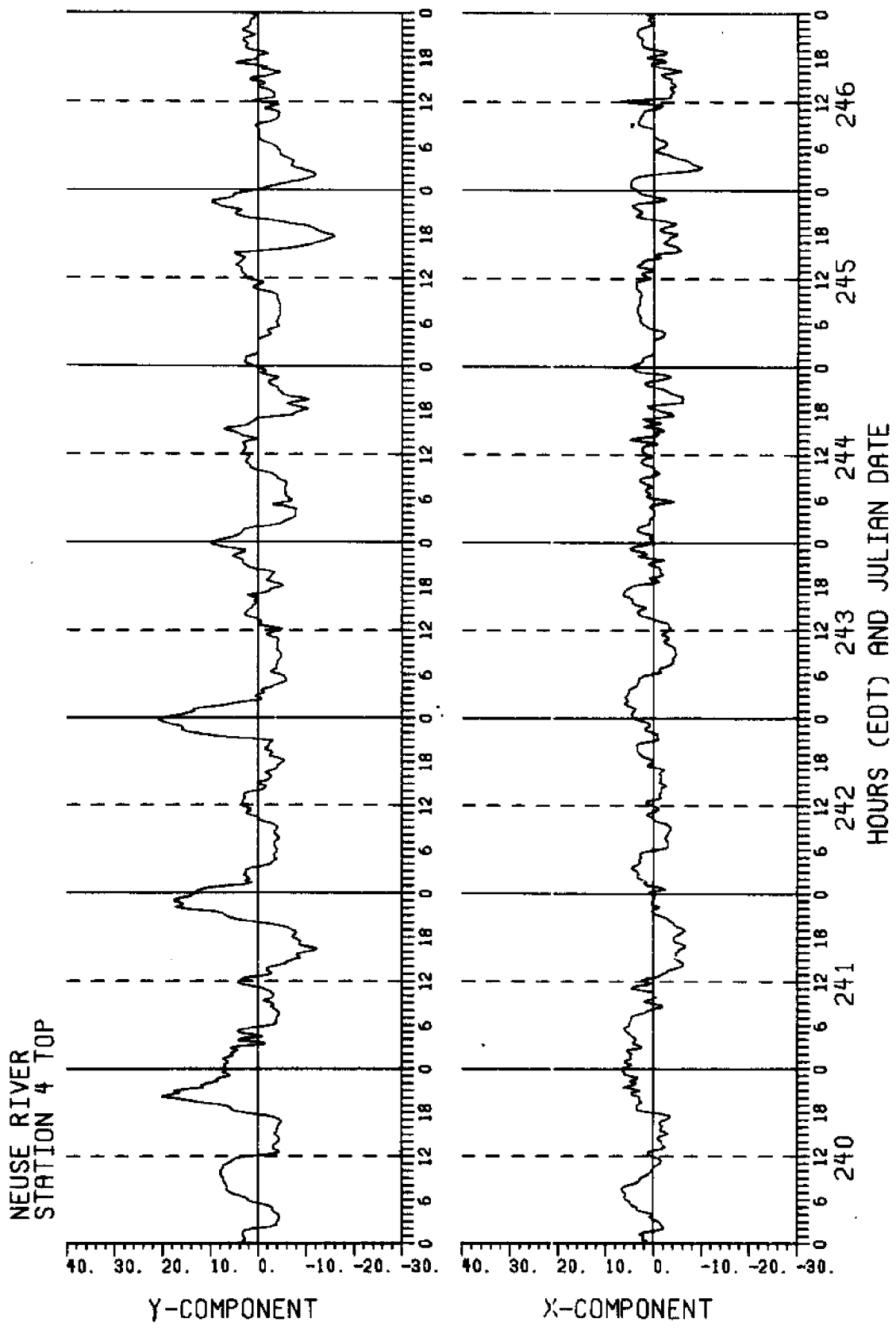


Figure D5

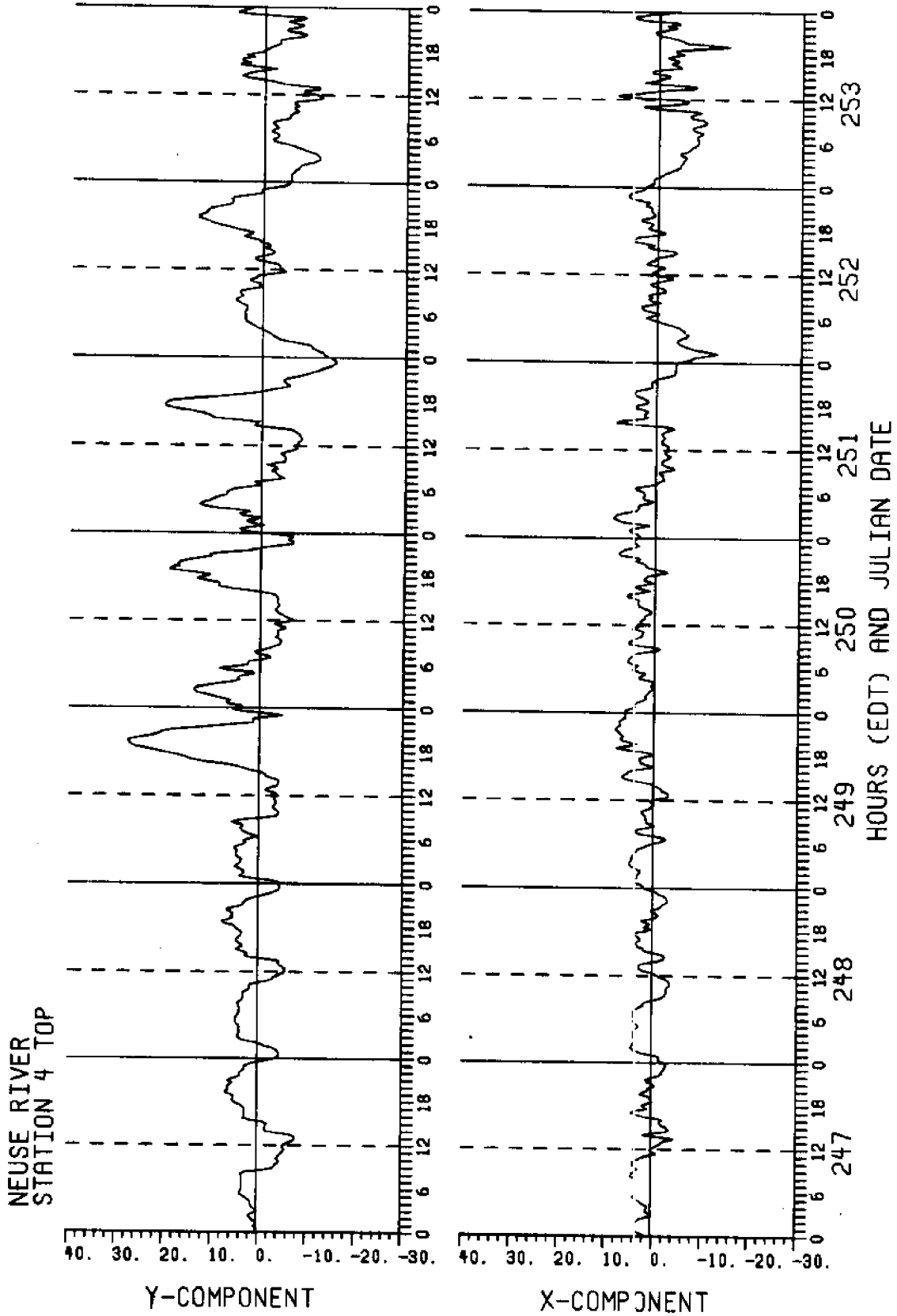


Figure D5

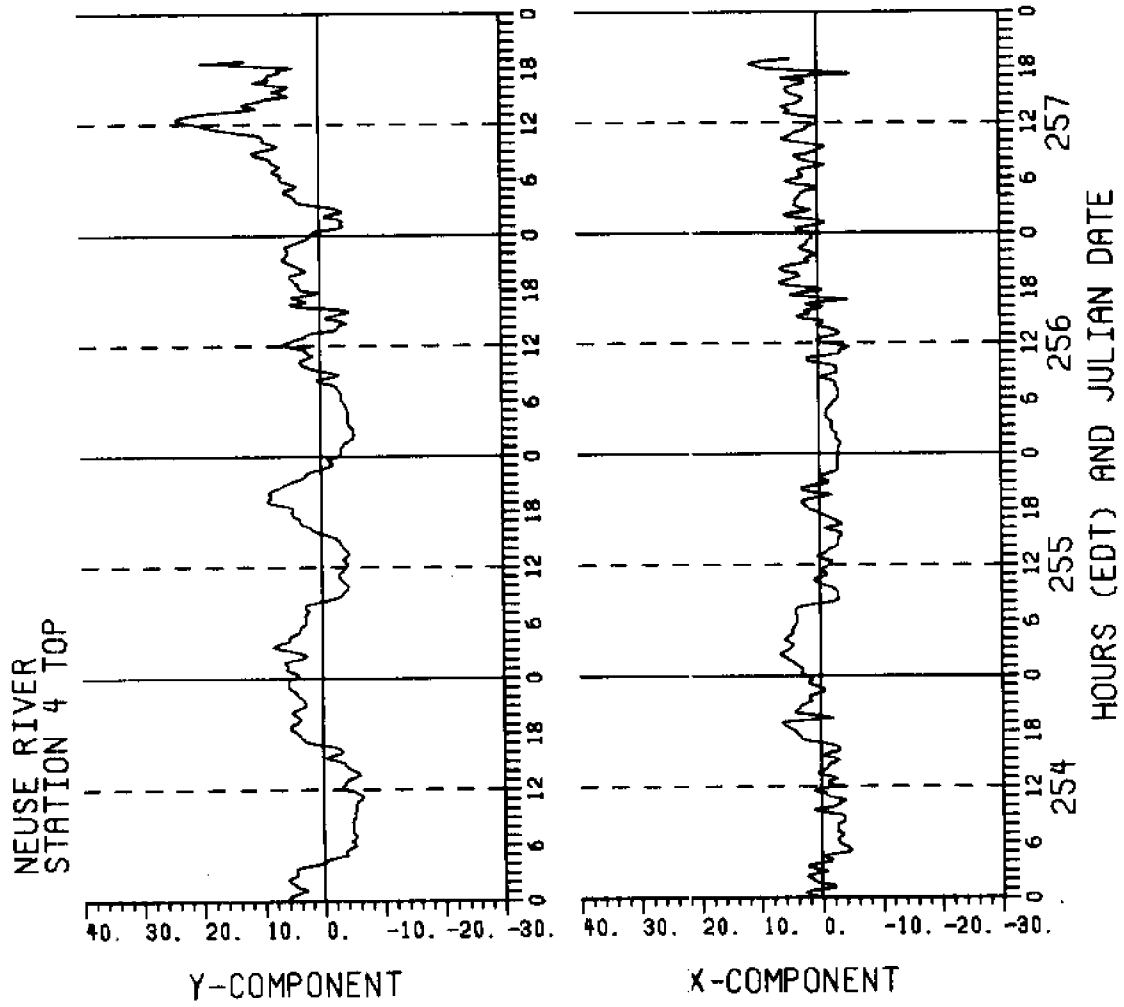


Figure D5

Figure D6. River flow at Station 4 Bottom, with channel axis of 045° mag.

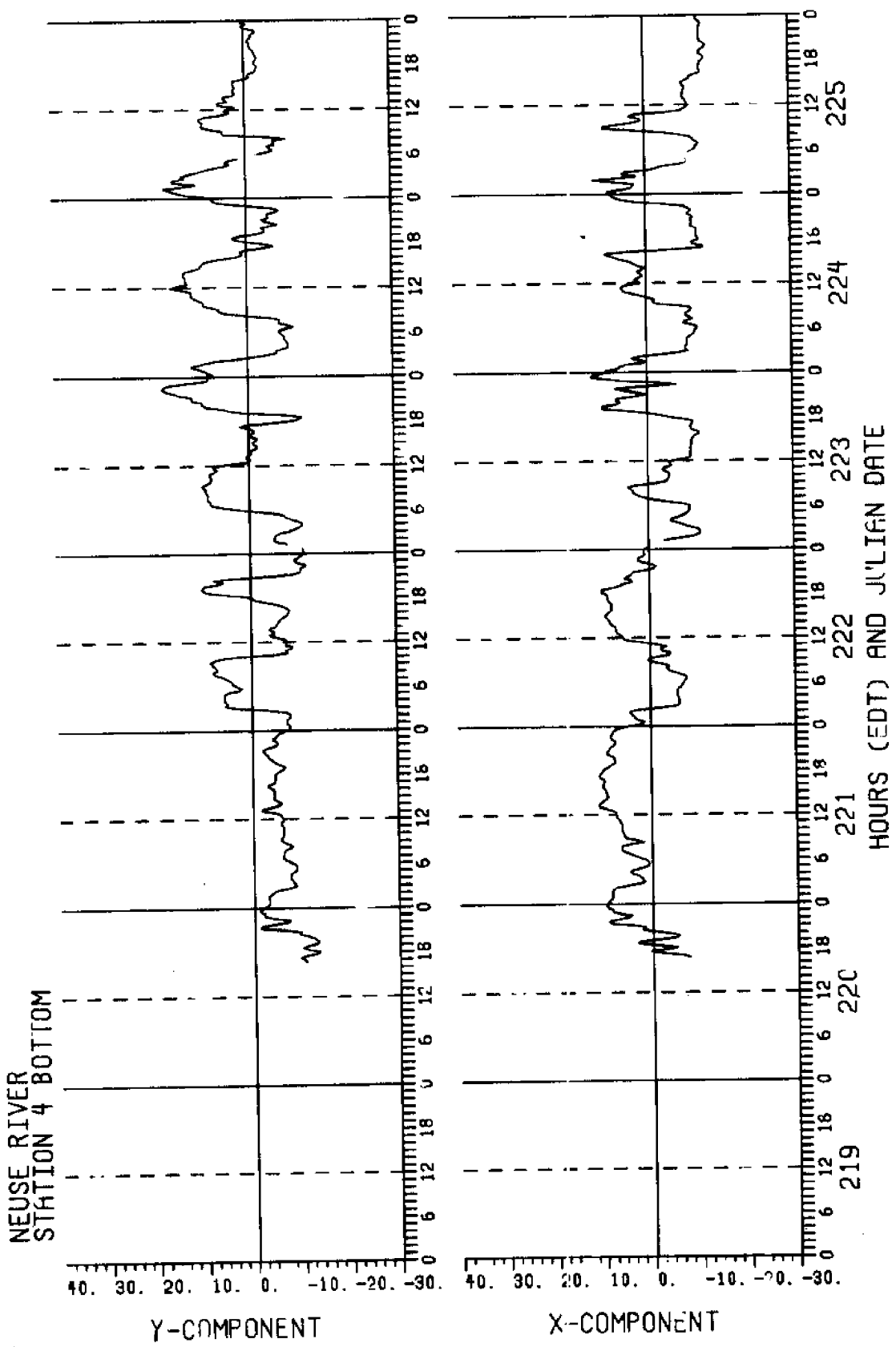


Figure D6

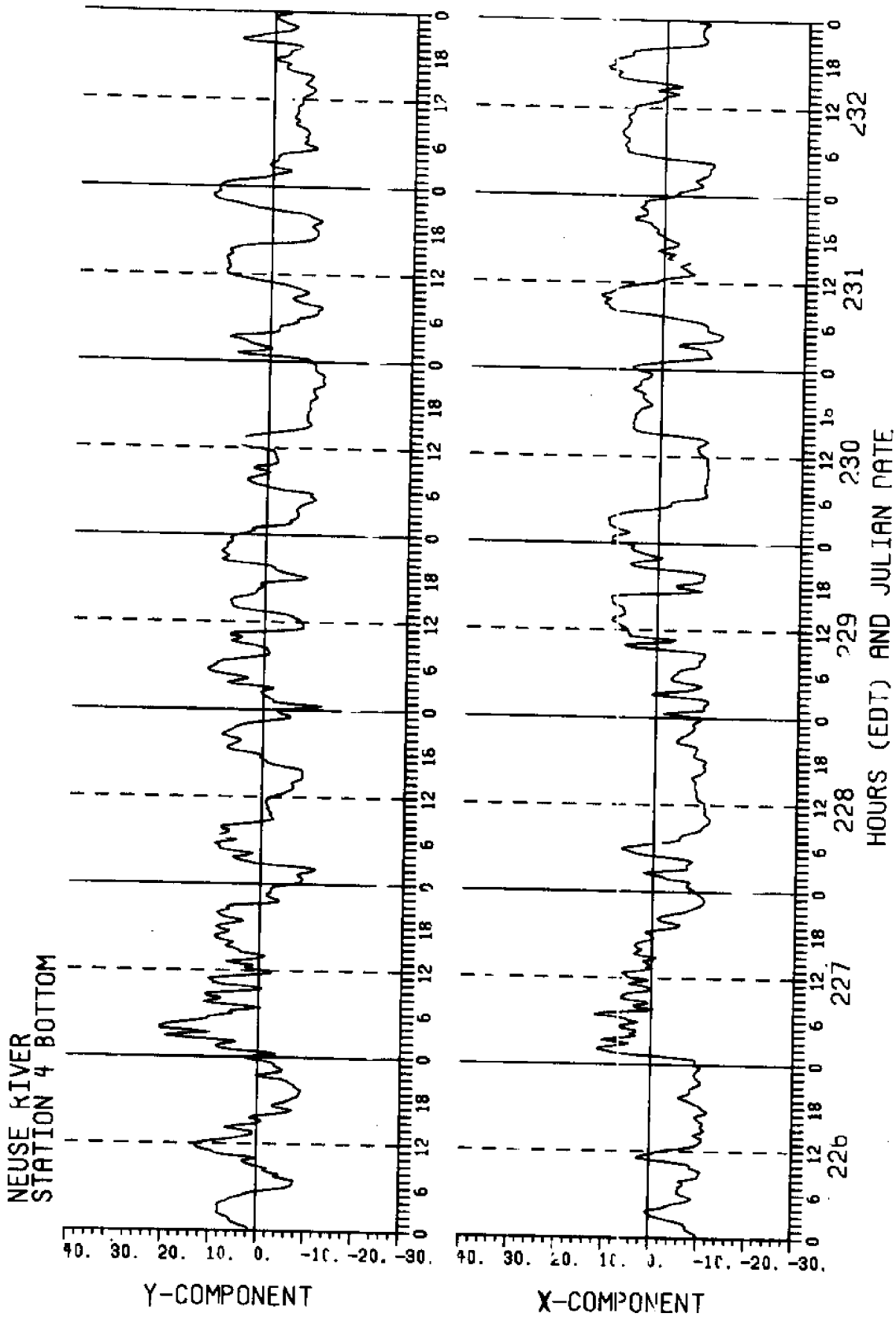


Figure D6

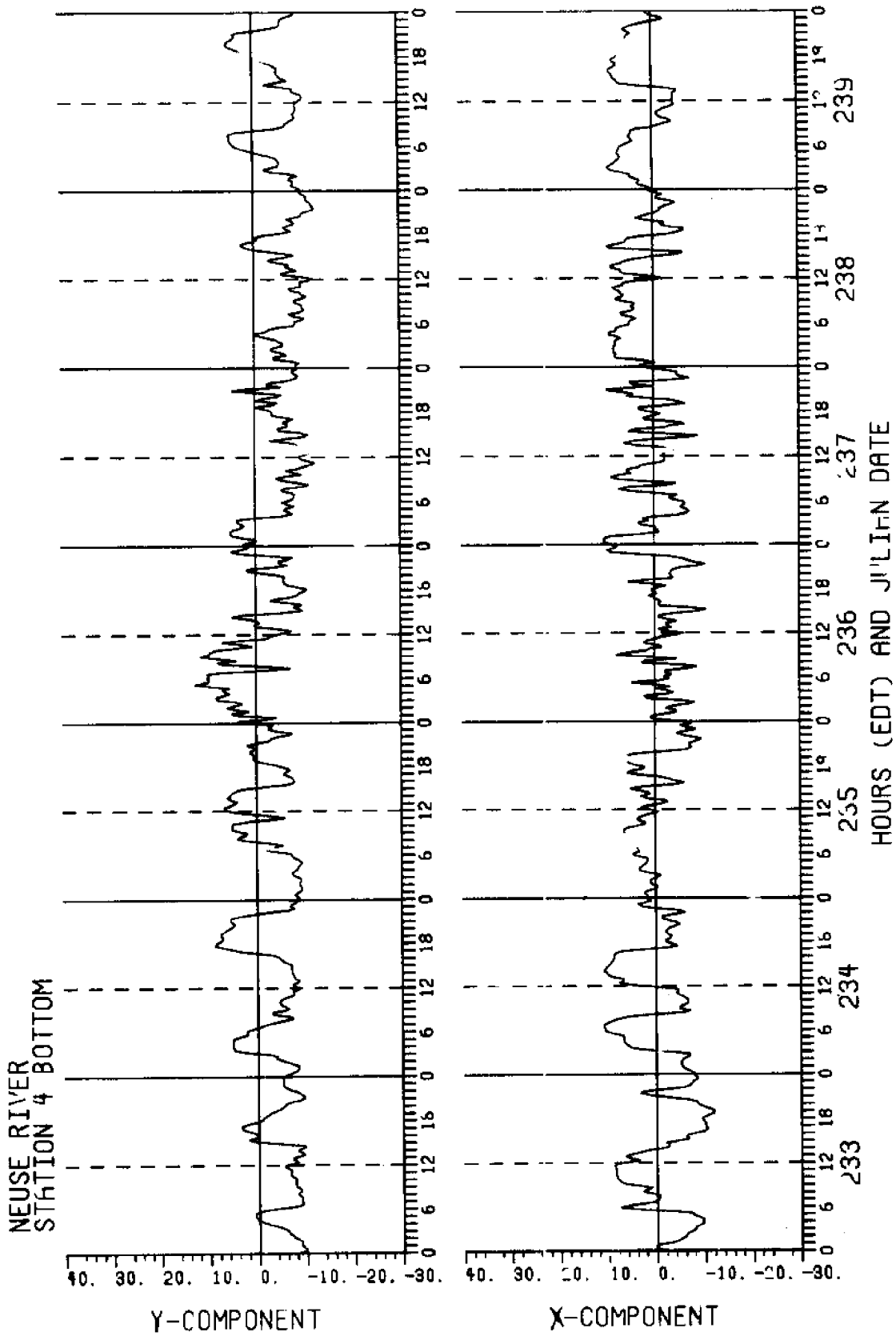


Figure D6

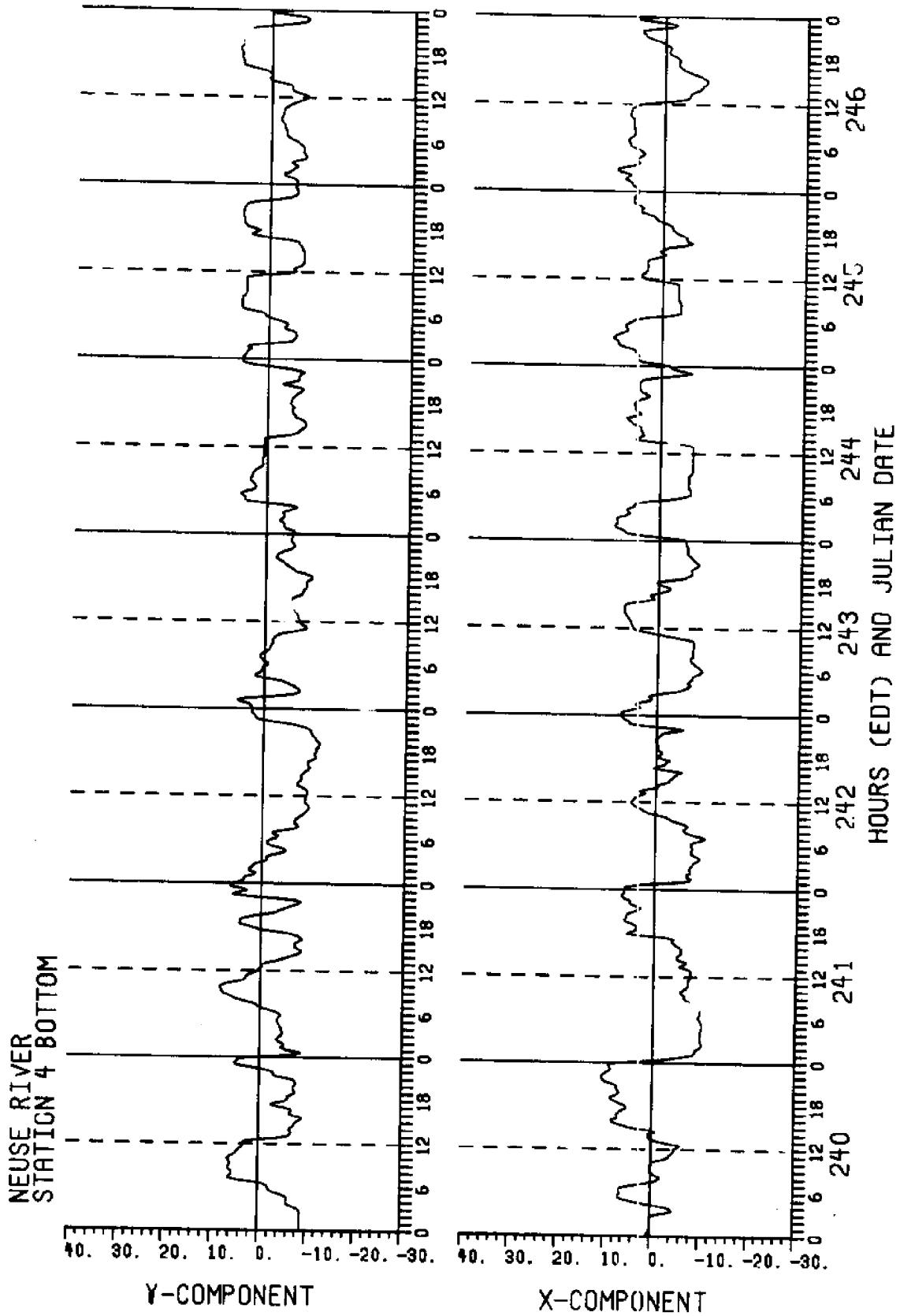


Figure D6

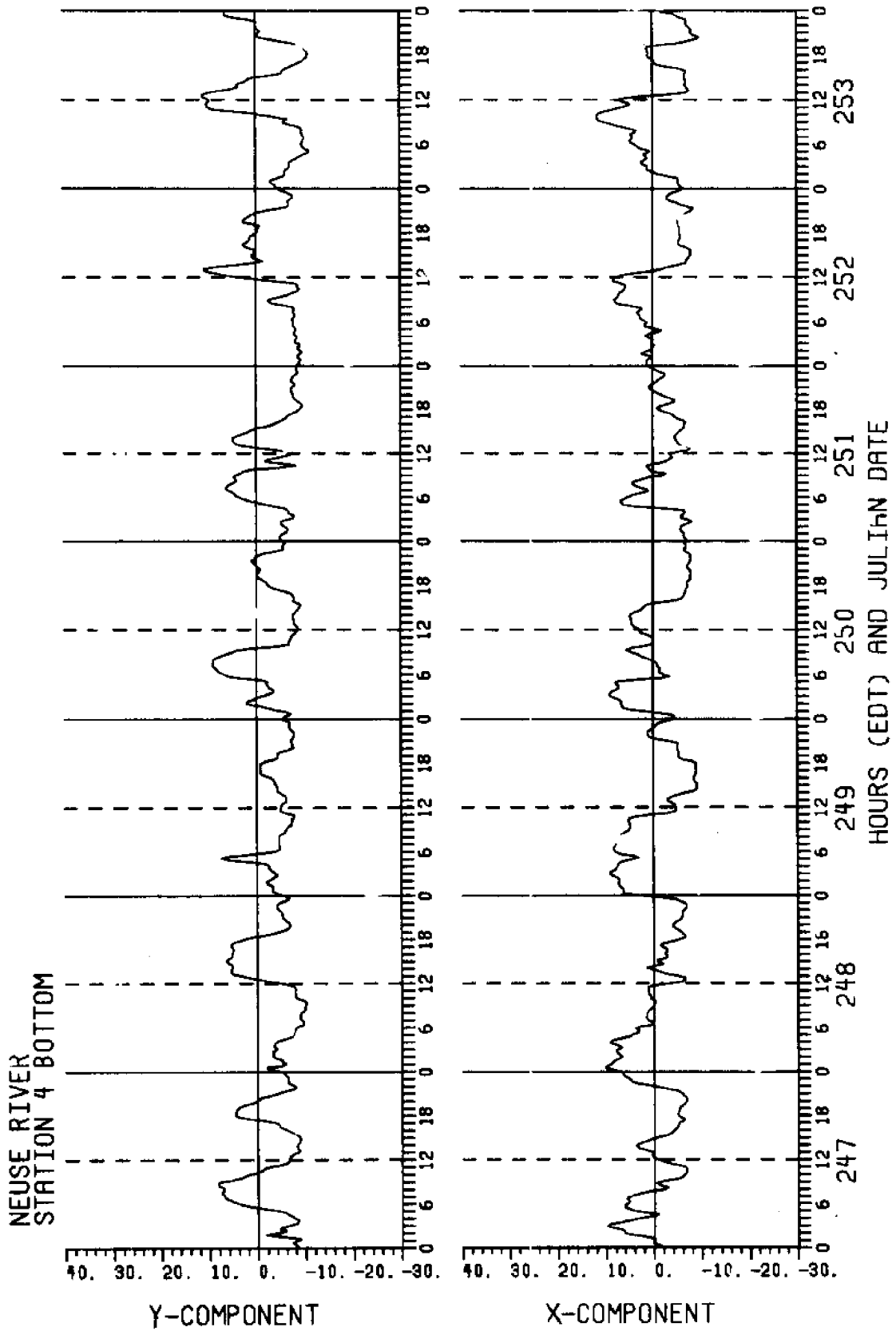


Figure D6

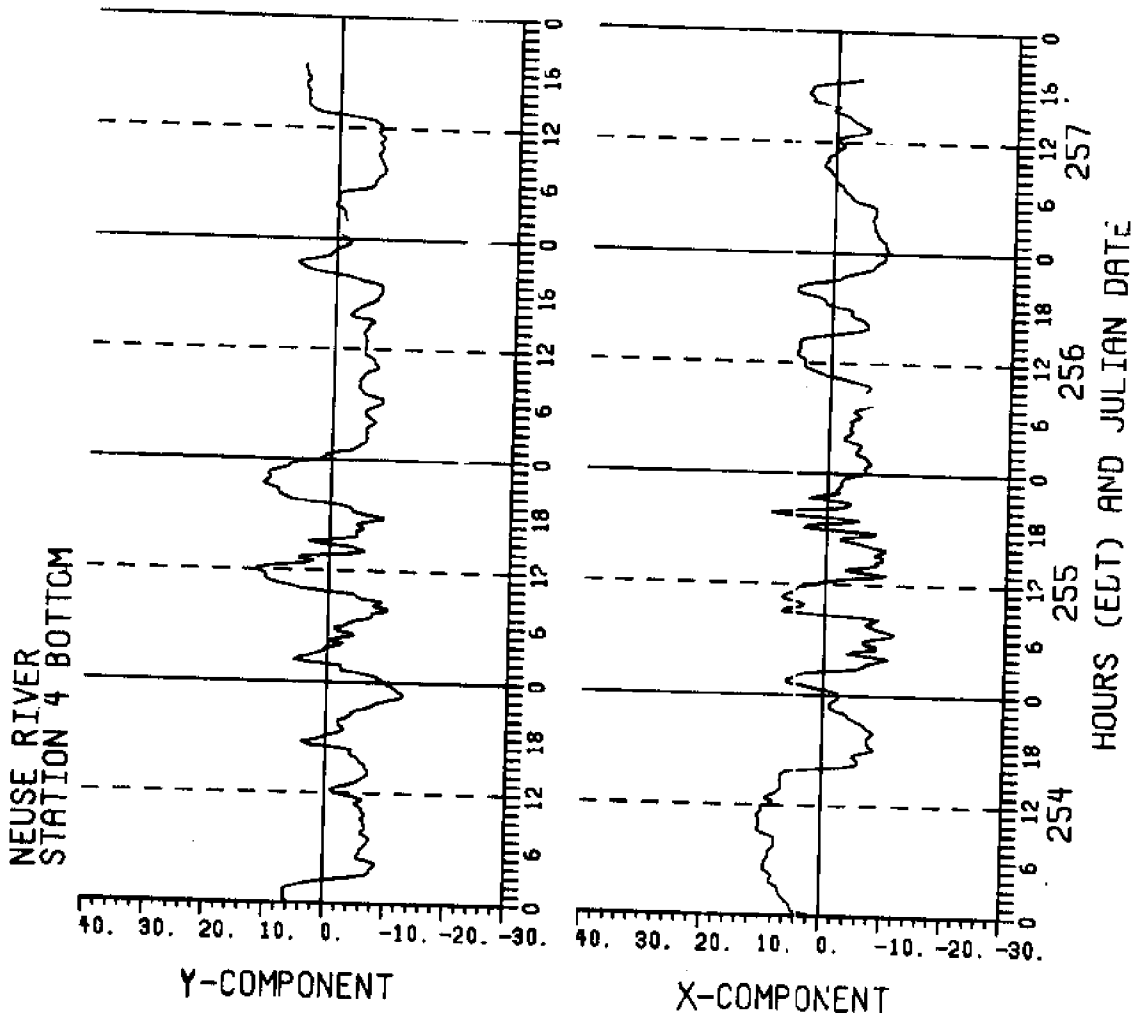


Figure D6

Figure D7. River flow at Station 5 Bottom, with channel axis of 045° mag.

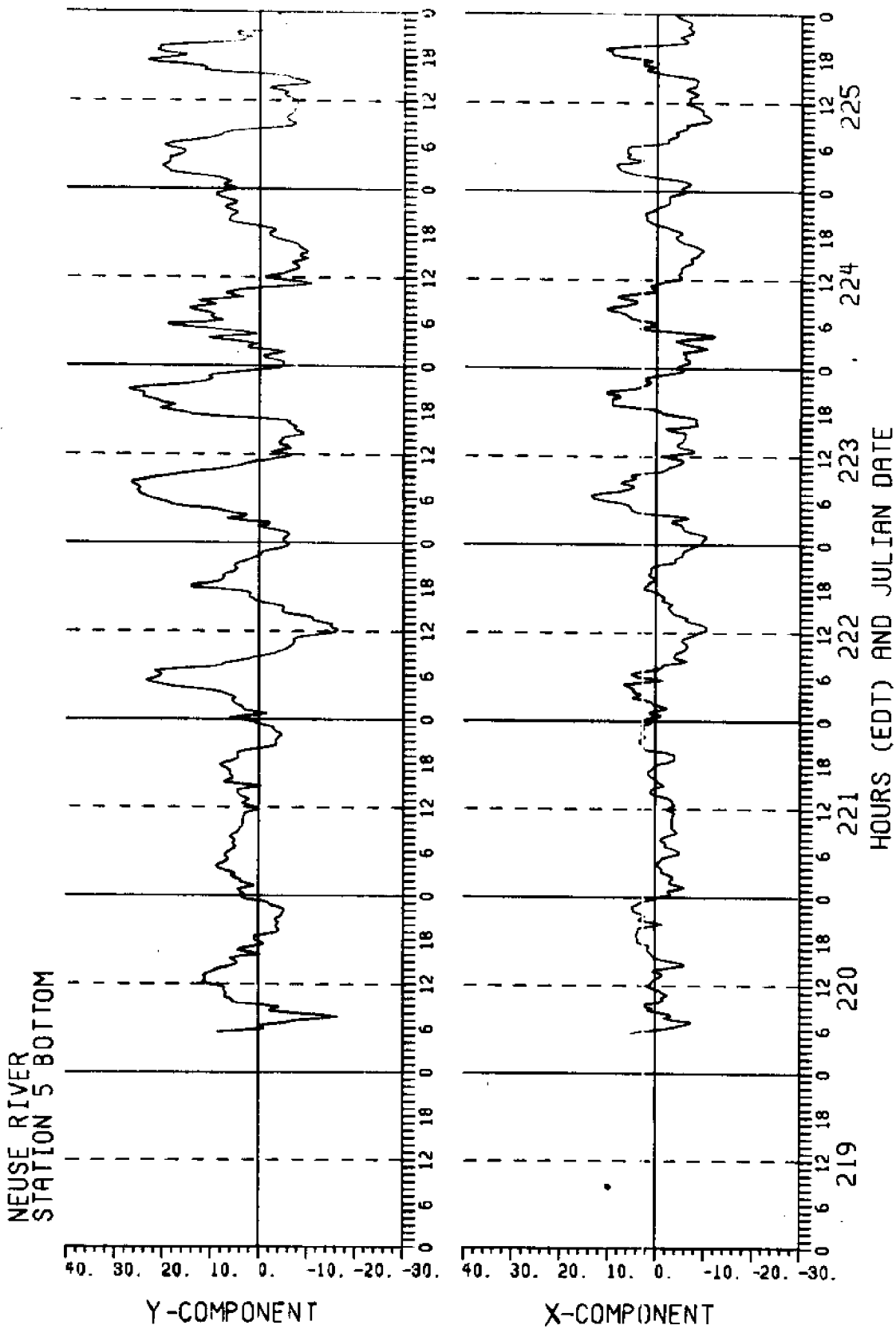


Figure D7

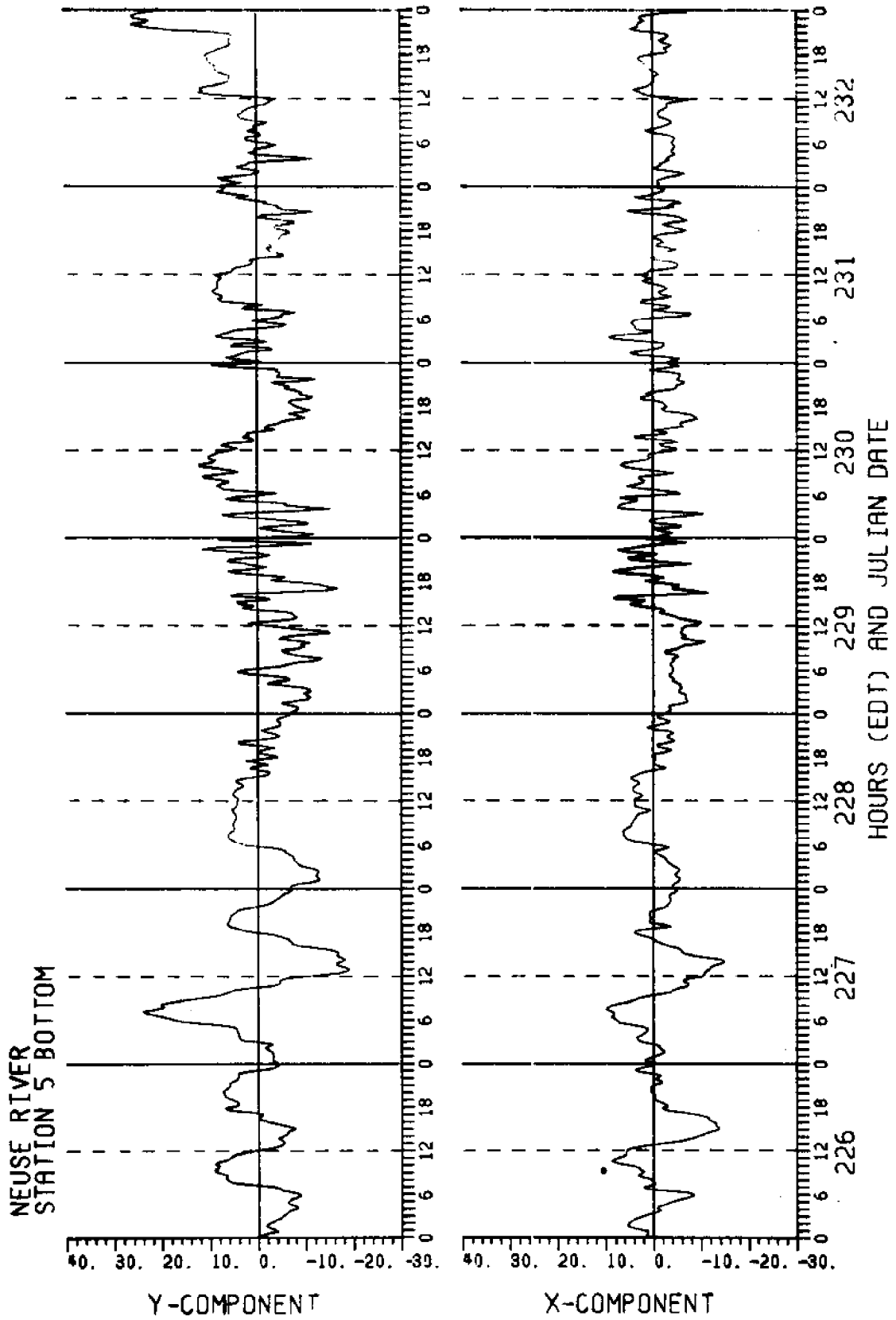


Figure D7

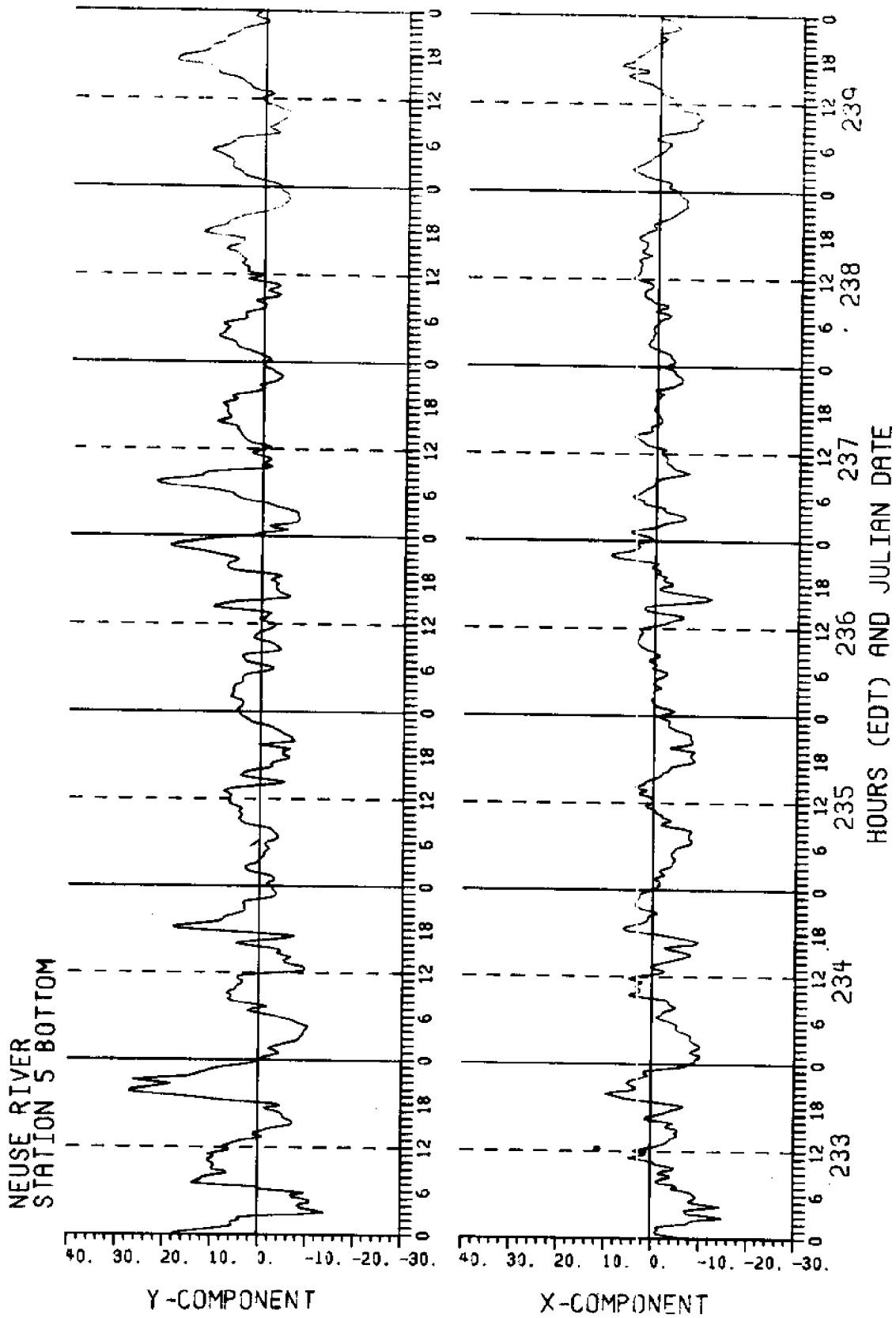


Figure D7

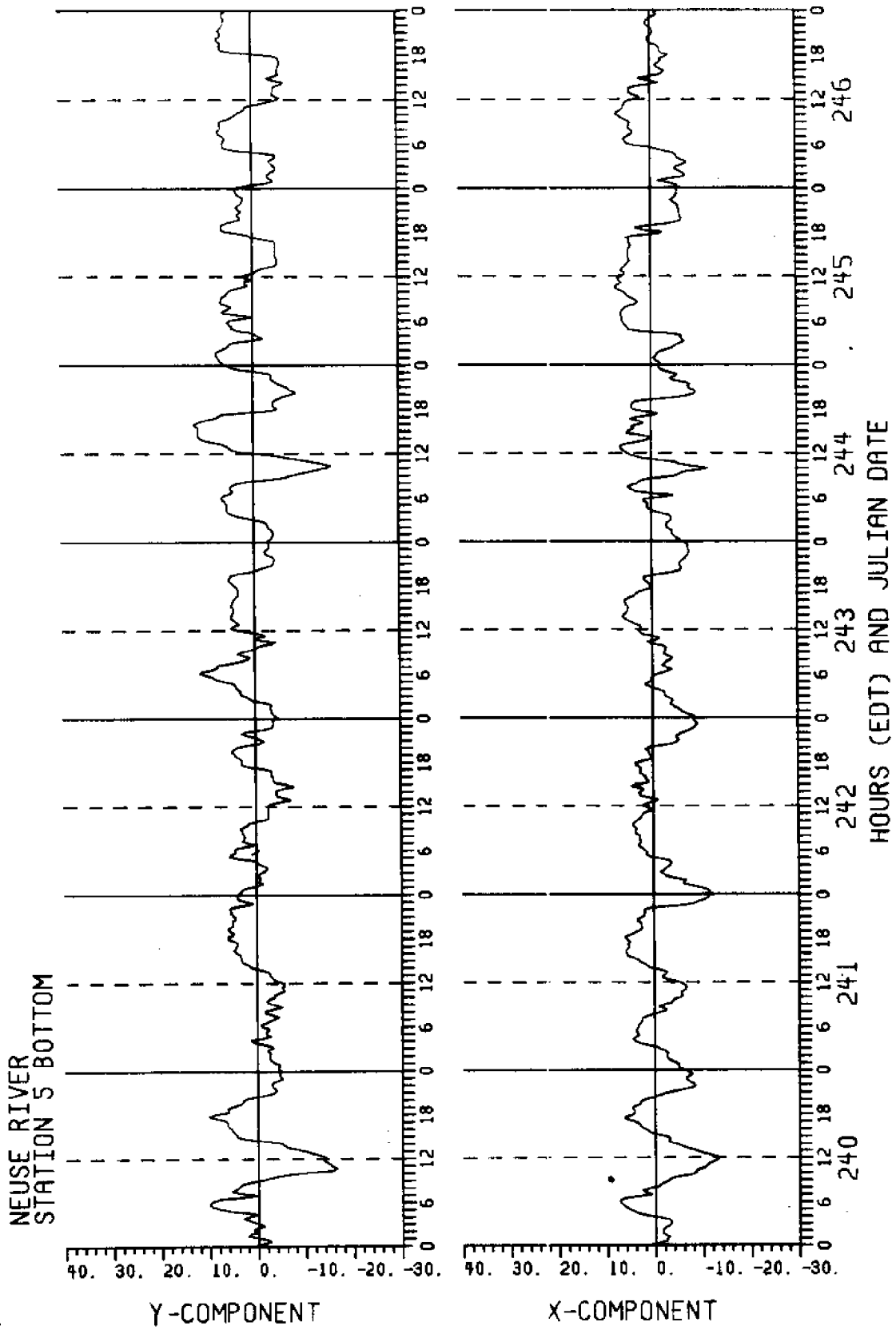


Figure D7

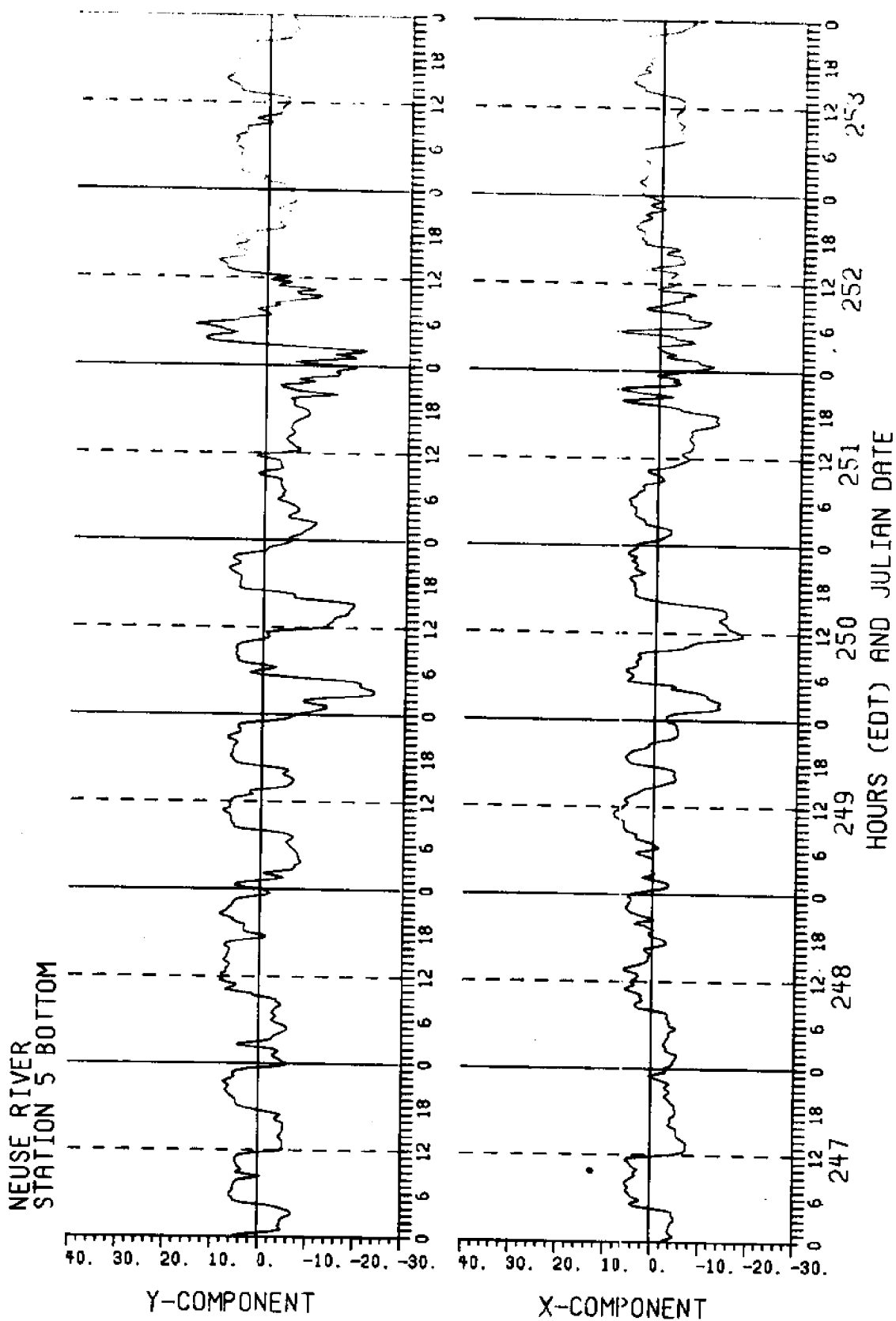


Figure D7

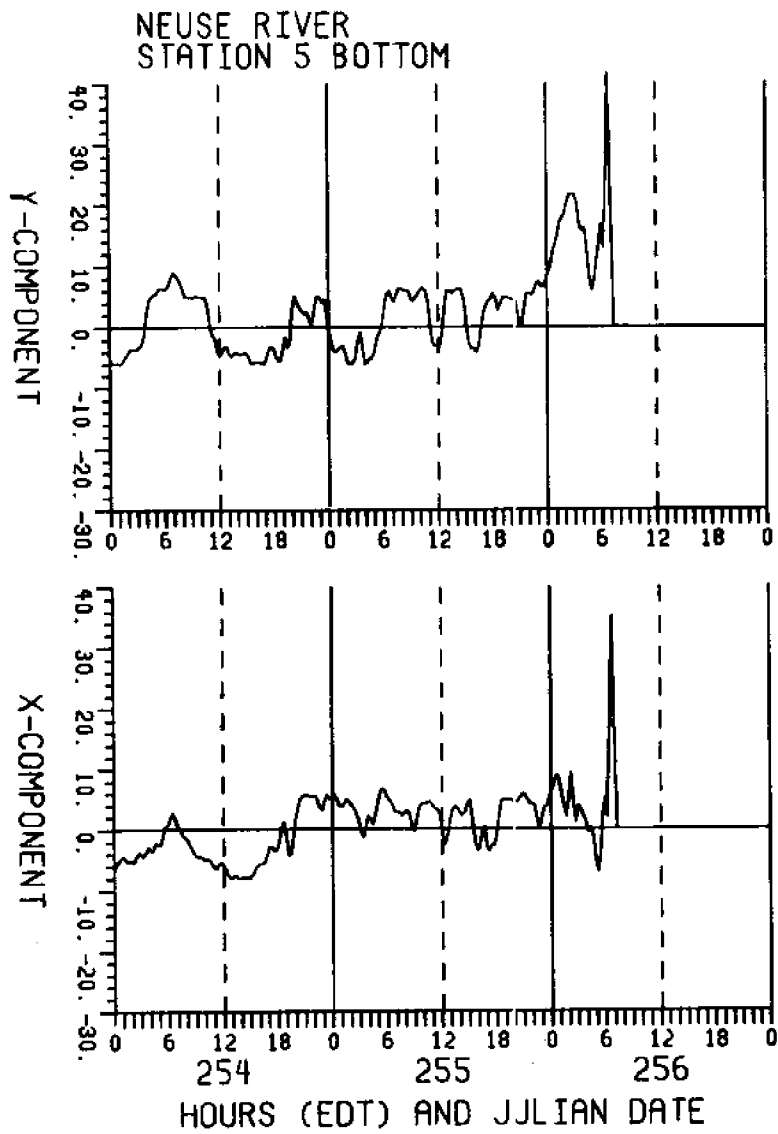


Figure D7

Figure D8. River flow at Station 6 Bottom, with channel axis of 040° mag.

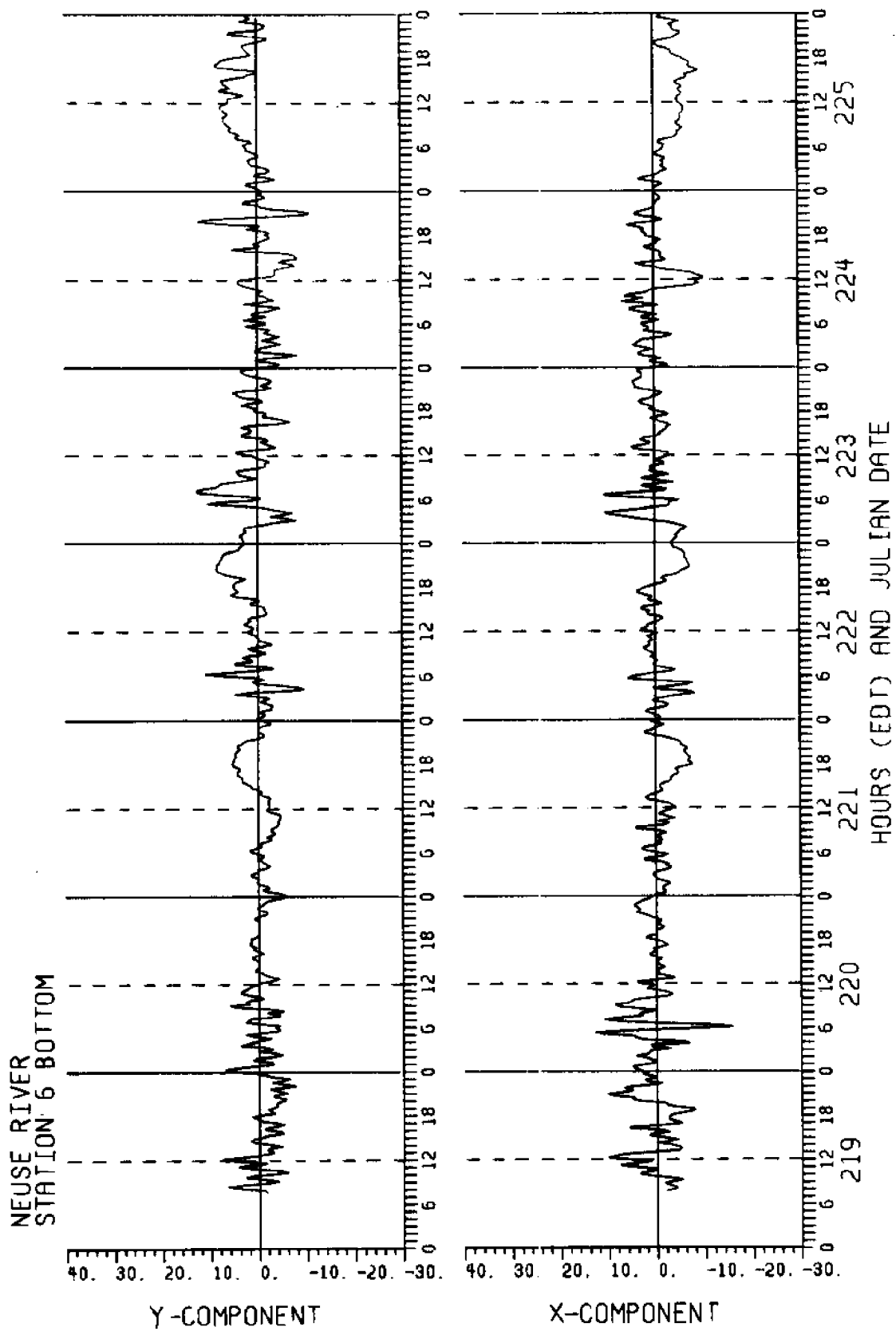


Figure D8

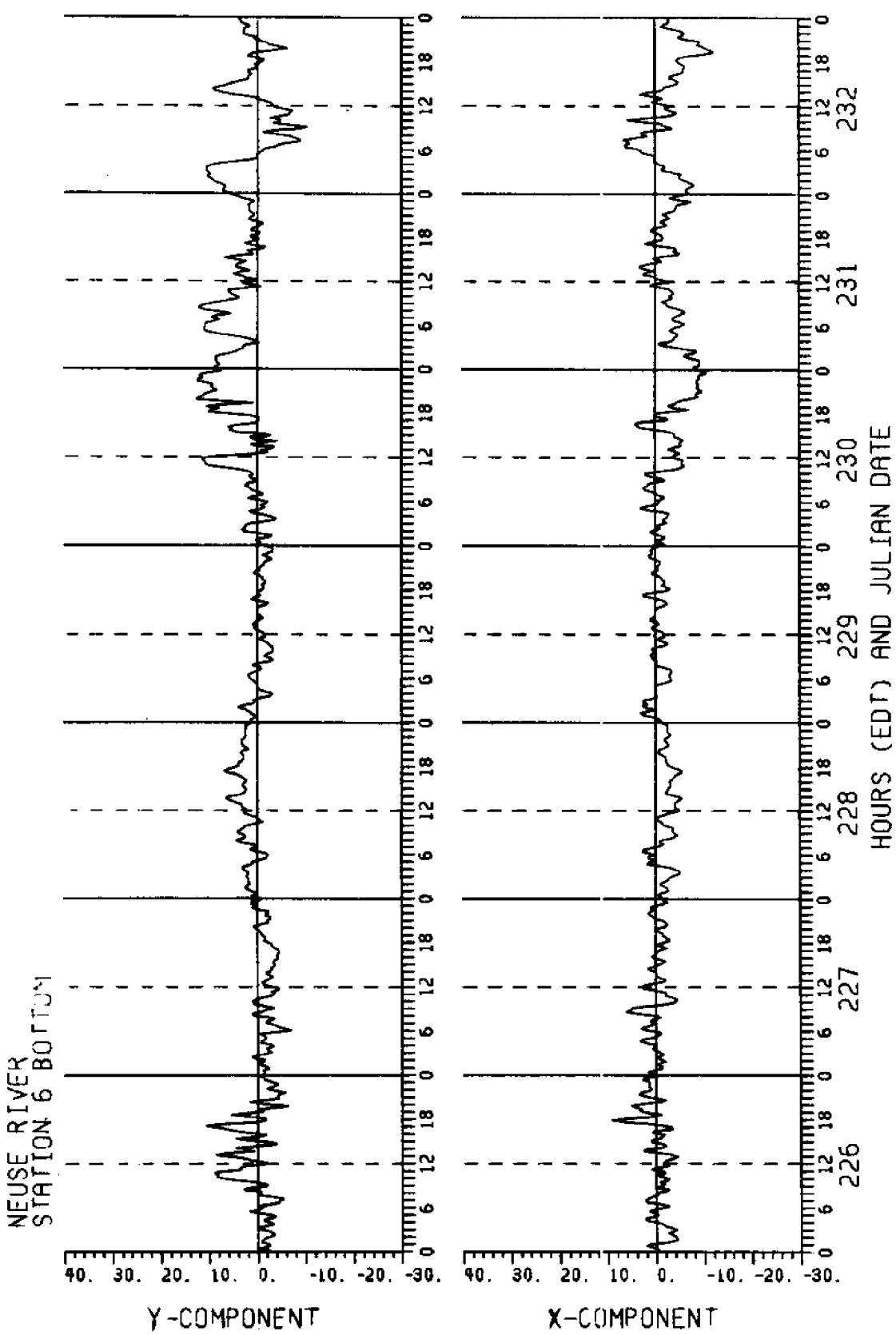


Figure D8

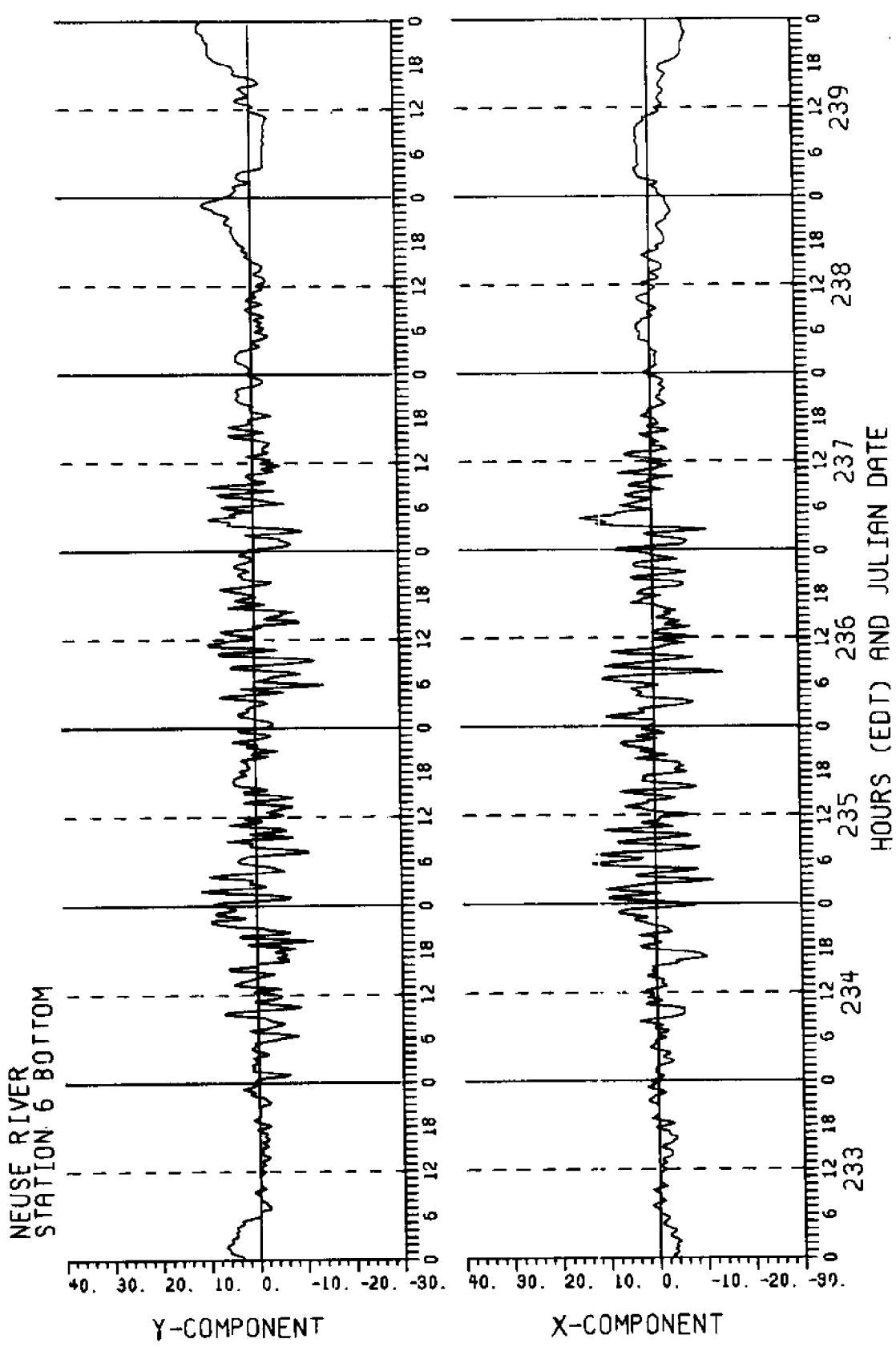


Figure D8

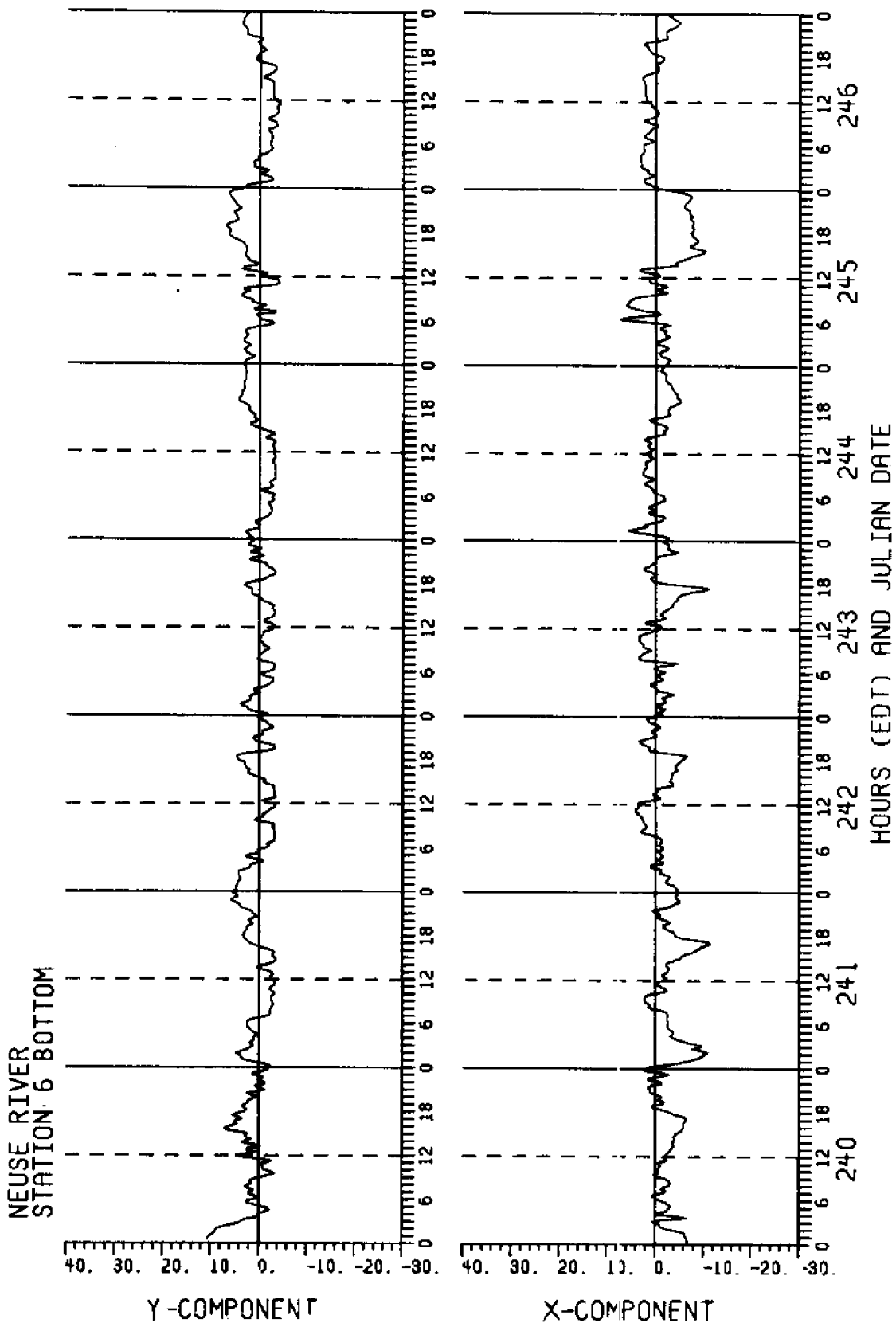


Figure D8

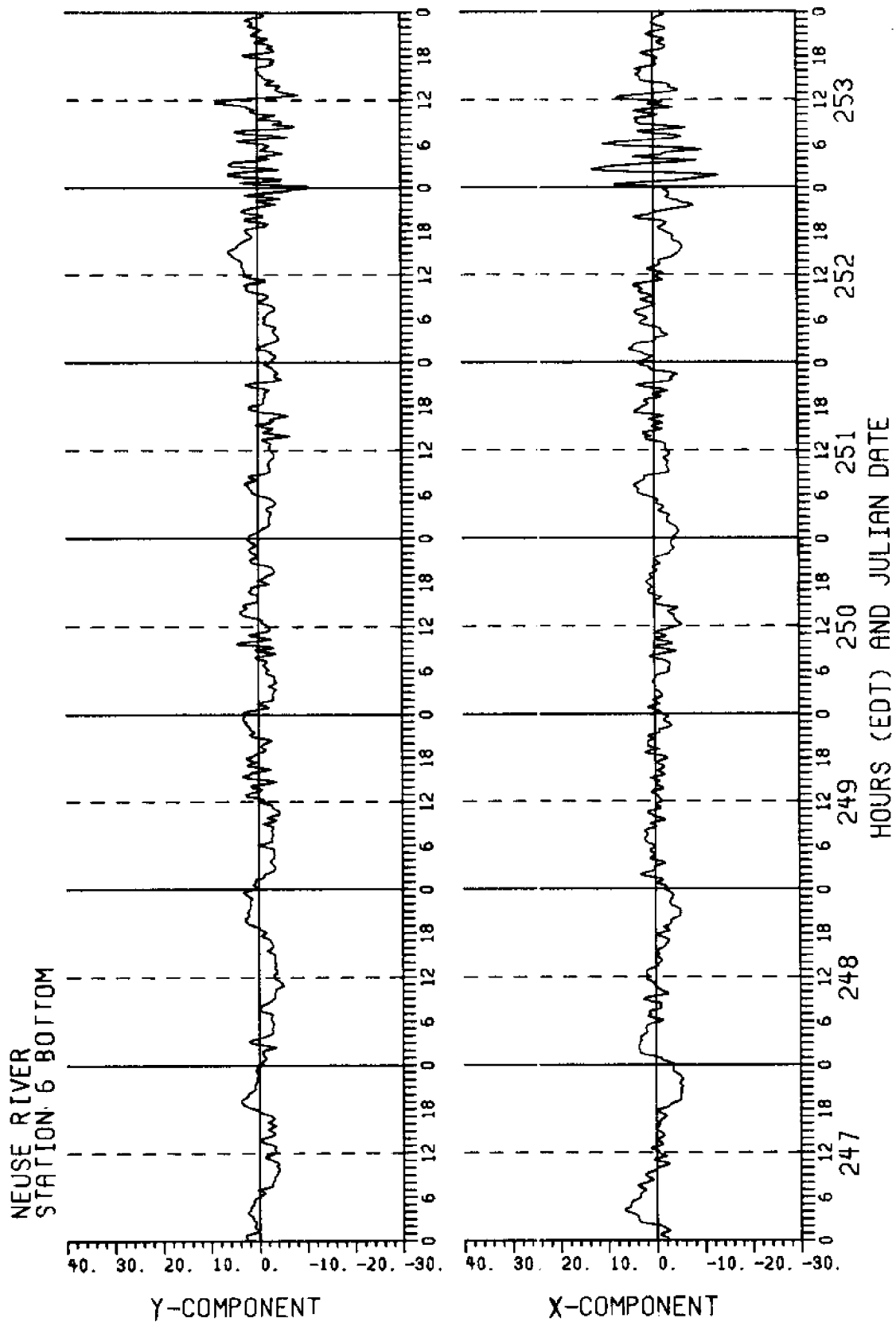


Figure D8

Figure D9. River flow at Station 7 Bottom, with channel axis of 040° mag.

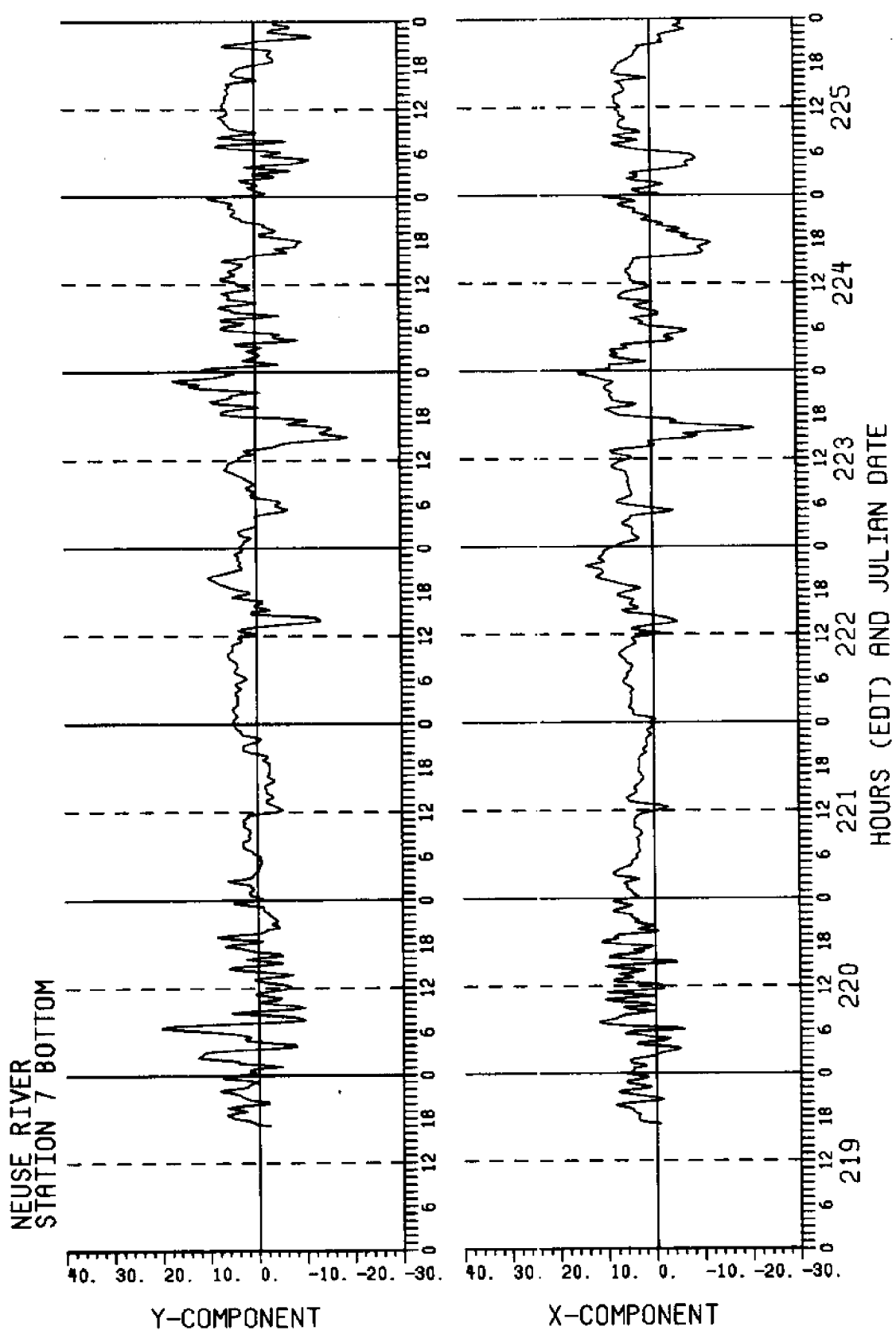


Figure D9

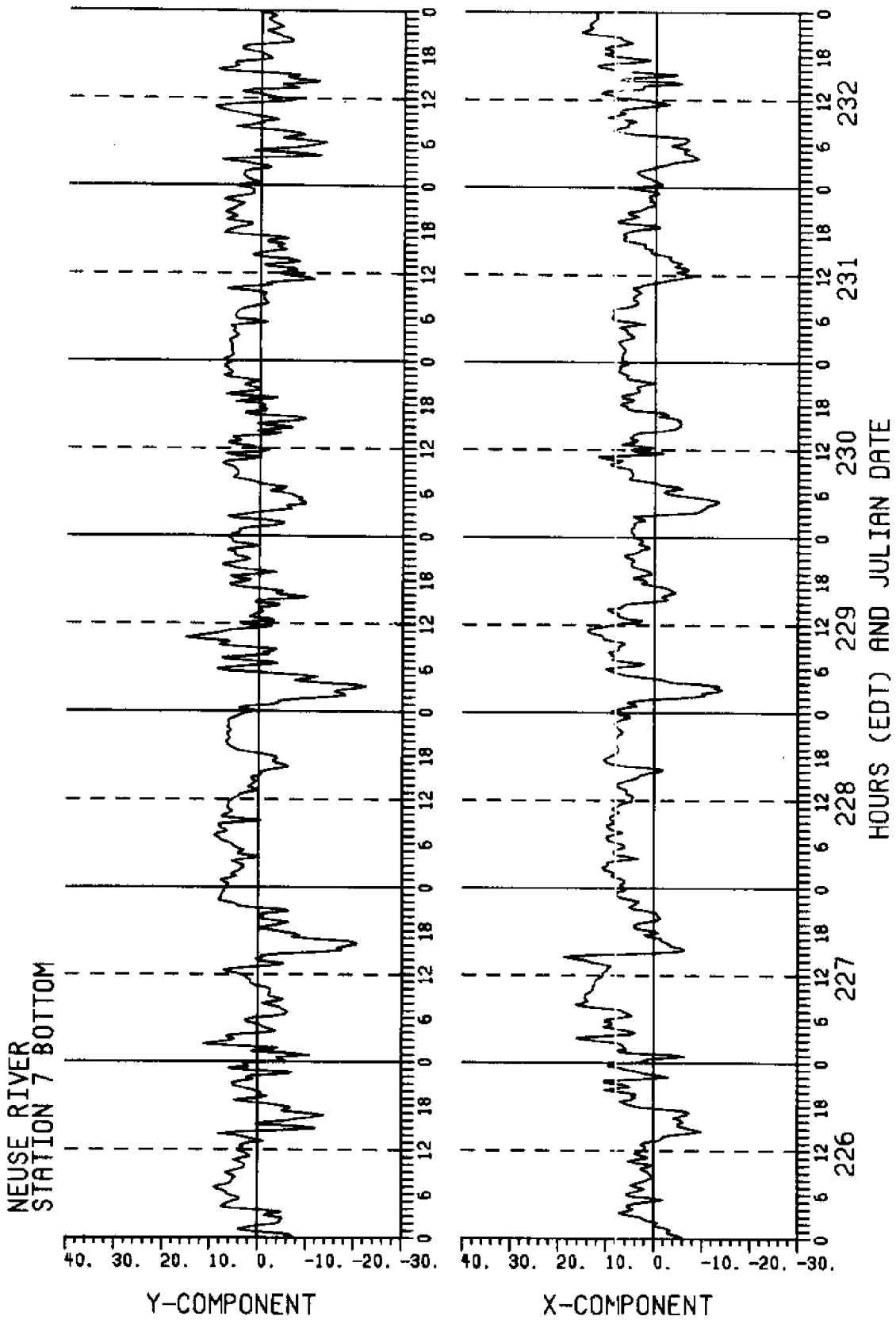


Figure D9

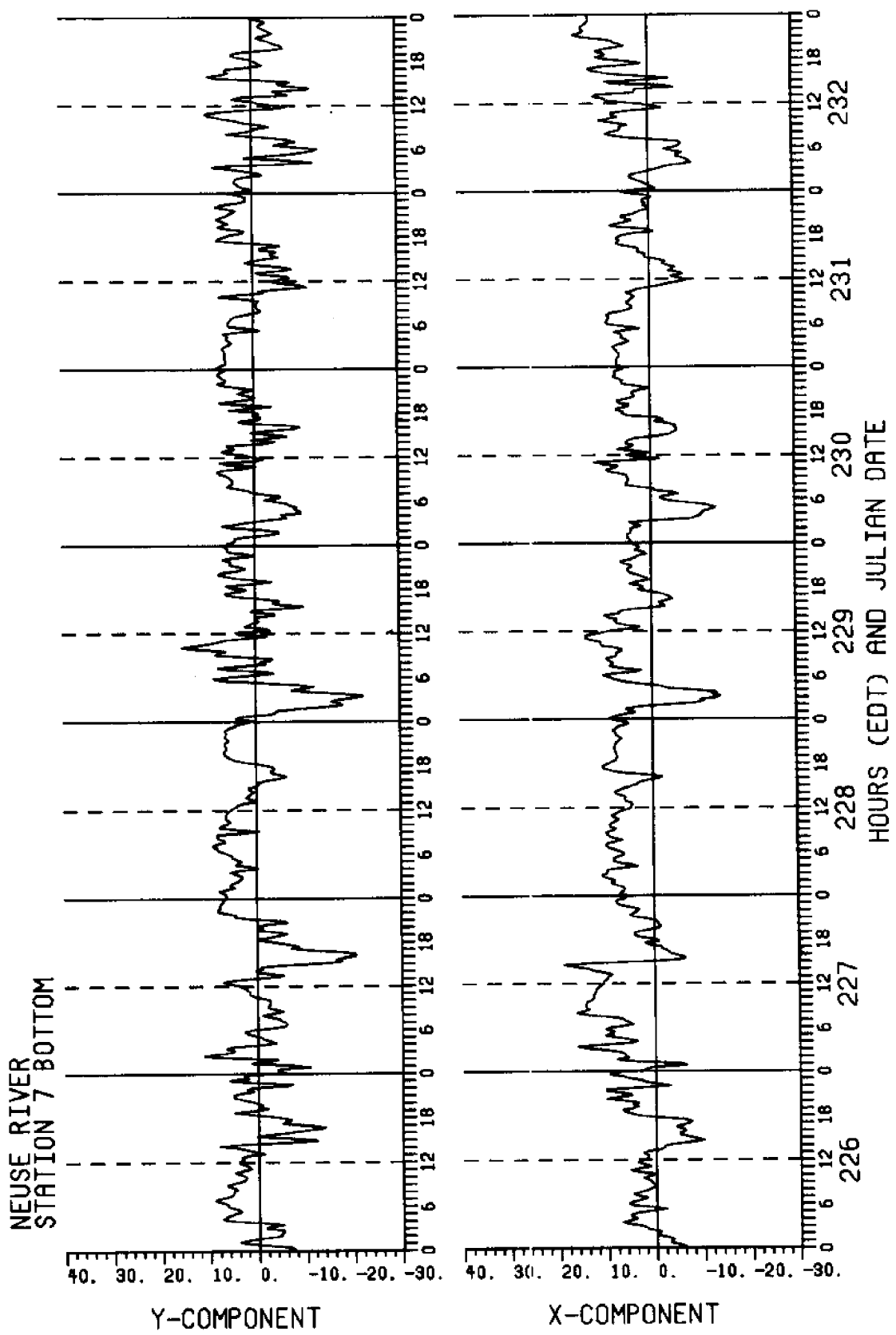


Figure D9

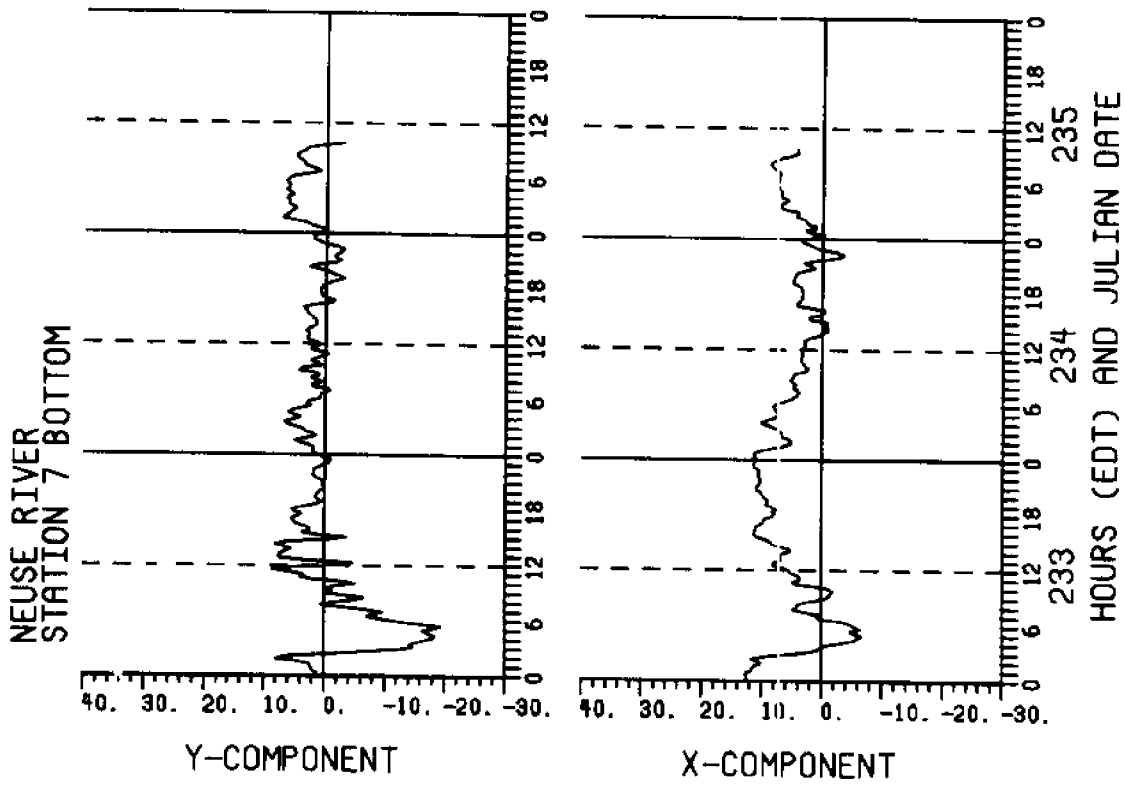


Figure D9

Appendix E. Water Temperature

Included in this appendix are the time history plots of (Figure E1) bottom water temperatures at Station 6 (top half of figure) and Station 7 (bottom half of figure). The ordinate shows temperature ($^{\circ}\text{F}$); the abscissa time (Julian Date and hours (EDT)).

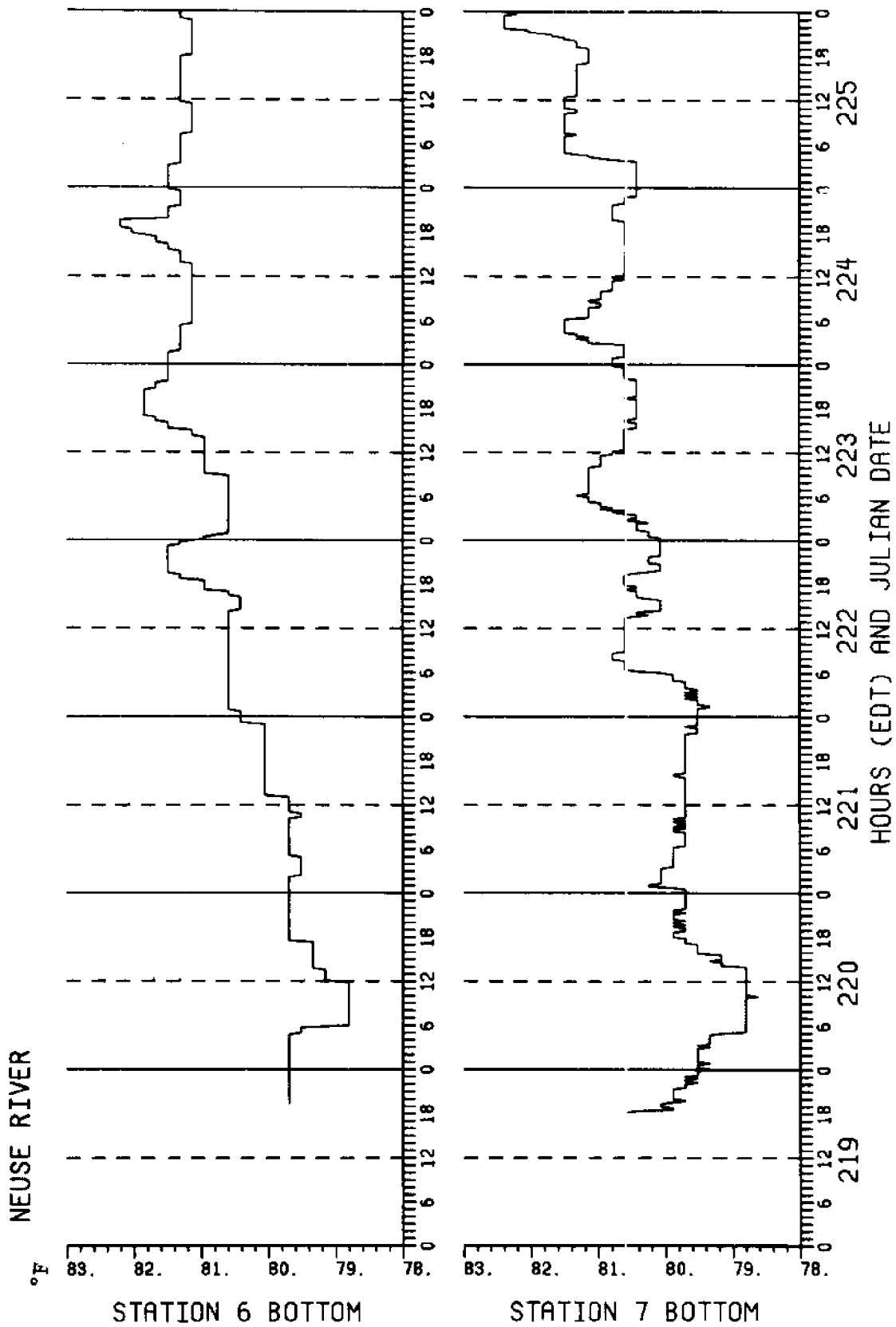


Figure E1

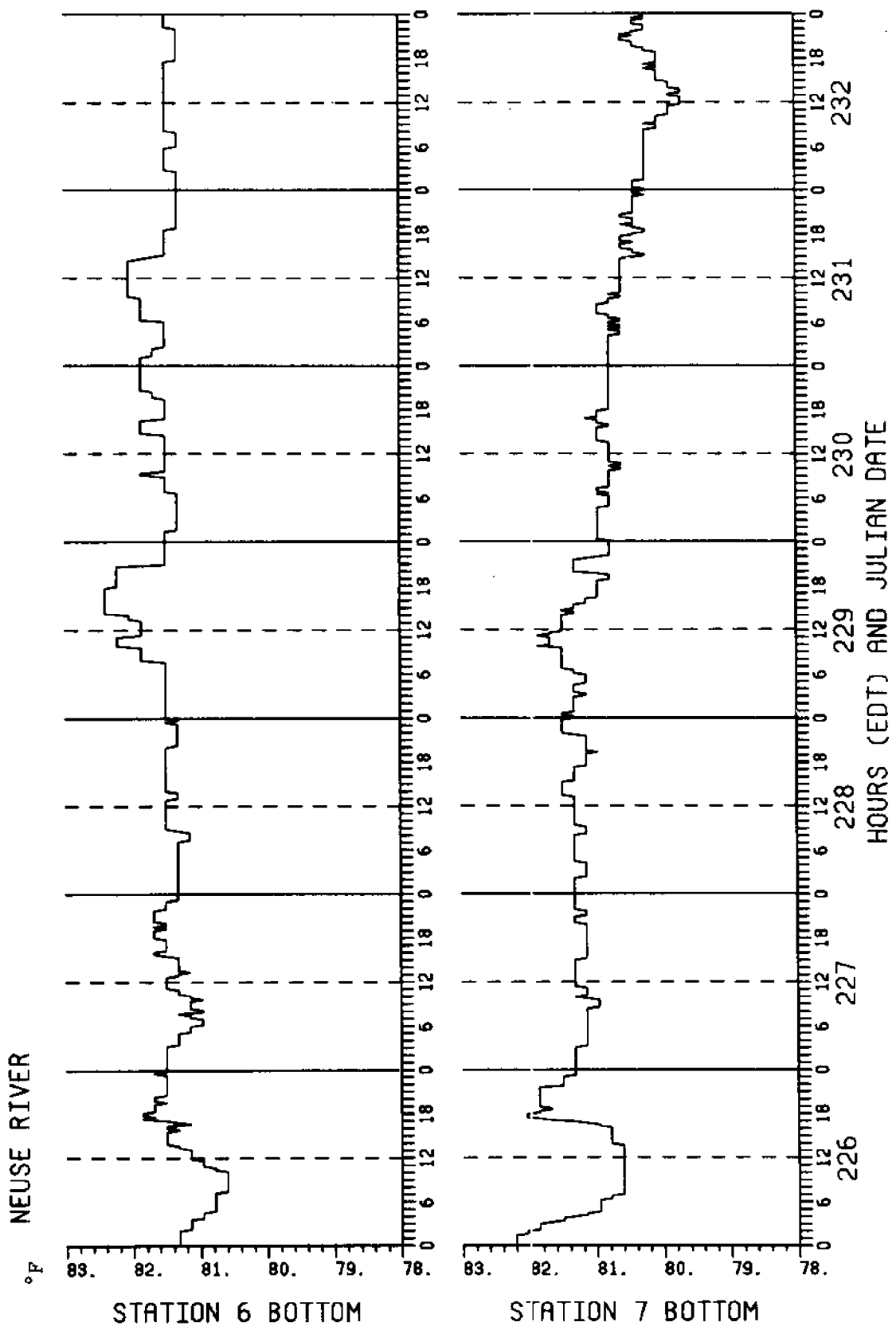


Figure E1

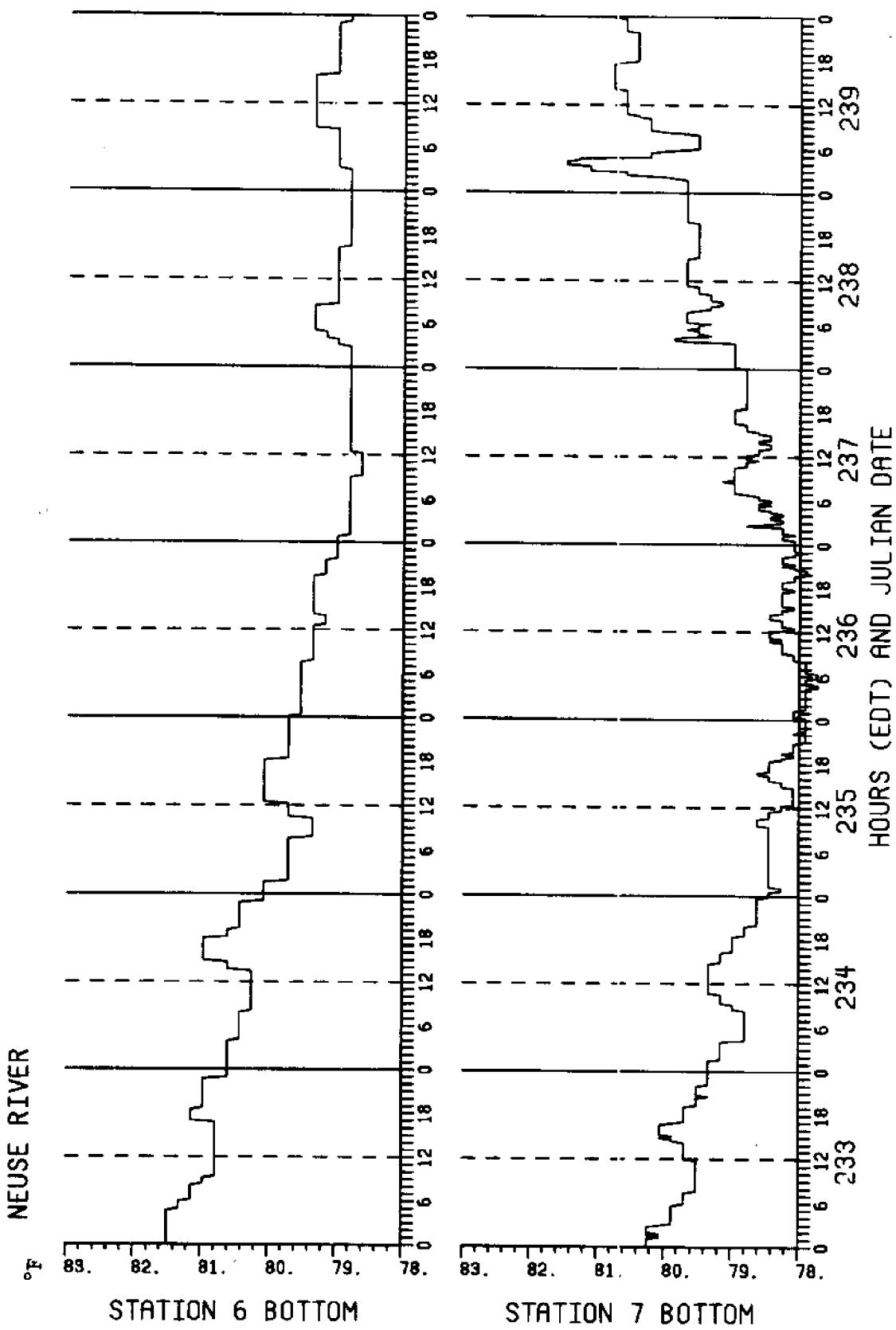


Figure E1

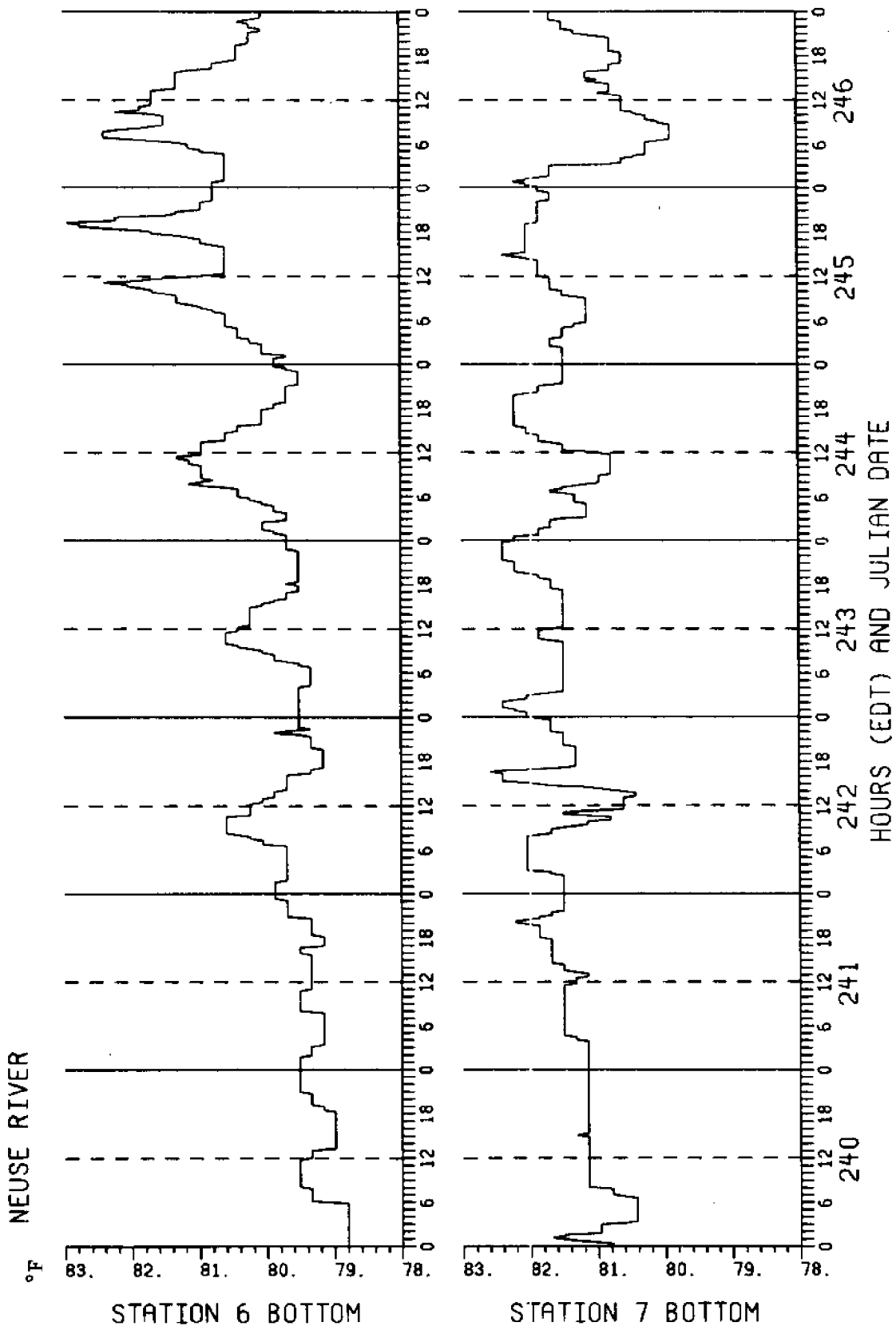


Figure E1

NEUSE RIVER

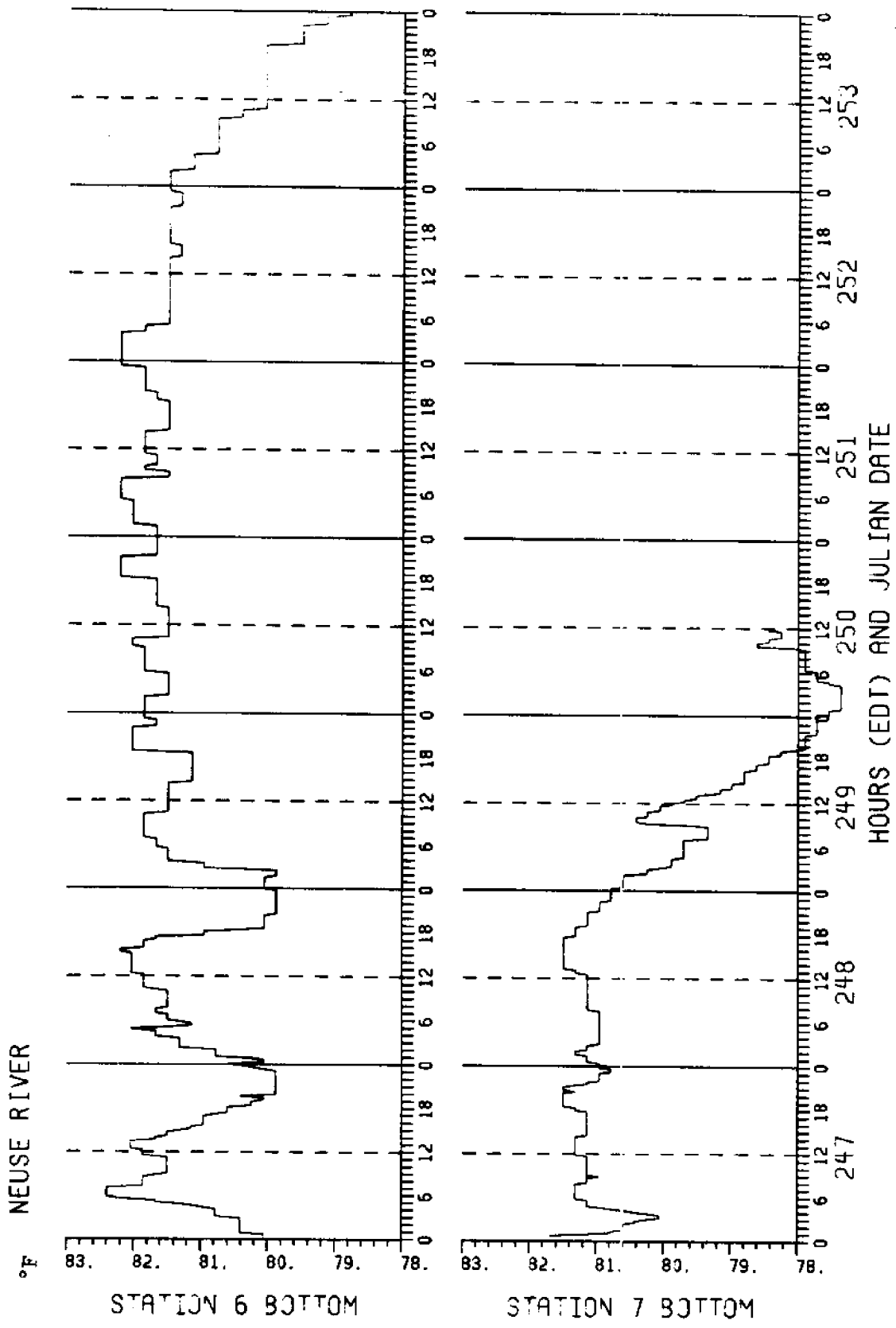


Figure E1

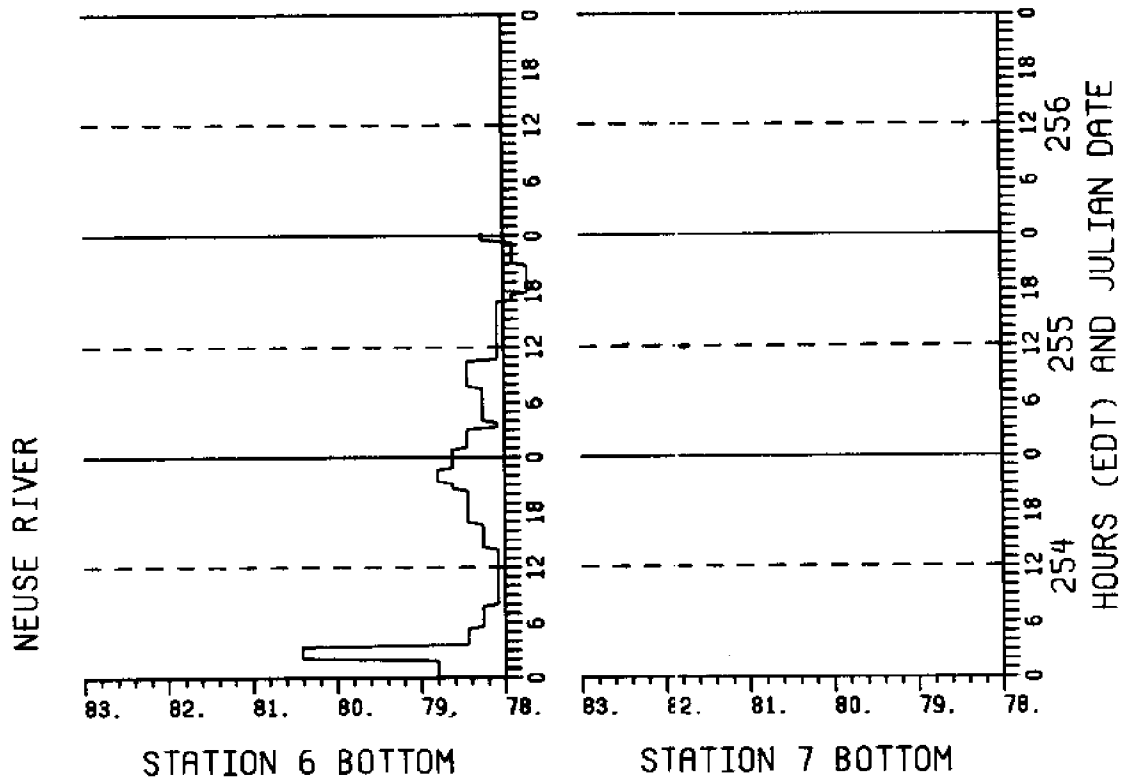


Figure E1

Appendix F. Power Spectral Density Analysis

Included in this appendix are semi-log plots of the power spectral density functions for the upstream-downstream component of river flow at all river stations ($(\text{cm/sec})^2/\text{CPH}$), and the N-S component of the wind field ($(\text{dynes/cm}^2/\text{CPH})$), where CPH is frequency in cycles per hours.

The ordinate shows the value of the spectral density function; the abscissa the period in hours. Black arrows are shown on the figures at 12 and 24 hours to aid in locating the period of the spectral peaks.

The list below includes the figure No., the Station No. and the page number of each plot.

<u>Figure</u>	<u>Station Number</u>	<u>Pages</u>
F1	1 Bottom	F-2
F2	2 Top	F-3
F3	2 Bottom	F-4
F4	3 Bottom	F-5
F5	4 Top	F-6
F6	4 Bottom	F-7
F7	5 Bottom	F-8
F8	6 Bottom	F-9
F9	7 Bottom	F-10
F10	(N-S) ORIENTAL Wind	F-11

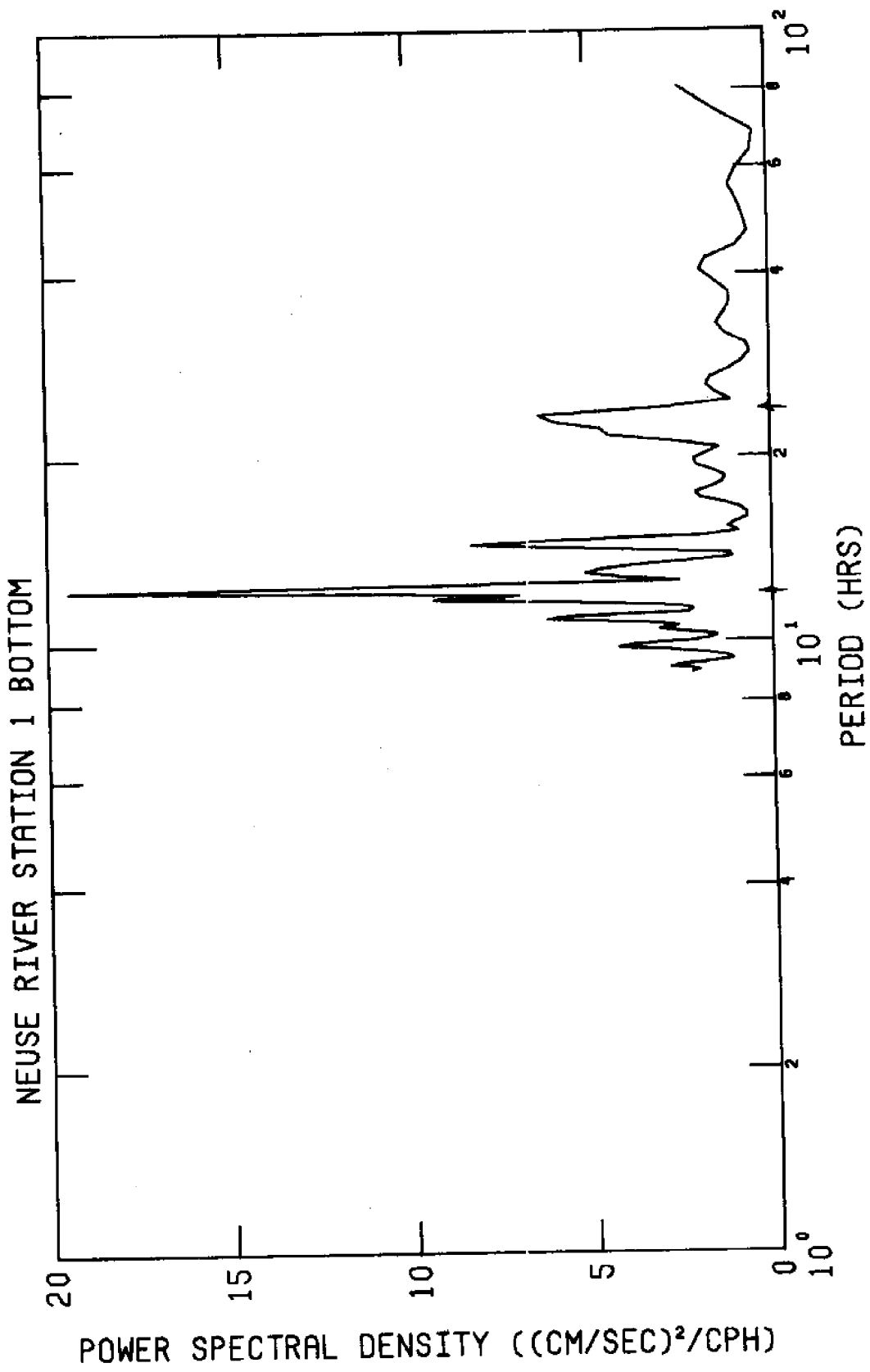


Figure F1

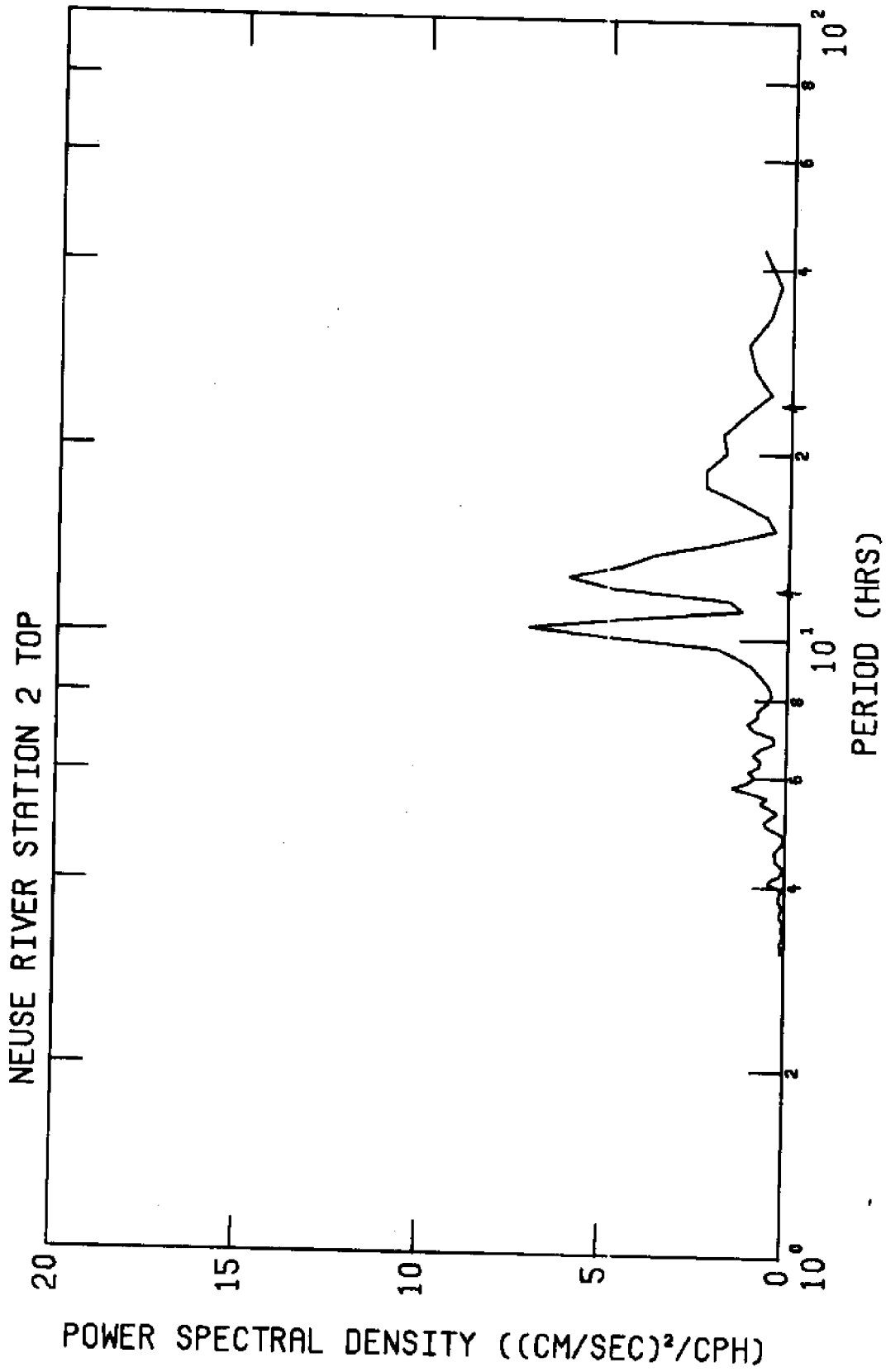


Figure F2

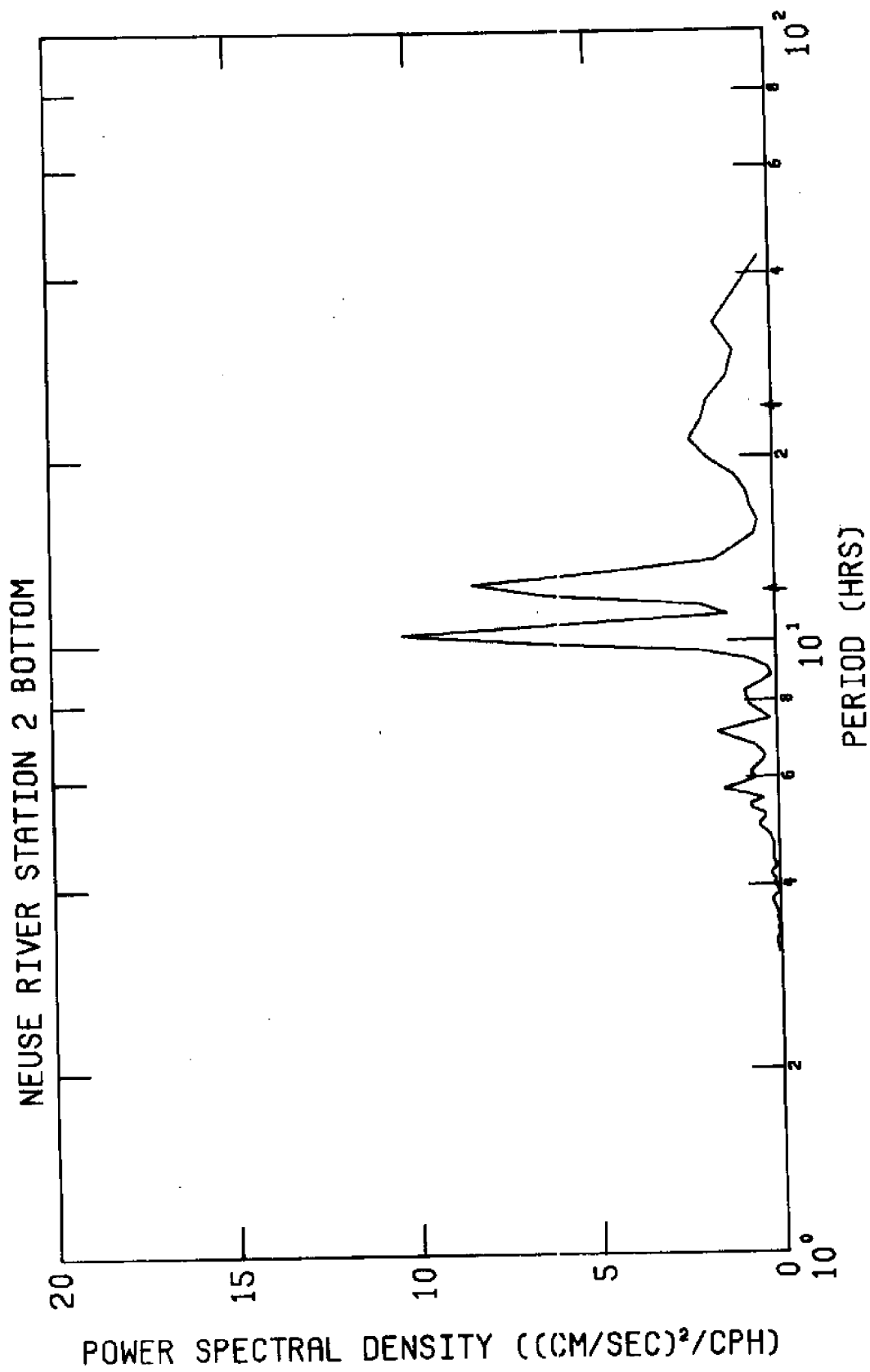


Figure F3

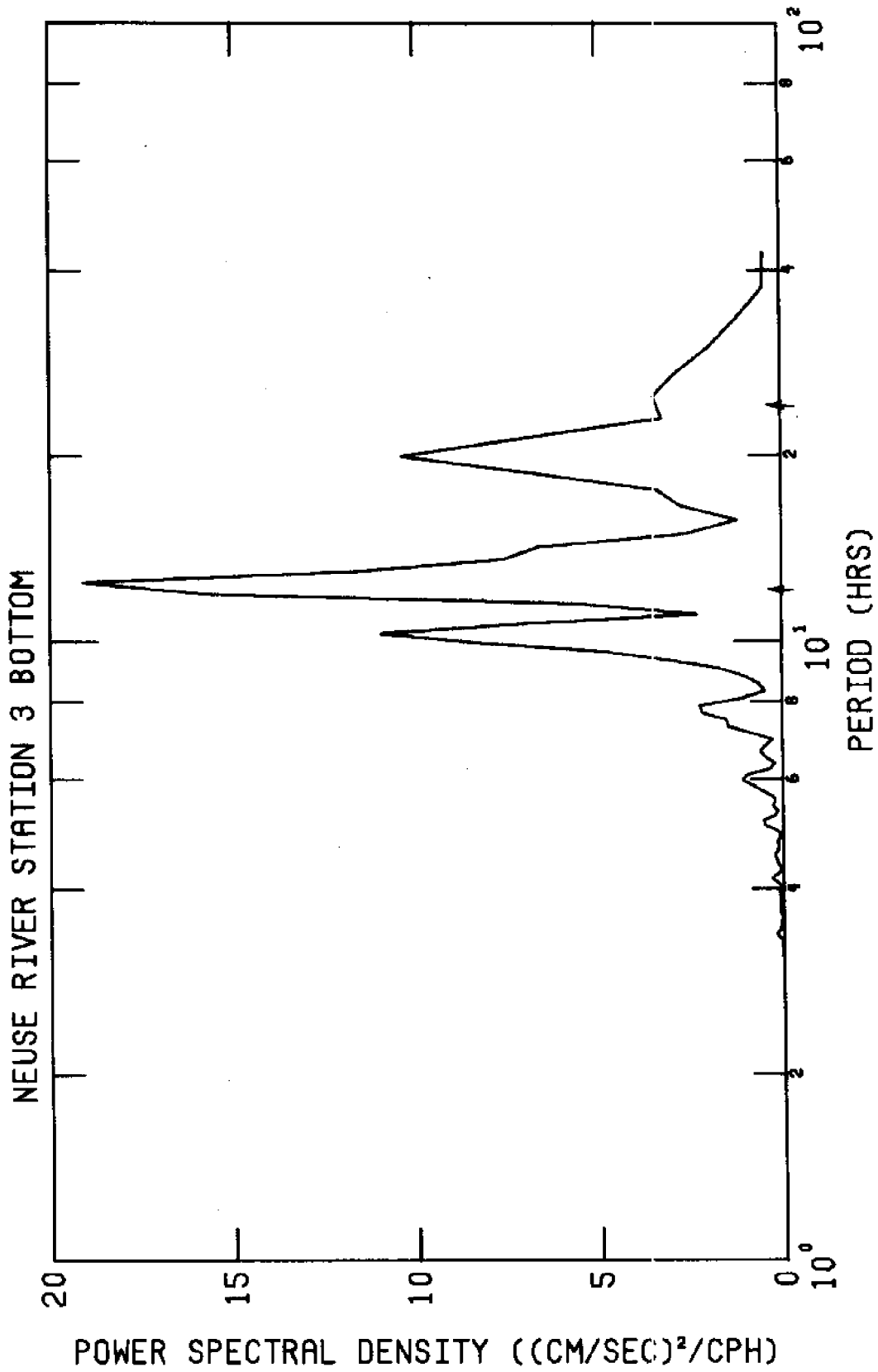


Figure F4

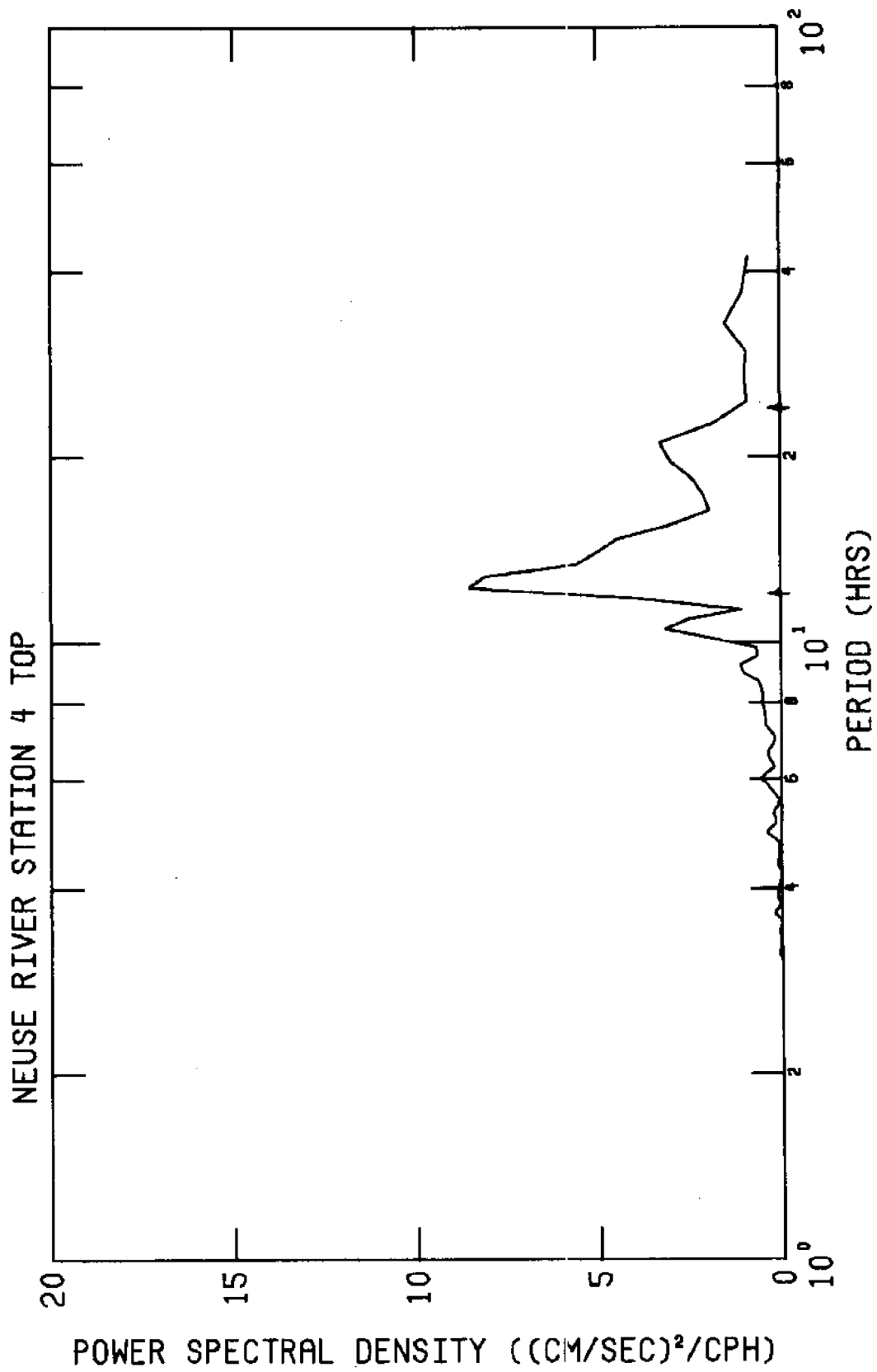


Figure F5

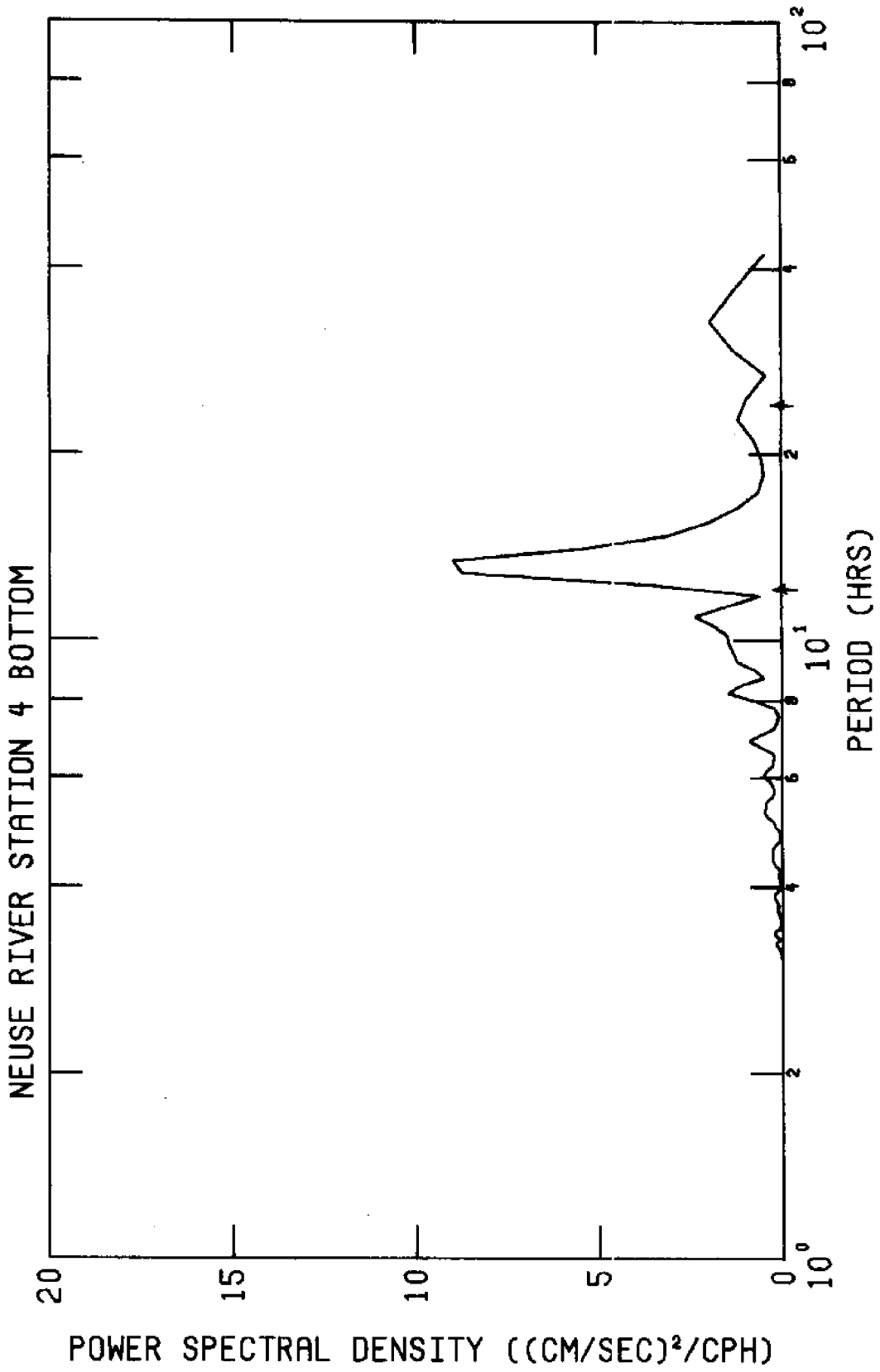


Figure F6

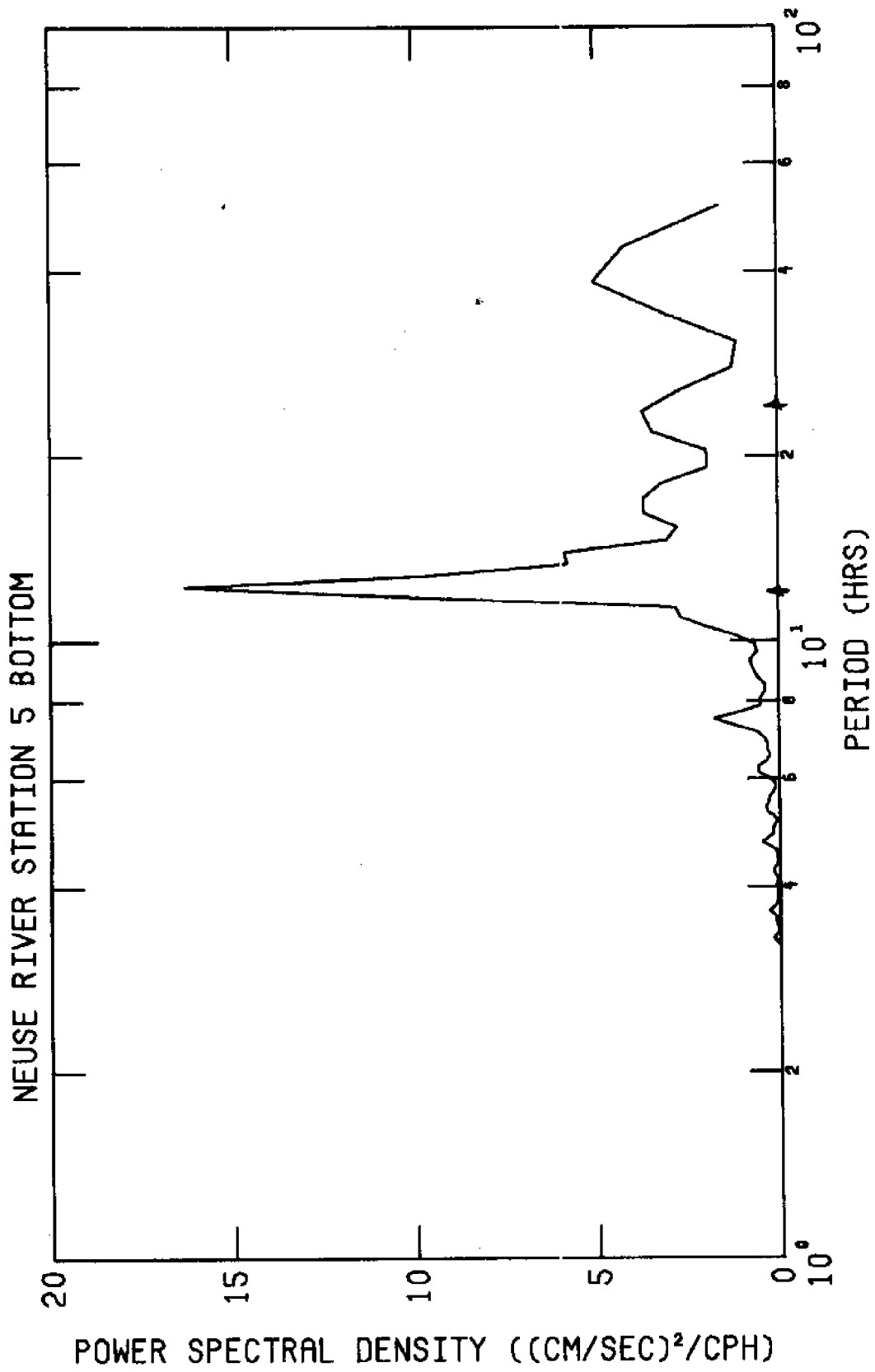


Figure F7

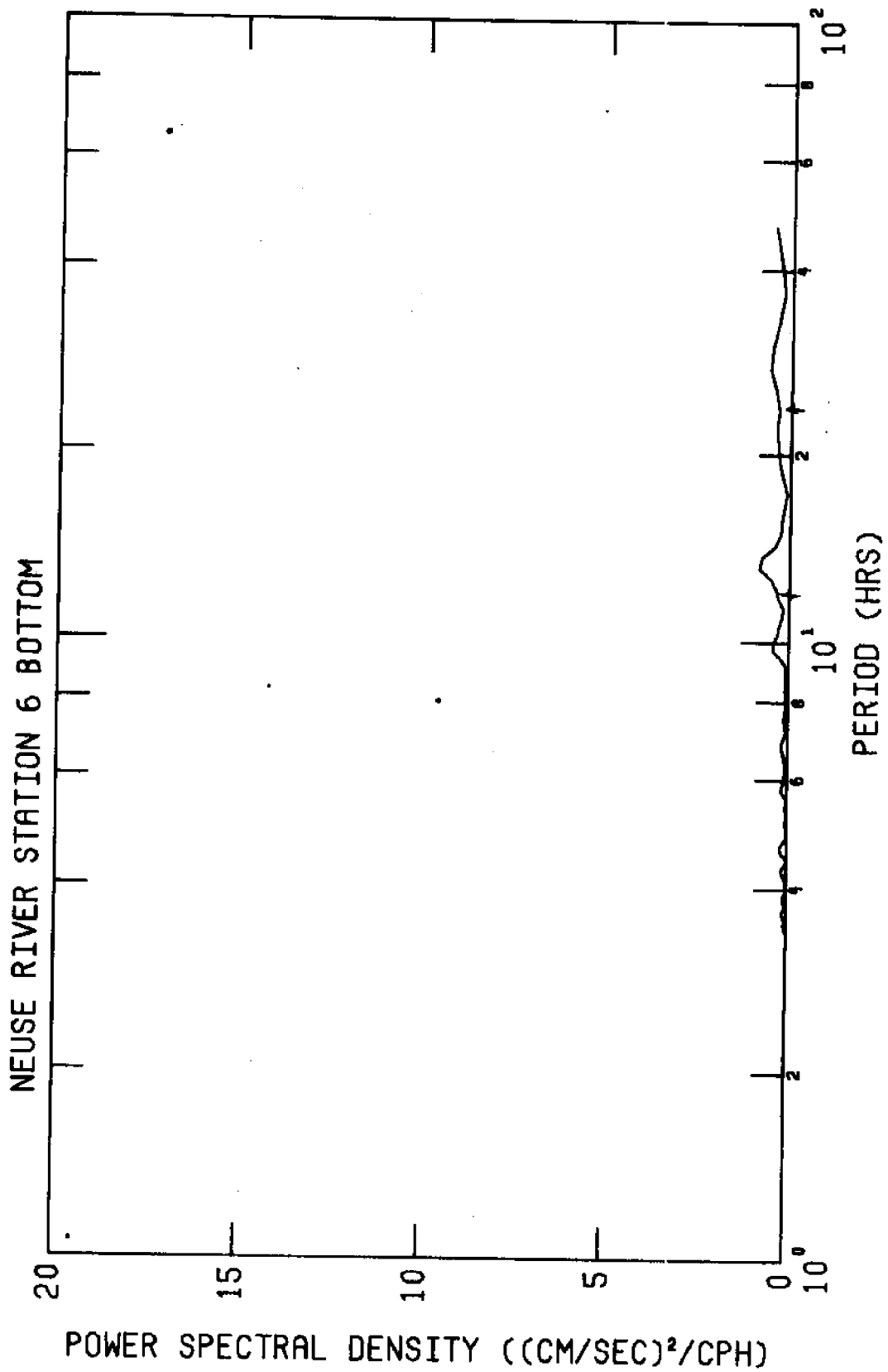


Figure F8

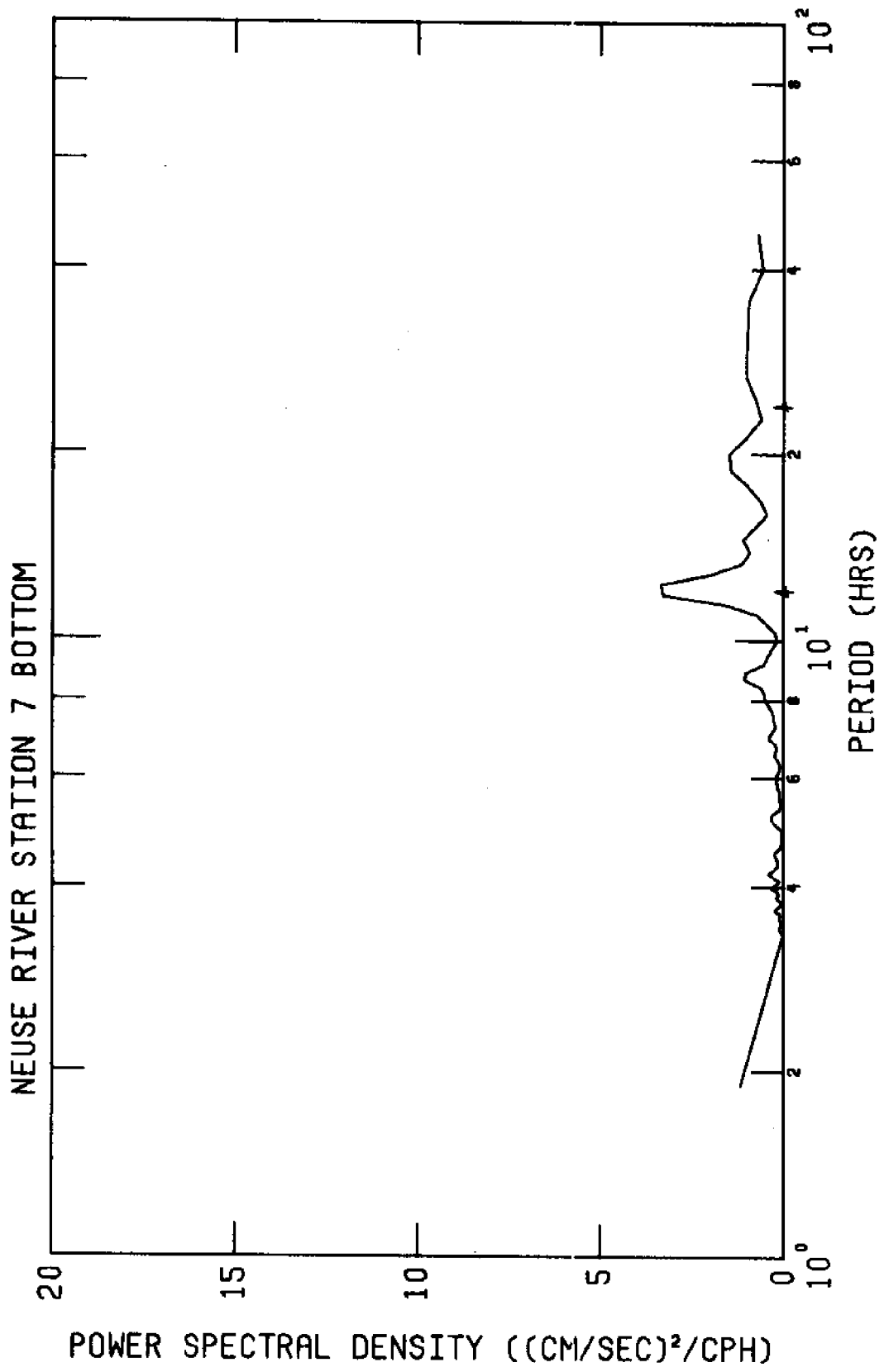


Figure F9

POWER SPECTRAL DENSITY

NEUSE RIVER ORIENTAL WIND

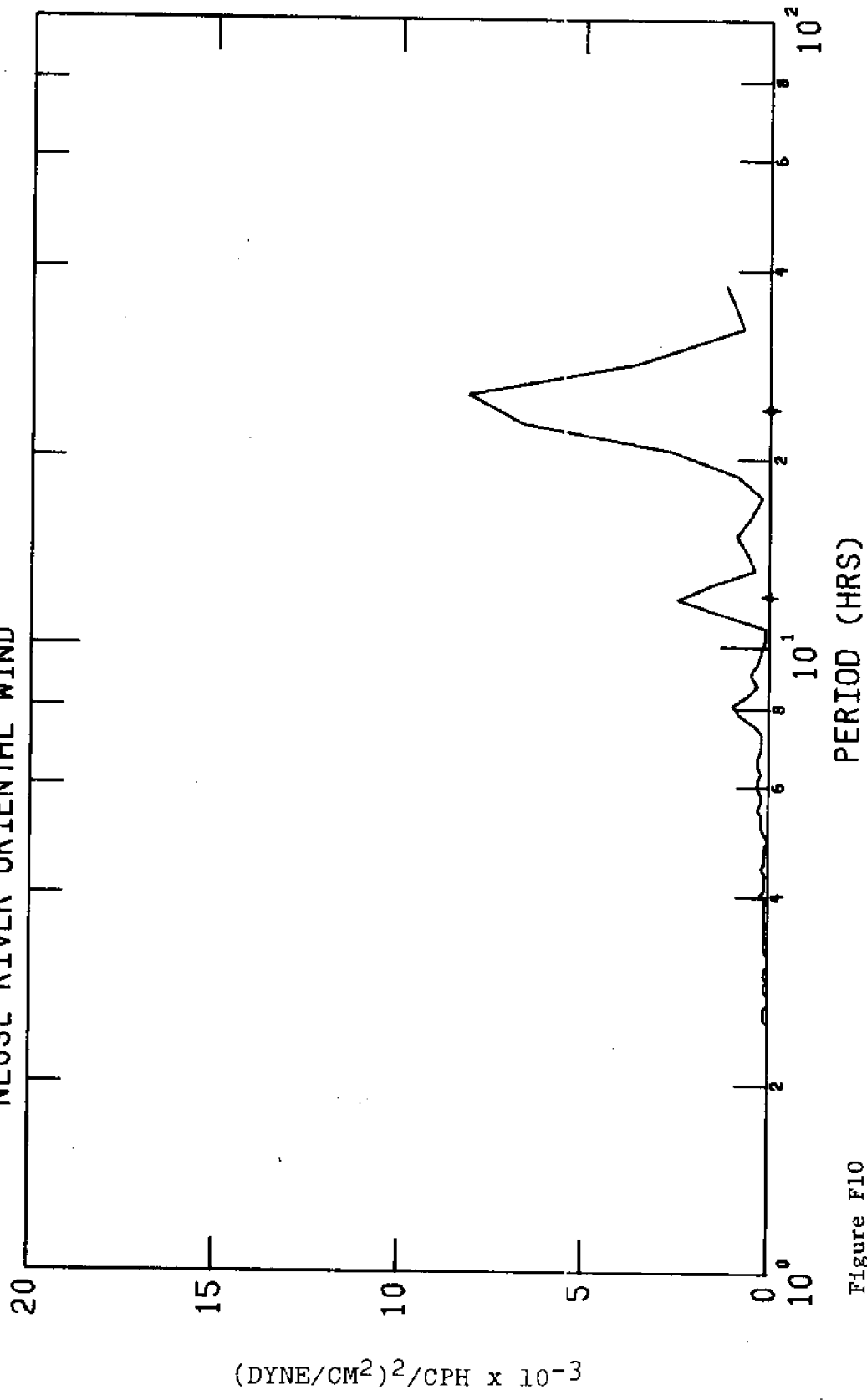


Figure F10

